

2-1-2008

Nonequilibrium Steady States of Driven Periodic Media

Leon Balents

University of California - Santa Barbara

M. Cristina Marchetti

Syracuse University

Leo Radzihovsky

University of Colorado at Boulder

Follow this and additional works at: <http://surface.syr.edu/phy>



Part of the [Physics Commons](#)

Repository Citation

arXiv:cond-mat/9707302v1

This Article is brought to you for free and open access by the College of Arts and Sciences at SURFACE. It has been accepted for inclusion in Physics by an authorized administrator of SURFACE. For more information, please contact surface@syr.edu.

Nonequilibrium Steady States of Driven Periodic Media

Leon Balents

Institute for Theoretical Physics, University of California, Santa Barbara, CA 93106-4030

M. Cristina Marchetti

Physics Department, Syracuse University, Syracuse, NY 13244-1130

Leo Radzihovsky

Physics Department, University of Colorado, Boulder, CO 80309-0390

(February 1, 2008)

We study a periodic medium driven over a random or periodic substrate, characterizing the non-equilibrium phases which occur by dynamic order parameters and their correlations. Starting with a microscopic lattice Hamiltonian, we perform a careful coarse-graining procedure to derive continuum hydrodynamic equations of motion in the laboratory frame. This procedure induces nonequilibrium effects (e.g. convective terms, KPZ nonlinearities, and non-conservative forces) which cannot be derived by a naive Galileian boost. Rather than attempting a general analysis of these equations of motion, we argue that in the random case instabilities will always destroy the LRO of the lattice. We suggest that the only periodicity that can survive in the driven state is that of a transverse smectic, with ordering wavevector perpendicular to the direction of motion. This conjecture is supported by an analysis of the linearized equations of motion showing that the induced nonequilibrium component of the force leads to displacements parallel to the mean velocity that diverge with the system size. In two dimensions, this divergence is extremely strong and can drive a melting of the crystal along the direction of motion. The resulting driven smectic phase should also occur in three dimensions at intermediate driving. It consists of a periodic array of flowing liquid channels, with transverse displacements and density (“permeation mode”) as hydrodynamic variables. We study the hydrodynamics of the driven smectic within the dynamic functional renormalization group in two and three dimensions. The finite temperature behavior is much less glassy than in equilibrium, owing to a disorder-driven effective “heating” (allowed by the absence of the fluctuation-dissipation theorem). This, in conjunction with the permeation mode, leads to a fundamentally *analytic* transverse response for $T > 0$.

PACS: 64.60.Fr, 74.20.D

I. INTRODUCTION

Non-equilibrium driven solids and liquids arise in a wide variety of different physical contexts. A common means of driving is to apply a constant or low frequency spatially uniform shear (either a constant shear rate or shear stress), which has been studied extensively in colloidal and polymeric systems¹. Such a driving is in a sense severe, since it is incompatible with a macroscopically ordered solid, requiring the continual breaking of a non-zero density of bonds per unit time. If translational symmetry is broken explicitly by the presence of, e.g. a periodic substrate or quenched impurities fixed in space, a gentler sort of driving is possible. In this case, even a uniform translation of the system is nontrivial, and it can be driven out of equilibrium simply by applying a constant force or pulling at a constant velocity.

A considerable number of such systems have been subjects of recent investigation. These include flux lattices in type-II superconductors^{2,3}, charge density waves (CDWs) in anisotropic conductors⁴, magnetic bubble arrays⁵, and the magnetically-induced Wigner crystal in

a two-dimensional electron gas^{6,7}. In all these systems the relevant degrees of freedom - be they vortices in superconductors or electrons in metals - form a lattice inside a solid matrix, provided by the superconducting or conducting material. Both a periodic potential (due to the underlying crystal lattice) and a quenched random one (due to material impurities and defects) are generally present, though their relative importance can vary from system to system. Closely related problems also arise in microscopic models of friction and lubrication, in which a surface or monolayer is brought into contact with another surface and forced to slide relative to it. Some recent simple models of earthquakes⁸, in which two elastic half-spaces are slowly driven past each other, also fall into the general class of driven disordered periodic elastic systems.

Much of the recent focus in these *pinned elastic media* has been on *equilibrium* behavior, since, unlike their colloidal and polymeric counterparts studied in the shear geometry, these systems exhibit a nontrivial competition between the external (substrate or disorder-induced) potential and the tendency for local order. In the random

case, this was argued by Larkin⁹ to generate long-range elastic distortions. More recent works have reinvestigated this problem in some detail, suggesting the existence of a novel “Bragg glass” phase in three and possibly two dimensions.^{10–12} In the periodic case (known as intrinsic pinning in the vortex community), the potential can either lock-in commensurate phases, generate finite (but qualitatively unimportant) incommensurate distortions of the lattice, or stabilize anisotropic *liquid-crystalline* states. Though for both types of matrix some detailed questions remain unanswered (in particular, the stability of the studied elastic glassy phases to proliferation of topological defects), the *equilibrium* phases and transitions in these systems have been extensively studied and are fairly well understood.

Once the elastic medium is driven, however, a host of new questions arises: Under a uniform applied external force $f_{\text{ext.}}$, what is the mean velocity $v(f_{\text{ext.}})$ (the IV curve, in the context of superconductors and CDWs), and is this uniquely determined or dependent upon history or other variables? Do ordered solid phases exist at low temperatures or weak disorder, and if so how are they characterized? Can one develop non-equilibrium phase diagrams, with phases classified by order parameters and symmetry analogous to equilibrium problems? What are the properties of the resulting non-equilibrium dynamic phase transitions and the nature of the fluctuations? Under what conditions does such a system reach a non-equilibrium *steady state*, and what are the hydrodynamic modes in this case?

Along with these new questions come a number of new physical variables which play important roles. While equilibrium behavior is relatively insensitive to detailed dynamical laws, there is no reason to expect this for a driven system. In particular, the nature of dissipation surely plays a crucial role. This distinguishes, e.g. friction and lubrication, in which (to a good approximation) energy can only be redistributed among vibrational modes of the solid, from charge-density-wave or vortex solids, in which energy can be transferred out of the collective modes to dissipate into electronic degrees of freedom. In the latter case, which we focus on here, it is appropriate to consider overdamped dynamics, while for the former inertial effects may be significant. Also crucial are conservation laws, which generally give rise to additional hydrodynamic modes. In equilibrium, the interactions of these with elastic degrees of freedom are constrained by the fluctuation-dissipation theorem (FDT) not to modify static correlations. For the nonequilibrium lattice, however, they must be treated explicitly. Finally, a driven system may exhibit complex dynamics even in the absence of external “thermal”, or time-dependent, noise. When the external noise level is low, this deterministic dynamics can give rise to steady, periodic, quasiperiodic, or (spatio-temporally) chaotic solutions. While in the latter case, dynamical chaos likely gives rise to an effective “temperature” and restoration of ergodicity, more regular solutions need not explore the full phase space and

can in principle behave with almost arbitrary complexity! Of course, factors such as the nature of the external potential, dimensionality, and range of inter-particle interactions, which control the equilibrium state, influence the driven dynamics as well.

A complete answer to these questions for all possible cases is beyond the scope of a single paper (or researcher!). Instead, we will focus here on systems with overdamped, dissipative dynamics which reach statistically steady states. This can occur either due to the presence of external time-dependent noise, which forces the system to explore the available phase space, or due to intrinsic chaotic dynamics. Note that this condition is violated by overdamped phase-only models (e.g. Fukuyama-Lee-Rice¹³) of CDWs, in which there is a unique periodic long-time attractor, as shown by Middleton.¹⁴ It may also be violated in zero-temperature simulations of vortex dynamics under some circumstances, as observed recently by Nori in some regimes for a strong periodic pinning potential.¹⁵ We expect, however, that in the presence of a random potential chaotic dynamics is much more germane, and furthermore, that most systems of experimental interest contain appreciable external thermal noise. Nevertheless, where possible, we will comment on the extensions of our conclusions to the noiseless case.

Our approach to the problem is first to devise a means of classifying the non-equilibrium phases, then to determine the dynamical equations of motion governing these phases. Finally, using these equations, we can begin to calculate the phase diagram and the properties thereof. We summarize the main results below, reserving a comparison with previous work for the discussion section of the paper. Some preliminary versions of some of the results of this paper appeared in Ref. 19.

A. Order parameters and correlation functions

A framework for classifying phases was introduced in Ref. 16 in the context of CDWs, and we generalize it here to more complex periodic media. As in equilibrium, phases are characterized by broken symmetry. An ordinary crystal is globally periodic, and hence has broken translational and rotational symmetry. Because the periodicity is sustained over long distances, we say that it has translational long range order (LRO). To quantify this notion, we must introduce suitable order parameters.

We consider initially a general model where the constituents of the driven lattice may be “oriented manifolds”, which are extended in some direction, such as magnetic flux lines in a three-dimensional superconductor. The configuration of such a lattice is described by labeling each manifold by its undisplaced equilibrium transverse position, \mathbf{x} . The internal coordinates parallel to the oriented manifold (e.g., along the magnetic field direction in the vortex lattice) are parameterized by a d_l -dimensional vector \mathbf{z} , and $\mathbf{r} = (\mathbf{x}, \mathbf{z})$. The number of

transverse dimensions is denoted by d_t and the dimensionality of space is $d = d_t + d_l$. The lattice may be described by a density field smoothed out on the scale of the lattice spacing, $\rho(\mathbf{x}, \mathbf{z})$, which in the ordered phase becomes periodic in the transverse direction. For the vortex lattice the density is the local magnetic induction, while for the CDW and the Wigner crystal it is the electronic charge density. In the ordered phase the collection of oriented manifolds acquires long-range periodicity, defined by a reciprocal lattice with basis vectors $\{\mathbf{Q}\}$. The density field is then written as

$$\rho(\mathbf{x}, \mathbf{z}) = \rho_0 + \frac{1}{2} \sum_{\mathbf{Q}} \tilde{\rho}_{\mathbf{Q}}(\mathbf{r}) e^{i\mathbf{Q}\cdot\mathbf{x}}, \quad (1.1)$$

where ρ_0 is the mean density. The complex Fourier components $\tilde{\rho}_{\mathbf{Q}}(\mathbf{r})$ satisfy $\tilde{\rho}_{-\mathbf{Q}} = \tilde{\rho}_{\mathbf{Q}}^*$. All the amplitudes transform as $\tilde{\rho}_{\mathbf{Q}} \rightarrow \tilde{\rho}_{\mathbf{Q}} e^{i\mathbf{Q}\cdot\mathbf{a}}$ under a lattice translation $\mathbf{x} \rightarrow \mathbf{x} + \mathbf{a}$ ¹⁷. A nonzero expectation value of the $\tilde{\rho}_{\mathbf{Q}}$'s thereby indicates broken translational symmetry. As a result of the broken translational symmetry, long-wavelength fluctuations in the ordered phase can be described in terms of long-wavelength distortions of the Fourier modes, which can in general be written in terms of an amplitude and a phase as

$$\tilde{\rho}_{\mathbf{Q}}(\mathbf{r}) = \tilde{\rho}_{\mathbf{Q},0}(\mathbf{r}) e^{i\mathbf{Q}\cdot\tilde{\phi}(\mathbf{r})}. \quad (1.2)$$

Note that the phase in each Fourier amplitude is not an independently fluctuating variable in the ordered state. It is constrained by, e.g. cubic interactions of the $\tilde{\rho}_{\mathbf{Q}}$, which leave only the vector of phases $\tilde{\phi}$. They correspond to distortions of the lattice, and indeed $\tilde{\phi}$ can be interpreted as a sort of displacement field (but see below).

So far, this discussion applies equally well to both equilibrium and driven solids. Consider now the *time-dependence* of the local density. In a moving solid, we expect $\tilde{\phi} = \mathbf{v}t + \phi$, so that

$$\rho(\mathbf{x}, \mathbf{z}, t) = \rho_0 + \frac{1}{2} \sum_{\mathbf{Q}} \rho_{\mathbf{Q}}(\mathbf{r}, t) e^{i\mathbf{Q}\cdot[\mathbf{x} + \mathbf{v}t]}, \quad (1.3)$$

where

$$\rho_{\mathbf{Q}}(\mathbf{r}, t) = \tilde{\rho}_{\mathbf{Q}}(\mathbf{r}, t) e^{-i\mathbf{Q}\cdot\mathbf{v}t}. \quad (1.4)$$

Physically, the oscillations in the density simply reflect the fact that individual constituents of the lattice pass any given point in a regular periodic fashion. The set of $\rho_{\mathbf{Q}}$ fields comprises the order parameters for the non-equilibrium system. Neglecting topological defects (i.e. dislocations) amounts to assuming that the amplitude $\rho_{\mathbf{Q},0}$ is constant. Elastic deformations of the solid are then described entirely by phase fluctuations in terms of a single-valued coarse-grained displacement field $\phi(\mathbf{r})$. It is important to distinguish between the displacement field defined in the moving or crystal frame (where the conventional phonon field is defined) and the displacement

field in the laboratory frame. Throughout this paper we denote by $\phi(\mathbf{r})$ the displacement field in the laboratory frame, while we reserve the symbol $\mathbf{u}(\mathbf{r})$ for the conventional phonon field. Many of the experimental systems of interest form triangular lattices. In this case, $\langle \rho_{\mathbf{Q}} \rangle \neq 0$ for three shortest wavevectors in the ordered phase (the brackets indicate a time average or average over thermal noise).

A quantity of immediate experimental interest is the static structure factor, which is the Fourier transform of the equal time density-density correlation function and is given by

$$\begin{aligned} S(\mathbf{q}) &= \langle |\delta\rho(\mathbf{q}, t)|^2 \rangle \\ &= \sum_{\mathbf{Q}} \int_{\mathbf{r}} e^{i(\mathbf{q}-\mathbf{Q})\cdot\mathbf{r}} \langle \rho_{\mathbf{Q}}(\mathbf{r}, t) \rho_{\mathbf{Q}}^*(\mathbf{0}, t) \rangle. \end{aligned} \quad (1.5)$$

Here $\mathbf{q} = (\mathbf{q}_t, \mathbf{q}_z)$ is the full wavevector. The order parameter correlator,

$$C_{\mathbf{Q}}(\mathbf{r}, t) = [\langle \rho_{\mathbf{Q}}(\mathbf{r}, t) \rho_{\mathbf{Q}}^*(\mathbf{0}, 0) \rangle]_{\text{ens.}}, \quad (1.6)$$

governs the behavior of the structure factor. We used angular (square) brackets to denote thermal (disorder) averages. If $C_{\mathbf{Q}}(\mathbf{r}, 0) \rightarrow \text{const.}$ for large $|r|$, $S(\mathbf{q})$ has a sharp (resolution limited) Bragg peak at $\mathbf{q}_t = \mathbf{Q}$. If $C_{\mathbf{Q}}(\mathbf{r}, 0) \sim |r|^{-\eta}$, these broaden to power-law form. If $C_{\mathbf{Q}}(\mathbf{r}, 0)$ decays exponentially for large $|r|$, only diffuse peaks if any exist. In these three cases, the system is said to possess long-range, quasi-long-range, and short-range translational order (at wavevector \mathbf{Q}), respectively. These will be abbreviated LRO, QLRO, and SRO, respectively, in the remainder of the paper.

$C_{\mathbf{Q}}(\mathbf{r}, t)$ also describes the extent of temporal periodicity. By analogy to the translational characterization, we say that the system possesses long-range, quasi-long-range, or short-range temporal order (at frequency $\omega = \mathbf{Q} \cdot \mathbf{v}$) if $C_{\mathbf{Q}}(\mathbf{0}, t)$ goes to a constant value, decays algebraically, or decays exponentially, respectively. This temporal order can be experimentally probed through the *dynamic* structure function

$$\begin{aligned} S(\mathbf{q}, \omega) &= \langle |\delta\rho(\mathbf{q}, \omega)|^2 \rangle \\ &= \sum_{\mathbf{Q}} \int_{\mathbf{r}, t} e^{i(\mathbf{q}-\mathbf{Q})\cdot\mathbf{r} - i(\omega - \mathbf{Q}\cdot\mathbf{v})t} \langle \rho_{\mathbf{Q}}(\mathbf{r}, t) \rho_{\mathbf{Q}}^*(\mathbf{0}, 0) \rangle. \end{aligned} \quad (1.7)$$

Systems with temporal LRO will display sharp peaks at multiples of the washboard frequency $\omega = \mathbf{Q} \cdot \mathbf{v}$ in the $S(\mathbf{q}, \omega)$ and in the related power spectrum of velocity fluctuations. Such system should also exhibit ‘‘complete mode locking’’ to an arbitrarily weak external periodic driving at these frequencies.

In a random system, temporal order is generally more robust than the translational order. Physically, the difference arises because impurities inhomogeneously stress the system. The responding non-uniform distortion, however, can have very little fluctuation in time, and

thereby can leave the temporal ordered relatively unaffected. It will, of course, have some effect on the dynamics, because disturbances propagate differently atop the non-uniform background, and because the local strains lower the barriers to defect nucleation. We cannot exclude the possibility of a phase in which dislocations are unbound, but frozen in the laboratory frame. Such a phase would exhibit translational SRO but temporal LRO, and would be the driven analog of the vortex glass phase originally proposed by Fisher, Fisher and Huse¹⁸. Given the relative instability of this phase in equilibrium, we think this scenario is, however, somewhat unlikely.

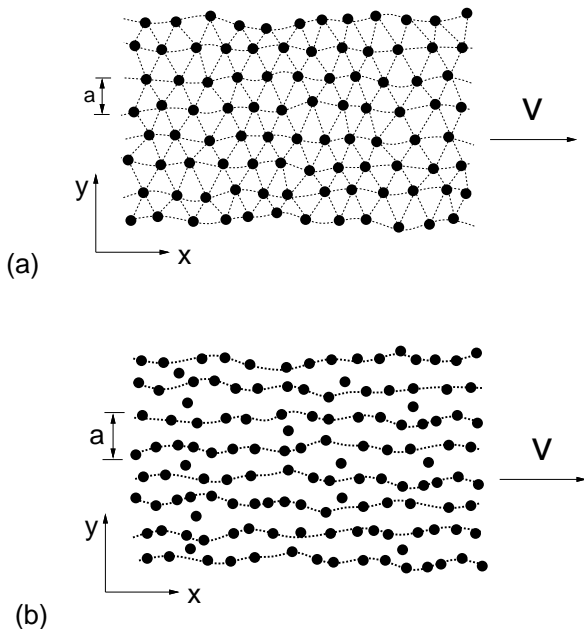


Fig.1:(a) Schematic illustration of a moving glass, which becomes unstable to the proliferation of dislocations with Burgers vectors along the direction of motion. At large velocities, we expect that unbound dislocations will be widely separated, with spacings x_{sm} and y_{sm} in the directions longitudinal and transverse to the motion, respectively. A naive estimate based on the linearized theory probably gives an upper bound for these scales: $x_{sm} \lesssim c_{66} a^8 (\gamma v)^7 / \Delta^4$ and $y_{sm} \lesssim c_{66} a^4 (\gamma v)^3 / \Delta^2$. Non-linear (KPZ) effects very likely shorten these lengths considerably. On larger scales, the “lattice” crosses over to the driven smectic state displayed in (b), with only transverse periodicity and liquid-like order along the direction of motion. The dislocations with Burgers vectors along the direction of motion allow the weakly coupled liquid channels to move at different velocities.

What particular types of translational order can in principle arise in a driven system? Of course, a disordered liquid state is possible (and may be the only stable phase in low dimensions). When translational order is present, it can occur at a variety of wavevectors \mathbf{Q} . For

weak disorder at low temperatures, it is natural to expect that a full reciprocal lattice of wavevectors characterizing a crystal should be important (i.e. have appreciable $C_{\mathbf{Q}}$). In two dimensions, for instance, the smallest of these would typically be arranged into a hexagon. If, as seems natural, and can be shown in some simple models, reflection symmetry perpendicular to the applied force is not broken, this can take one of two orientations, with a diagonal oriented either parallel or perpendicular to the force. Since the applied force breaks rotational symmetry, however, there is no reason for the correlations at all six points to be identical. Instead, if the system evolves continuously with increasing temperature or disorder, it is natural to expect that LRO will be lost first at some subset of these wavevectors. The surviving state has a lesser periodicity, with only a single line of Bragg peaks (symmetry requires that the other solid peaks disappear pairwise). It represents therefore a layered liquid or *smectic* state. This can be either a longitudinal smectic, with ordering wavevector parallel to the velocity, or a transverse smectic, with periodicity in the direction perpendicular to the velocity. We argue below that only the case of a transverse smectic shown in Figure 1(b) is stable, and indeed, that this is likely to be a more generic state than the true solid when the system is driven.

B. Hydrodynamics and elasticity

There are at least two analytical approaches to calculating $C_{\mathbf{Q}}(\mathbf{r}, t)$. One is to construct a density-functional or Landau-like theory for the order parameters $\rho_{\mathbf{Q}}$. For the non-equilibrium driven system considered here, this would be a set of stochastic partial differential equations. This has the advantage of allowing large amplitude fluctuations, and hence including dislocations in a natural way. The disadvantage of this approach is its intractability. It is often difficult to recover relatively simple properties in the ordered phase. A second approach is to assume a large degree of local order, so that the amplitude of the order parameters fluctuates very little. In this case, a phase-only or elastic approximation is natural, and only the ϕ fields remain in the description. This method has the disadvantage of excluding topological defects, which must be reintroduced by hand to complete the description, as has been successfully done for equilibrium systems, such as for example Kosterlitz and Thouless treatment of 2d superfluids and 2d melting²⁰. Determining the relevance or irrelevance of such defects upon the elastic description in disordered systems is a difficult and unsolved problem. If, however, the phase-only approximation predicts only small displacements in the ordered phase, it can be expected to be a self-consistent approximation out to a rather long length scale. If, by contrast, large distortions are found, the original assumption of order is inconsistent, and we have discovered an instability of the solid phase.

To determine the nature and stability of the possible ordered non-equilibrium phases, this paper focuses on the elastic approach. Assuming constant amplitude of the order parameters, $C_{\mathbf{Q}}$ can be written in terms of the displacement field correlation as

$$C_{\mathbf{Q}}(\mathbf{r}, t) = |\rho_{\mathbf{Q}, \mathbf{0}}|^2 \left[\langle e^{i\mathbf{Q} \cdot [\phi(\mathbf{r}, t) - \phi(\mathbf{0}, 0)]} \rangle \right]_{\text{ens.}}, \quad (1.8)$$

where we have pulled out the amplitude factor. If ϕ is a Gaussian random variable,

$$C_{\mathbf{Q}}(\mathbf{r}, t) = |\rho_{\mathbf{Q}, \mathbf{0}}|^2 \exp\{-Q_i Q_j B_{ij}(\mathbf{r}, t)\}, \quad (1.9)$$

where i and j denote Cartesian components and $B_{ij}(\mathbf{r})$ are the components of a mean-square displacement tensor,

$$B_{ij}(\mathbf{r}, t) = [\langle [\phi_i(\mathbf{r}, t) - \phi_i(\mathbf{0}, 0)][\phi_j(\mathbf{r}, t) - \phi_j(\mathbf{0}, 0)] \rangle]_{\text{ens.}}. \quad (1.10)$$

Generally, the displacements fluctuate in a non-Gaussian manner, so that Eq. 1.10 is not strictly correct. However, we expect its qualitative implications to hold. If $B_{ij}(\mathbf{r}, t)$ goes to a constant at long distances (times), then so does $C_{\mathbf{Q}}(\mathbf{r}, t)$. If $B_{ij}(\mathbf{r}, t)$ grows algebraically, then $C_{\mathbf{Q}}(\mathbf{r}, t)$ has stretched exponential form (though not necessarily with the naive stretching exponent), suggesting that in a physical system topological defects might proliferate and lead to short-range order, and if $B_{ij}(\mathbf{r}, t)$ grows logarithmically, then $C_{\mathbf{Q}}(\mathbf{r}, t)$ decays as or slower than a power-law.

To calculate $B_{ij}(\mathbf{r}, t)$, we employ the analog of hydrodynamic equations of motion. In general, the hydrodynamics of systems far from equilibrium is far more complex than its equilibrium counterpart. In particular, fluctuations about the nonequilibrium steady state do not satisfy a fluctuation-dissipation theorem and the external driving force breaks both the rotational and reflection (parallel to the force) invariance of the equilibrium system. As a result, the hydrodynamic equations contain many more parameters than in equilibrium. A general construction based only on symmetry constraints is thus not very useful, and a concrete derivation, which provides precise values for these parameters, is desirable. We perform such a derivation in Section II. Our first main result is the complete non-equilibrium hydrodynamic equation of motion for the driven lattice,

$$\begin{aligned} \gamma_{ij} \partial_t \phi_j &= A_{i\alpha j} \partial_\alpha \phi_i + B_{i\alpha\beta j} \partial_\alpha \partial_\beta \phi_j \\ &+ C_{i\alpha j\beta k} \partial_\alpha \phi_j \partial_\beta \phi_k + \tilde{F}_i[\mathbf{r}, \phi, t] + \eta_i(\mathbf{r}, t), \end{aligned} \quad (1.11)$$

where the coefficients A, B , and C are non-zero only when the number of subscripts taking values of axes perpendicular to the driving force is even. Explicit expressions for these are given in Section II. \tilde{F} and η represent quenched random and external ‘‘thermal’’ forces, respectively. Eq. 1.11 remedies the deficiencies of various ad-hoc equations of motion proposed in previous works²¹.

One noteworthy feature of Eq. 1.11 is the proliferation of gradient terms beyond the usual equilibrium elastic ones (contained in the B term). These represent convective effects and dependence of the substrate-lattice interaction upon the local deformation of the lattice. To properly account for them, it is crucial to treat the phonon modes near the zone boundary, not considered in previous calculations. Especially important are the A terms, which lead to propagating modes at low frequencies and wavevectors.

Another key feature is the random force $\tilde{F}_i[\mathbf{r}, \phi, t]$. It is distinguished from the equilibrium form in two ways. First, it contains non-trivial time-dependence, as can be seen from

$$\tilde{F}_i[\mathbf{r}, \phi, t] = \sum_{\mathbf{Q}} e^{i\mathbf{Q} \cdot (\mathbf{x} - \mathbf{v}t - \phi(\mathbf{r}, t))} F_i(\mathbf{r}), \quad (1.12)$$

where $F_i(\mathbf{r})$ is a time-*independent* quenched random variable, which we will refer to as a *static* pinning force (the exponential factor in Eq. 1.12 comes from the transformation from the moving to the laboratory frame). The terms with $\mathbf{Q} \cdot \mathbf{v} \neq 0$ therefore oscillate in the sliding solid. The second distinction is seen from the decomposition

$$F_i(\mathbf{r}) = F_i^{\text{eq}}(\mathbf{r}) + F_i^{\text{neq}}(\mathbf{r}). \quad (1.13)$$

The first term on the right hand side of Eq. 1.13 is the *equilibrium* component of the static pinning force and can be written as the gradient of a potential, as required by the fluctuation-dissipation theorem. Its correlations are approximately given by

$$[F_i^{\text{eq}}(\mathbf{r}) F_j^{\text{eq}}(\mathbf{r}')]_{\text{ens.}} = -\partial_i \partial_j \Gamma(\mathbf{r} - \mathbf{r}'), \quad (1.14)$$

where $\Gamma(\mathbf{r})$ is the correlator of the Gaussian random potential. The second term in Eq. 1.13 is the *nonequilibrium* part of the static pinning force, with correlator

$$[F_i^{\text{neq}}(\mathbf{r}) F_j^{\text{neq}}(\mathbf{r}')]_{\text{ens.}} = g_{ij} \delta(\mathbf{r} - \mathbf{r}'). \quad (1.15)$$

The variance g_{ij} of this static force is given in Eq. 2.51 and vanishes in the absence of external drive. A non-zero g_{ij} implies that F_i^{neq} is non-conservative, violating the fluctuation-dissipation theorem.

C. Analysis

A general analysis of Eq. 1.11 is quite difficult. In principle, the stability and behavior of the putative moving glass can be determined by an RG analysis of the full equations of motion (Eqs. 1.11), including *both* the KPZ nonlinearities ($C_{i\alpha j\beta k}$) and the random forces ($F_i(\mathbf{r}, \phi, t)$). Past experience with other nonequilibrium KPZ-like equations^{16,22} suggests that instabilities are quite ubiquitous in low dimensions. We expect such instabilities will occur also in this case, at least in two dimensions and quite possibly in three, and leave an analytical check of this hypothesis to younger researchers who

may have enough career years ahead of them to complete the calculation. Provided such an instability occurs, can any residual order survive in the driven state? Two physical realizations of partially ordered moving states have already been suggested: the longitudinal and the transverse smectic. A longitudinal smectic is equivalent to a conventional driven CDW, studied earlier by Chen et al.²² and by Balents and Fisher¹⁶. These authors concluded that this phase is unstable in two dimensions, but may exist at large velocities in three dimensions (although the role of dislocations and KPZ nonlinearities in three dimensions deserves further study).

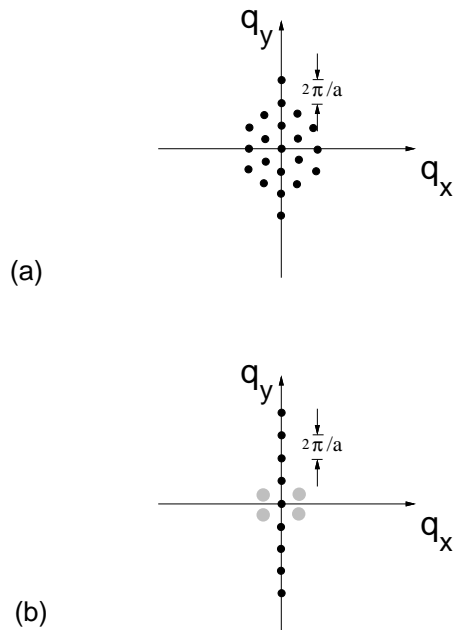


Fig.2:(a) The static structure factor for the moving glass sketched in Fig.1(a), with sharp peaks at all the reciprocal lattice vectors of a triangular lattice. The static structure factor of the driven transverse smectic is shown in (b). Sharp peaks (dark spots) only appear along the q_y axis; some remnant of short-range local triangular lattice order can appear in the form of weak and diffuse peaks at finite q_x (light spots).

The only possible ordered phase in $d = 2$ is thus a transverse smectic (discussed in the previous subsection and illustrated in Fig. 1(b)) with some degree of order at a periodic set of \mathbf{Q} perpendicular to the velocity. This is of course also a possibility in $d = 3$, regardless of the stability of the lattice. The marginal stability of the driven lattice in three dimensions allows for a dynamic phase transition between the driven smectic (at intermediate velocities) to a moving lattice (at high velocities). We illustrate the corresponding dynamic phase diagrams in Fig. 3.

The latter part of the paper is devoted to an analy-

sis of this possibility. In Section IV, we present the hydrodynamic equations of motion for the smectic. These include a simplified version of Eq. 1.11, supplemented by an additional one for the conserved particle density. Unlike in a vacancy/interstitial-free solid, this is not generally slaved to the smectic displacement, and constitutes a separate hydrodynamic mode.²³ This is the well-known permeation mode in smectic liquid crystals.

Even these equations are somewhat intractable, so in Sections V–VI we study the “toy model” in which the permeation mode is decoupled from the smectic displacement $\phi_y \equiv \phi$. This is best done using renormalization group (RG) techniques, which are controlled in two limits. At and near $d = 3$, the RG is controlled by a low-temperature fixed point, which is analyzed using a *functional* RG in Section V. The fixed-point temperature T^* increases with decreasing dimension until in $d = 2$, more conventional sine-Gordon RG techniques can be applied. Directly in three dimensions, there is a slow asymptotic approach to zero temperature.

From these RG calculations come several concrete predictions. In a three-dimensional smectic, the structure factor has power-law Bragg peaks along the axis in momentum space perpendicular to the velocity, as illustrated in Fig. 2(b). Because these peaks are entirely transverse, the smectic exhibits neither narrow-band-noise nor complete mode locking (although incomplete mode locking is of course possible for sizeable ac drives). The response to a force \mathbf{f}_\perp transverse to the mean direction of motion is a superposition of two effects. First, the permeation mode provides a non-vanishing linear component of the velocity $\mathbf{v}_\perp^{\text{perm.}} = \mu_{\text{perm.}} \mathbf{f}_\perp$. Secondly, the smectic responds in a non-linear manner, *resembling* a threshold at low temperatures but crossing over to linear response at very low forces for $T \neq 0$.

In two dimensions, the RG study of the elastic model also predicts only short-range *asymptotic transverse* translational correlations and quasi-long-range temporal correlations. These calculations actually indicate that the system is outside the regime of validity of the elastic approximation. We expect that in $d = 2$ an eventual instability of even the smectic state to unbinding of transverse dislocations may occur at larger length scales. Nevertheless, the RG results should hold up to this length, and, as in three dimensions, also predict superimposed linear and non-linear transverse velocity responses.

We conclude the Introduction with a summary of the remainder of the text. Section II describes the derivation of hydrodynamic equations of motion for the driven lattice, which we study perturbatively in Section III. Sections IV presents the equations of motion for the transverse smectic, which are analyzed using renormalization group techniques in Sections V and VI. The specific predictions of the RG for correlation and response functions are given in section VII. Section VIII summarizes our results, makes comparisons with other work, and gives a synopsis of remaining open questions and future applications of these ideas. Finally, six Appendices give

technical details unsuitable for the body of the paper.

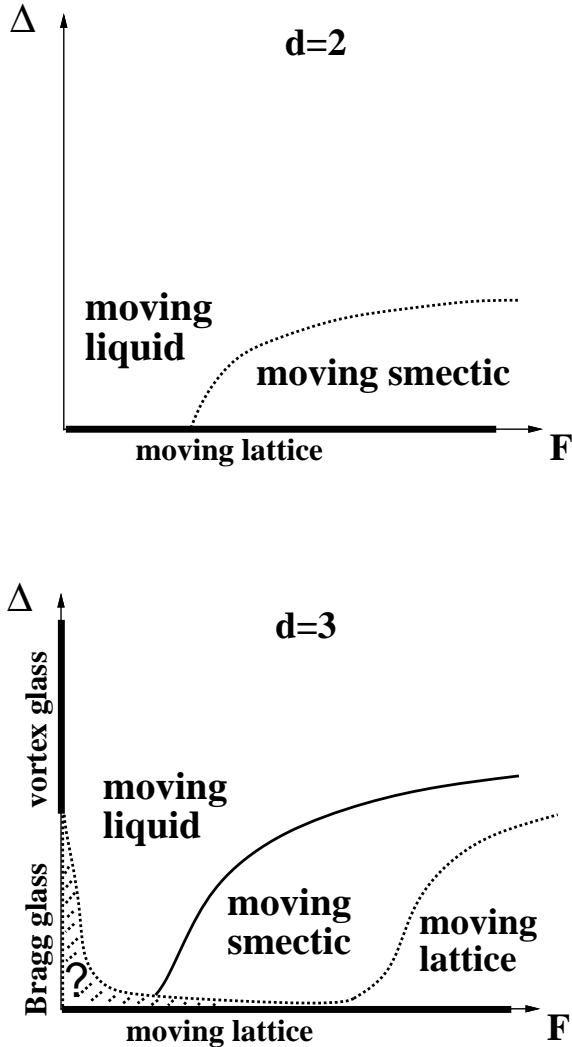


Fig.3: Schematic phase diagram for a finite temperature driven solid in (a) $d = 2$ and (b) $d = 3$ dimensions. In (a) we have used a dashed line as a boundary between the moving liquid and the transverse smectic to emphasize that the smectic might be unstable in 2d and therefore asymptotically indistinguishable from a moving liquid. In (b) we have similarly used a dashed boundary between the moving smectic and lattice, to emphasize that it is likely that the moving lattice is unstable even in 3d. In (b) the hatched “?” region indicates the interesting possibility of a moving Bragg glass in 3d, at low drives.

II. DERIVATION OF HYDRODYNAMICS

As discussed above, the goal of this paper is to study the non-equilibrium steady states that arise in driven periodic media. We will focus on the low-energy and long-wavelength properties of these steady states, in cases where these are uniquely defined. This should be the case provided ergodicity is achieved, either through a

small non-zero “thermal” noise or via intrinsic chaotic dynamics of the system in the absence of external noise. We will not discuss zero-temperature systems in which relatively simple global attractors exist with non-chaotic (e.g. periodic) dynamics.

In the limit of interest, then, we expect a sort of hydrodynamic description to hold. Such hydrodynamics is particularly successful in equilibrium because it is highly constrained. It must respect both detailed balance (to reduce to equilibrium statistical mechanics) and the symmetries of the system – in this case translations, rotations, and reflections. Out of equilibrium, a putative steady state equation of motion can be much more general. The fluctuations around the driven state need not satisfy any fluctuation–dissipation relation, and the external driving force breaks both rotational and reflection invariance.

For this reason, there are many more parameters in the hydrodynamic description. In the absence of further input, it is therefore considerably less powerful than equilibrium hydrodynamics. To make it useful, we need a means of calculating these parameters “microscopically”. This is possible for weak external potentials.

The calculation proceeds in two stages. Beginning with a microscopic lattice Hamiltonian, we first explicitly coarse-grain the equations of motion. This is a mode-elimination procedure in momentum space, reminiscent of a single step of rescaling in a renormalization group calculation. It is this stage which requires a weak external potential, since the elimination can only be performed perturbatively in these mode-coupling terms. The end result is an effective equation of motion for the phonon modes with momenta within a small sphere of radius $\Lambda \ll 2\pi/a$ in momentum space (a is the lattice spacing).

The second step is to transform the equation of motion from the moving frame (in which the conventional phonon coordinate or displacement field is defined) to the laboratory frame (more relevant for physical measurements). While technically much simpler than the previous mode-elimination step, it is possible only at this stage, since the transformation can be carried out only as a gradient expansion, with the small parameter $\Lambda a \ll 1$.

A. Formulation

The formulation of the problem begins with some microscopic Hamiltonian, describing particles connected by springs. The natural degrees of freedom are thus the displacements of these particles, whose gradients are expected to be small provided the potential acting on the particles is weak. The high-momentum modes being eliminated here therefore describe *small* relative displacements of nearby (say, neighboring) particles. Small though these are, they are crucial to the physics of the *sliding* solid.

Furthermore, the effects of the fixed external potential are expected to be most pronounced when it has strong periodic components commensurate with the driven lattice. This is intuitively reasonable, and indeed comes out of our more detailed calculations. This physics, however, comes precisely from these high-momentum modes at the scale of the lattice spacing. Even if the lattice is not pinned into a static configuration, these modes are the most strongly coupled to the static matrix, and thereby give rise to the seeds of interesting non-linear dynamics.

We consider a general model in which the constituents of the driven lattice may be ‘‘oriented manifolds’’, which are extended in some directions. This allows for systems including, for example, vortex lines in a three-dimensional superconductor. The conformation of a manifold with undisplaced equilibrium transverse position \mathbf{x} in a distorted lattice is described by the displacement vector $\mathbf{u}(\mathbf{x}, \mathbf{z})$, such that the true position is

$$\mathbf{X}(\mathbf{x}, \mathbf{z}) = \mathbf{x} + \mathbf{u}(\mathbf{x}, \mathbf{z}), \quad (2.1)$$

where \mathbf{u} and \mathbf{x} are d_t -component vectors, while \mathbf{z} has d_l components.

A natural microscopic Hamiltonian, valid in most cases, is

$$H = \sum_{\mathbf{xx}'} \int_{\mathbf{zz}'} V[\mathbf{x} - \mathbf{x}' + \mathbf{u}(\mathbf{x}, \mathbf{z}) - \mathbf{u}(\mathbf{x}', \mathbf{z}'), \mathbf{z} - \mathbf{z}'] + \sum_{\mathbf{x}} \int_{\mathbf{z}} U[\mathbf{x} + \mathbf{u}(\mathbf{x}, \mathbf{z}), \mathbf{z}]. \quad (2.2)$$

Here $V[\mathbf{x}, \mathbf{z}]$ is a two-body manifold-manifold interaction, and $U[\mathbf{x}, \mathbf{z}]$ is the external potential of the static medium.

Expanding the interaction potential in the usual way gives the elastic energy

$$H \approx \frac{1}{2} \sum_{\mathbf{x}, \mathbf{x}'} \int_{\mathbf{z}, \mathbf{z}'} K_{ij}(\mathbf{x} - \mathbf{x}', \mathbf{z} - \mathbf{z}') u^i(\mathbf{x}, \mathbf{z}) u^j(\mathbf{x}', \mathbf{z}') + \sum_{\mathbf{x}} \int_{\mathbf{z}} U[\mathbf{x} + \mathbf{u}(\mathbf{x}, \mathbf{z}), \mathbf{z}], \quad (2.3)$$

where the elastic matrix

$$K_{ij}(\mathbf{r}) = \sum_{\mathbf{x}'} \int_{\mathbf{z}'} \partial_i \partial_j V(\mathbf{r}') \delta_{\mathbf{x}, \mathbf{0}} \delta(\mathbf{z}) - \partial_i \partial_j V[\mathbf{r}]. \quad (2.4)$$

At this point, it pays to establish some notation. In the previous equation, we have already adopted a convention for indices. Latin indices alphabetically following i denote transverse (\mathbf{x}) coordinates, while a, b, \dots, h denote longitudinal (\mathbf{z}) ones. If an index may range over the full space, a Greek index α, β, \dots will be used. We will attempt to use \mathbf{x} and \mathbf{z} (with primes, etc.) exclusively as transverse and longitudinal coordinate vectors, with corresponding momenta \mathbf{q}_t and \mathbf{q}_z . These will often be assembled into vectors in the full d -dimensional space denoted $\mathbf{r} = (\mathbf{x}, \mathbf{z})$ and $\mathbf{q} = (\mathbf{q}_t, \mathbf{q}_z)$.

In Fourier space, using reflection symmetry, the elastic matrix is

$$K_{ij}(\mathbf{q}) \equiv \sum_{\mathbf{x}} \int_{\mathbf{z}} K_{ij}(\mathbf{r}) e^{i\mathbf{q}\cdot\mathbf{r}} = \sum_{\mathbf{x}} \int_{\mathbf{z}} \partial_i \partial_j V(\mathbf{r}) [1 - e^{i\mathbf{q}\cdot\mathbf{r}}]. \quad (2.5)$$

Overdamped relaxational dynamics is defined by

$$\gamma \partial_t u_i(\mathbf{r}, t) = -\frac{\delta H}{\delta u_i(\mathbf{r}, t)} + f_i, \quad (2.6)$$

where \mathbf{f} is an external force. This is equivalent to the equation of motion

$$\gamma \partial_t u_i(\mathbf{r}, t) = -\sum_{\mathbf{x}'} \int_{\mathbf{z}'} K_{ij}(\mathbf{r} - \mathbf{r}') u_j(\mathbf{r}', t) + \tilde{F}_i[\mathbf{x} + \mathbf{u}(\mathbf{r}, t) + \mathbf{v}t, \mathbf{z}], \quad (2.7)$$

where we have shifted \mathbf{u} to remove the external force, $\mathbf{v} = \mathbf{f}/\gamma$, and

$$\tilde{F}_i(\mathbf{r}) = -\partial_i U(\mathbf{r}). \quad (2.8)$$

In general, $\mathbf{v} = \mathbf{f}/\gamma$ is not the true steady-state velocity for a given force \mathbf{f} , since interactions with the impurities intermittently pin the lattice and thereby reduce the sliding speed. This finite renormalization (which is quantitatively small at large velocities) can, however, be neglected for the current purpose of studying the properties of the steady state. This is analogous to ignoring the mass renormalization in field theory (or T_c shift in critical phenomena). Of course from the experimental point of view, the velocity curve $v(f)$ (like the true T_c) is an important and measurable quantity.

B. Mode elimination

Having set up the dynamics, we are now in a position to perform the coarse-graining. We will use the Martin-Siggia-Rose (MSR) formalism²⁴, which allows the mode-elimination to be performed by functional integration. The object of interest in the MSR method is the statistical weight

$$W[\hat{\mathbf{u}}, \mathbf{u}] = e^{-\tilde{S}}, \quad (2.9)$$

where the action $\tilde{S} = S_0 + \tilde{S}_1$, with

$$S_0 = \sum_{\mathbf{x}} \int_{\mathbf{z}t} \hat{u}_i(\mathbf{r}, t) \left[\gamma \partial_t u_i(\mathbf{r}, t) + \sum_{\mathbf{x}'} \int_{\mathbf{z}'} K_{ij}(\mathbf{r} - \mathbf{r}') u_j(\mathbf{r}', t) \right] \quad (2.10)$$

and

$$\tilde{S}_1 = -\sum_{\mathbf{x}} \int_{\mathbf{z}t} \hat{u}_i(\mathbf{r}, t) \tilde{F}_i[\mathbf{x} + \mathbf{u}(\mathbf{r}, t) + \mathbf{v}t, \mathbf{z}]. \quad (2.11)$$

With this choice of weight, correlation functions are given by the functional integral

$$\langle u_i(\mathbf{r}, t) u_j(\mathbf{r}', t') \dots \rangle = \int [d\hat{\mathbf{u}}][d\mathbf{u}] u_i(\mathbf{r}, t) u_j(\mathbf{r}', t') \dots e^{-\tilde{S}}. \quad (2.12)$$

In this expression, the left-hand side should be interpreted as simply the product of the specified u_i evaluated along the solution of Eq. 2.7. The right-hand side is the result of functional integration over *all* functions $\mathbf{u}, \hat{\mathbf{u}}$. Because of this identity, we will freely employ angular brackets in either context. We note that this equality relies crucially on proper regularization of the equal-time correlators in the field theory. In particular, we will choose the causal convention

$$\langle u_i(\mathbf{r}, t) \hat{u}_j(\mathbf{r}', t) \rangle = 0. \quad (2.13)$$

Correlation functions involving the field $\hat{\mathbf{u}}$ have the physical interpretation of *response functions*, as can be seen by simply differentiating a correlation function with respect to an applied force. This convention then simply implies that there is no instantaneous (and hence discontinuous) response to a perturbation.

Within the MSR formalism, we can now readily carry out the mode elimination. The fields are first separated into two parts via

$$\begin{aligned} \mathbf{u}(\mathbf{r}, t) &= \mathbf{u}_<(\mathbf{r}, t) + \mathbf{u}_>(\mathbf{r}, t), \\ \hat{\mathbf{u}}(\mathbf{r}, t) &= \hat{\mathbf{u}}_<(\mathbf{r}, t) + \hat{\mathbf{u}}_>(\mathbf{r}, t), \end{aligned} \quad (2.14)$$

Here the slow and fast fields are defined by

$$\mathbf{u}_<(\mathbf{r}, t) \equiv \int_{|\mathbf{q}_t| < \Lambda} \int_{\mathbf{q}_z \omega} \mathbf{u}(\mathbf{q}, \omega) e^{i\mathbf{q} \cdot \mathbf{r} - i\omega t}, \quad (2.15)$$

$$\hat{\mathbf{u}}_<(\mathbf{r}, t) \equiv \int_{|\mathbf{q}_t| < \Lambda} \int_{\mathbf{q}_z \omega} \hat{\mathbf{u}}(\mathbf{q}, \omega) e^{-i\mathbf{q} \cdot \mathbf{r} + i\omega t}, \quad (2.16)$$

$$\mathbf{u}_>(\mathbf{r}, t) \equiv \int_{|\mathbf{q}_t| > \Lambda} \int_{\mathbf{q}_z \omega} \mathbf{u}(\mathbf{q}, \omega) e^{i\mathbf{q} \cdot \mathbf{r} - i\omega t}, \quad (2.17)$$

$$\hat{\mathbf{u}}_>(\mathbf{r}, t) \equiv \int_{|\mathbf{q}_t| > \Lambda} \int_{\mathbf{q}_z \omega} \hat{\mathbf{u}}(\mathbf{q}, \omega) e^{-i\mathbf{q} \cdot \mathbf{r} + i\omega t}, \quad (2.18)$$

where we have adopted opposite Fourier sign conventions for the displacement and response fields, and all momentum integrations are restricted to within the Brillouin zone. Correlation functions of the slow fields describe all the long-wavelength (i.e. hydrodynamic and elastic) behaviors of the system, and can be obtained from the effective weight

Inserting the above Fourier decomposition and evaluating the expectation value in Eq. 2.22 to second order in U gives corrections to S_0 which correspond to a renormalized equation of motion (see Appendix A). Since for small Λ , the remaining ‘‘slow’’ fields have small gradients, the corrected equation of motion may be written in the continuum approximation. It takes the general form

$$\tilde{\gamma}_{ij} \partial_t u_j = \tilde{A}_{i\alpha j} \partial_\alpha u_j + \tilde{B}_{i\alpha\beta j} \partial_\alpha \partial_\beta u_j + \tilde{C}_{i\alpha j\beta k} \partial_\alpha u_j \partial_\beta u_k + F_i^s[\mathbf{x} + \mathbf{u}(\mathbf{r}, t) + \mathbf{v}t, \mathbf{z}]. \quad (2.24)$$

$$W_{\text{eff}}[\mathbf{u}_<, \hat{\mathbf{u}}_<] = e^{-\tilde{S}_{\text{eff}}} = \int [d\mathbf{u}_>][d\hat{\mathbf{u}}_>] e^{-\tilde{S}}. \quad (2.19)$$

For simplicity, let us consider the model at zero temperature – i.e., in the absence of any external time-dependent noise. Because the potential couples the slow and fast modes, we will nevertheless obtain non-trivial renormalizations of the slow dynamics from the mode elimination.

We proceed by inserting the decomposition in Eq. 2.14 into the action \tilde{S} . Furthermore assuming that the potential U is weak, we may expand the exponential and perform the functional integrations over the fast modes order by order, re-exponentiating the resulting expressions, which then depend only upon the slow fields. The elastic part of the Hamiltonian is diagonal in momentum space,

$$S_0 = \int_{\mathbf{q}, \omega} \hat{u}_i(\mathbf{q}, \omega) \left[i\gamma\omega + K_{ij}(\mathbf{q}, \omega) \right] u_i(\mathbf{q}, \omega), \quad (2.20)$$

so that upon decomposition the slow and fast fields are decoupled in this term:

$$S_0[\mathbf{u}, \hat{\mathbf{u}}] = S_0[\mathbf{u}_<, \hat{\mathbf{u}}_<] + S_0[\mathbf{u}_>, \hat{\mathbf{u}}_>]. \quad (2.21)$$

The effective potential is therefore

$$\tilde{S}_{\text{eff}} = S_0[\mathbf{u}_<, \hat{\mathbf{u}}_<] - \ln \left\langle e^{-\tilde{S}_1} \right\rangle_{0>}, \quad (2.22)$$

where the angular bracket with the subscripts indicates integration over the fast modes ($>$) with the additional weight factor e^{-S_0} (0).

From this point onward, the treatment differs for the periodic and random potential, so we divide the remainder of this subsection into two parts. Each involves the conceptually straightforward perturbative calculation of the average in Eq. 2.22. This is somewhat tedious technically, so details will be given in Appendices A and B.

1. Periodic potential

We can specify a periodic potential by the Fourier decomposition,

$$U(\mathbf{x}) = \sum_{\mathbf{Q}} e^{i\mathbf{Q} \cdot \mathbf{x}} U_{\mathbf{Q}}. \quad (2.23)$$

Note that we have taken the potential to be independent of the continuous longitudinal coordinates \mathbf{z} .

Here the gradients may be understood either as lattice differences or as the corresponding expressions in momentum space. The coefficients are

$$\tilde{\gamma}_{ij} = \gamma\delta_{ij} - \sum_{\mathbf{Q}} Q_i Q_j Q_k Q_l |U_{\mathbf{Q}}|^2 i \frac{\partial}{\partial \omega} G_{kl}(\mathbf{Q}, \mathbf{v} \cdot \mathbf{Q}), \quad (2.25)$$

$$\tilde{A}_{i\alpha j} = \sum_{\mathbf{Q}} Q_i Q_j Q_k Q_l |U_{\mathbf{Q}}|^2 i \frac{\partial}{\partial q^\alpha} G_{kl}(\mathbf{Q}, \mathbf{v} \cdot \mathbf{Q}), \quad (2.26)$$

$$\tilde{B}_{i\alpha\beta j} = B_{i\alpha\beta j}^0 - \frac{1}{2} \sum_{\mathbf{Q}} Q_i Q_j Q_k Q_l |U_{\mathbf{Q}}|^2 \frac{\partial}{\partial q^\alpha} \frac{\partial}{\partial q^\beta} G_{kl}(\mathbf{Q}, \mathbf{v} \cdot \mathbf{Q}), \quad (2.27)$$

$$\tilde{C}_{i\alpha j\beta k} = \frac{i}{2} \sum_{\mathbf{Q}} Q_i Q_j Q_k Q_l Q_m |U_{\mathbf{Q}}|^2 \frac{\partial}{\partial q^\alpha} \frac{\partial}{\partial q^\beta} G_{lm}(\mathbf{Q}, \mathbf{v} \cdot \mathbf{Q}), \quad (2.28)$$

where

$$B_{i\alpha\beta j}^0 \equiv \frac{\partial}{\partial q^\alpha} \frac{\partial}{\partial q^\beta} K_{ij}(\mathbf{q} = \mathbf{0}) \quad (2.29)$$

is the bare linearized elastic matrix. To leading order, the force is unrenormalized,

$$F_i^s[\mathbf{r}] = \tilde{F}_i[\mathbf{r}]. \quad (2.30)$$

Here we have written the expressions in terms of the Fourier transform of the Green's function, $G(\mathbf{q}, \omega)$, which is defined in the extended zone scheme (i.e. it is periodically repeated in each translated copy of the fundamental Brillouin zone). It is

$$G(\mathbf{q}, \omega) = \left[i\omega I + K(\mathbf{q}) \right]^{-1} \theta(|q| - \Lambda). \quad (2.31)$$

The θ -function is present because only a partial mode elimination has been performed, so that the slow modes remain as dynamical variables in the coarse-grained theory. Note that these expressions *diverge* in the limit of zero velocity and identical periodicities, since in this case all the \mathbf{Q} are equivalent to the origin in momentum space.

2. Random potential

In the case of the random potential, we adopt the approach of disorder pre-averaging the MSR functional, thereby working directly with the variance of the random force. This is done purely for technical reasons: identical results are obtained by coarse-graining for a fixed realization of disorder and eventually averaging only physical quantities.

We take the simplest model for disorder, in which $U(\mathbf{r})$ is Gaussian distributed and statistically translationally invariant, with zero mean and second cumulant

$$[U(\mathbf{r})U(\mathbf{r}')]_{\text{ens.}} = \tilde{\Gamma}(\mathbf{r} - \mathbf{r}'). \quad (2.32)$$

The force-force correlator is thus

$$\left[\tilde{F}_i(\mathbf{r})\tilde{F}_j(\mathbf{r}') \right]_{\text{ens.}} = -\partial_i \partial_j \tilde{\Gamma}(\mathbf{r} - \mathbf{r}'). \quad (2.33)$$

The averaged statistical weight is readily computed:

$$[W[\hat{\mathbf{u}}, \mathbf{u}]]_{\text{ens.}} = e^{-S}, \quad (2.34)$$

with $S = S_0 + S_1$, and

$$S_1 = \frac{1}{2} \sum_{\mathbf{r}, \mathbf{r}'} \int_{\mathbf{z}\mathbf{z}'t t'} \hat{u}^i(\mathbf{r}, t) \hat{u}^j(\mathbf{r}', t') \times \partial_i \partial_j \tilde{\Gamma}[\mathbf{x} - \mathbf{x}' + \mathbf{u} - \mathbf{u}' + \mathbf{v}(t - t'), \mathbf{z} - \mathbf{z}']. \quad (2.35)$$

As before, we can coarse-grain by integrating out the fast ($>$) modes. The analog of Eq. 2.22 is

$$S_{\text{eff}} = S_0[\mathbf{u}_{<}, \hat{\mathbf{u}}_{<}] - \ln \langle e^{-S_1} \rangle_{>}. \quad (2.36)$$

In Appendix B, we compute this average to second order in S_1 . This again gives an equation of motion of the form, Eq. 2.24, but with

$$\tilde{A}_{i\alpha j} = - \sum_{\mathbf{x}} \int_{\mathbf{z}\mathbf{t}} \tilde{\Gamma}_{ijkl}[\mathbf{x} + \mathbf{v}t, \mathbf{z}] r^\alpha G_{kl}(\mathbf{r}, t), \quad (2.37)$$

$$\tilde{\gamma}_{ij} = \gamma\delta_{ij} + \sum_{\mathbf{x}} \int_{\mathbf{z}\mathbf{t}} \tilde{\Gamma}_{ijkl}[\mathbf{x} + \mathbf{v}t, \mathbf{z}] t G_{kl}(\mathbf{r}, t), \quad (2.38)$$

$$\tilde{B}_{i\alpha\beta j} = B_{i\alpha\beta j}^0 + \frac{1}{2} \sum_{\mathbf{x}} \int_{\mathbf{z}\mathbf{t}} \tilde{\Gamma}_{ijkl}[\mathbf{x} + \mathbf{v}t, \mathbf{z}] r^\alpha r^\beta G_{kl}(\mathbf{r}, t), \quad (2.39)$$

$$\tilde{C}_{i\alpha j\beta k}$$

$$= -\frac{1}{2} \sum_{\mathbf{x}} \int_{\mathbf{z}\mathbf{t}} \tilde{\Gamma}_{ijklm}[\mathbf{x} + \mathbf{v}\mathbf{t}, \mathbf{z}] r^\alpha r^\beta G_{lm}(\mathbf{r}, t), \quad (2.40)$$

where we have abbreviated $\tilde{\Gamma}_{ij\dots} \equiv \partial_i \partial_j \dots \tilde{\Gamma}$. Also useful are the corresponding expressions in momentum space,

$$\tilde{A}_{i\alpha j} = \int_{\mathbf{q}} q_i q_j q_k q_l \tilde{\Gamma}(\mathbf{q}) i \frac{\partial}{\partial q^\alpha} G_{kl}(\mathbf{q}, \mathbf{v} \cdot \mathbf{q}_t), \quad (2.41)$$

$$\tilde{\gamma}_{ij} = \gamma \delta_{ij} - \int_{\mathbf{q}} q_i q_j q_k q_l \tilde{\Gamma}(\mathbf{q}) i \frac{\partial}{\partial \omega} G_{kl}(\mathbf{q}, \mathbf{v} \cdot \mathbf{q}_t), \quad (2.42)$$

$$\begin{aligned} \tilde{B}_{i\alpha\beta j} &= B_{i\alpha\beta j}^0 \\ &- \frac{1}{2} \int_{\mathbf{q}} q_i q_j q_k q_l \tilde{\Gamma}(\mathbf{q}) \frac{\partial}{\partial q^\alpha} \frac{\partial}{\partial q^\beta} G_{kl}(\mathbf{q}, \mathbf{v} \cdot \mathbf{q}_t), \end{aligned} \quad (2.43)$$

$$\begin{aligned} \tilde{C}_{i\alpha j \beta k} &= \frac{i}{2} \int_{\mathbf{q}} q_i q_j q_k q_l q_m \tilde{\Gamma}(\mathbf{q}) \frac{\partial}{\partial q^\alpha} \frac{\partial}{\partial q^\beta} G_{kl}(\mathbf{q}, \mathbf{v} \cdot \mathbf{q}_t). \end{aligned} \quad (2.44)$$

A correction $\delta\Gamma_{ij}(\mathbf{r})$ is also obtained to the random force correlator. Because it is unpardonably ugly, we quote it only in Appendix B. It is, however, straightforward to show that the renormalized force-force correlator *cannot* be written in terms of a random potential correlator, i.e.

$$\Gamma_{ij}(\mathbf{r}) \equiv \tilde{\Gamma}_{ij}(\mathbf{r}) + \delta\Gamma_{ij}(\mathbf{r}) \neq -\partial_i \partial_j \Gamma(\mathbf{r}), \quad (2.45)$$

for any function $\Gamma(\mathbf{r})$. The difference from the equilibrium form can be accounted for by separating the force into two components:

$$F_i^s(\mathbf{r}) = F_i^{\text{eq.}}(\mathbf{r}) + F_i^{\text{neq.}}(\mathbf{r}), \quad (2.46)$$

where the equilibrium component $F_i^{\text{eq.}}$ is the gradient of a potential, so that

$$[F_i^{\text{eq.}}(\mathbf{r}) F_j^{\text{eq.}}(\mathbf{r}')]_{\text{ens.}} = -\partial_i \partial_j \Gamma^{\text{eq.}}(\mathbf{r} - \mathbf{r}'). \quad (2.47)$$

The other component we denote a (\mathbf{u} -independent) *static force*, with the correlator

$$[F_i^{\text{neq.}}(\mathbf{r}) F_j^{\text{neq.}}(\mathbf{r}')]_{\text{ens.}} = g_{ij} \delta(\mathbf{r} - \mathbf{r}'). \quad (2.48)$$

Clearly, since the correction term $\delta\Gamma_{ij}$ is small, we have

$$\Gamma^{\text{eq.}}(\mathbf{r}) \approx \tilde{\Gamma}(\mathbf{r}). \quad (2.49)$$

The static force variance is determined, however, entirely by the correction. It can be obtained by integrating

$$g_{ij} = \int_{\mathbf{r}} \delta\Gamma_{ij}(\mathbf{r}). \quad (2.50)$$

Substituting in Eq. (8.25) from Appendix B, all but the first and fourth terms are total derivatives and hence integrate to zero. After a certain amount of manipulation, we find

$$\begin{aligned} g_{ij} &= \int_{\mathbf{q}} q_i q_j q_k q_l q_m q_n |\tilde{\Gamma}(\mathbf{q})|^2 G_{km}(\mathbf{q}, \mathbf{q}_t \cdot \mathbf{v}) \\ &\times [G_{ln}(\mathbf{q}, -\mathbf{q}_t \cdot \mathbf{v}) - G_{ln}(\mathbf{q}, \mathbf{q}_t \cdot \mathbf{v})]. \end{aligned} \quad (2.51)$$

As expected, this expression vanishes for $\mathbf{v} = 0$, i.e. in order to satisfy the fluctuation-dissipation relation in equilibrium, the random force *must* be the derivative of a random potential.

C. Transformation to Laboratory Frame

Up to this point, we have worked with conventional displacement fields, defined in the crystal frame. This means that each particle in the lattice is labeled by its equilibrium position $\mathbf{r} = (\mathbf{x}, \mathbf{z})$, and that its actual transverse position is given by

$$\mathbf{X} = \mathbf{x} + \mathbf{v}\mathbf{t} + \mathbf{u}(\mathbf{x}, \mathbf{z}, t). \quad (2.52)$$

Most measurements in the systems of interest are, however, conducted in the laboratory frame. It is therefore advantageous to adopt a description based directly in this frame. To do so, we define a new field $\phi(\mathbf{r}, t)$ to be the displacement of the particle which is located at position \mathbf{r} at time t . Formally, this is described by the implicit equation

$$\phi_i(\mathbf{X}, \mathbf{z}, t) = \phi_i(\mathbf{x} + \mathbf{v}\mathbf{t} + \mathbf{u}(\mathbf{r}, t), \mathbf{z}, t) = \tilde{u}_i(\mathbf{r}, t). \quad (2.53)$$

Here, because \mathbf{u} is defined only at a discrete set of points $\{\mathbf{x}\}$, we have written the previous equation in terms of a smoothed continuum field $\tilde{\mathbf{u}}$ defined at all space points. For many purposes this distinction is insignificant, but it will return at one important juncture.

At this point the need for coarse-graining *prior* to the frame transformation is clear. Eq. (2.53) has an unambiguous solution defining ϕ only when $\partial_\alpha u_i \ll 1$. In this case, we can obtain the transformation rules for gradients by simply differentiating. They are

$$\partial_t \tilde{u}_i = (\delta_{ij} + \partial_j \phi_i) (\partial_t + \mathbf{v} \cdot \nabla) \phi_j + \dots, \quad (2.54)$$

$$\partial_\alpha \tilde{u}_i = \partial_\alpha \phi_i + \partial_\alpha \phi_j \partial_j \phi_i + \dots, \quad (2.55)$$

$$\partial_\alpha \partial_\beta \tilde{u}_i = \partial_\alpha \partial_\beta \phi_i + \dots \quad (2.56)$$

We are now in a position to transform the equation of motion, Eq. (2.24). The first step is change from \mathbf{u} field to the $\tilde{\mathbf{u}}$ field. This is done by multiplying by a smoothing function and summing, using

$$\tilde{\mathbf{u}}(\mathbf{x}, \mathbf{z}, t) = a^{dt} \sum_{\mathbf{x}'} D(\mathbf{x} - \mathbf{x}') \mathbf{u}(\mathbf{x}', \mathbf{z}, t), \quad (2.57)$$

where $D(\mathbf{x})$ is a delta-like function smoothed-out on the scale of the lattice spacing a , i.e. $\int_{\mathbf{x}'} D(\mathbf{x}' - \mathbf{x}) f(\mathbf{x}') = f(\mathbf{x})$ and $D(\mathbf{0}) = 1$.

Carrying out this procedure, the gradient and time-derivative terms are essentially unchanged, with $\mathbf{u} \rightarrow \tilde{\mathbf{u}}$ to a good approximation. The discreteness of the lattice sum is important for the force term, however. It becomes

$$\begin{aligned}
& a^{dt} \sum_{\mathbf{x}'} D(\mathbf{x} - \mathbf{x}') F_i^s[\mathbf{x}' + \mathbf{v}t + \mathbf{u}(\mathbf{x}', \mathbf{z}, t), z] \\
&= \sum_{\mathbf{Q}} \int_{\mathbf{x}'} e^{i\mathbf{Q}\cdot\mathbf{x}'} D(\mathbf{x} - \mathbf{x}') F_i^s[\mathbf{x}' + \mathbf{v}t + \mathbf{u}(\mathbf{x}', \mathbf{z}, t), z] \\
&\approx \sum_{\mathbf{Q}} e^{i\mathbf{Q}\cdot\mathbf{x}} F_i^s[\mathbf{x} + \mathbf{v}t + \tilde{\mathbf{u}}(\mathbf{x}, \mathbf{z}, t), z]. \quad (2.58)
\end{aligned}$$

Making the final transformation from $\tilde{\mathbf{u}}$ to ϕ , the force term becomes

$$F_i[\mathbf{X}, \mathbf{z}; \phi, t] = \sum_{\mathbf{Q}} e^{i\mathbf{Q}\cdot(\mathbf{X} - \mathbf{v}t - \phi(\mathbf{X}, \mathbf{z}, t))} F_i^s[\mathbf{X}, \mathbf{z}]. \quad (2.59)$$

Putting this together with the gradient transformations, Eq. (2.24) becomes

$$\begin{aligned}
\gamma_{ij} \partial_t \phi_j(\mathbf{X}, \mathbf{z}, t) &= A_{i\alpha j} \partial_\alpha \phi_j + B_{i\alpha\beta j} \partial_\alpha \partial_\beta \phi_j \\
&+ C_{i\alpha j \beta k} \partial_\alpha \phi_j \partial_\beta \phi_k + F_i[\mathbf{X}, \mathbf{z}; \phi, t]. \quad (2.60)
\end{aligned}$$

At this point, we can regard \mathbf{X} as a dummy variable and treat Eq. 2.60 as simply a continuum partial differential equation. The transformed gradient coefficients are

$$\gamma_{ij} = \tilde{\gamma}_{ij}, \quad (2.61)$$

$$A_{i\alpha j} = \tilde{A}_{i\alpha j} - v^\alpha \tilde{\gamma}_{ij}, \quad (2.62)$$

$$B_{i\alpha\beta j} = \tilde{B}_{i\alpha\beta j}, \quad (2.63)$$

$$C_{i\alpha j \beta k} = \tilde{C}_{i\alpha j \beta k} - \tilde{\gamma}_{ij} \delta_{\alpha k} v^\beta + \tilde{A}_{i\alpha k} \delta_{j\beta}. \quad (2.64)$$

III. LINEARIZED THEORY

In the previous section we derived the proper form of the hydrodynamic equations, Eqs. 1.11, describing the low-energy, long-wavelength properties of a periodic medium driven through either a periodic or quenched random potential. These equations are distinct from their equilibrium counterpart in three respects. First, in addition to the well-known convective term arising when transforming from the crystal to the laboratory frame, the coupling of the driven system to the external potential yields several other terms linear in the gradients of the displacement field; these are collectively described by non-zero coefficients $A_{i\alpha j}$. Second, the equations contain nonequilibrium KPZ-type nonlinearities that can be thought of as corrections to linear elasticity. Third, in the random case there is a *nonequilibrium* component of the static (i.e., ϕ -independent) pinning force. This force is a genuine nonequilibrium effect, as it cannot be represented as the gradient of a potential and vanishes in the absence of external drive.

The remainder of this paper focuses on the random case, which is of more immediate experimental relevance. Although, as discussed in the Introduction, a general analysis of Eqs. 1.11, is beyond the scope of this paper, we take this section to discuss the weak-disorder limit, in

which only the leading (in $\tilde{\Gamma}$) contributions to each term are kept. In this approximation the damping $\gamma_{ij} = \gamma \delta_{ij}$ is diagonal, and the leading linear gradient term is simply the convective derivative, $A_{i\alpha j} \approx -\gamma \delta_{ij} v^\alpha$. Similarly keeping only the bare elastic matrix, we obtain the simplified set of nonequilibrium elastic-hydrodynamic equations for the driven lattice,

$$\begin{aligned}
\gamma(\partial_t + \mathbf{v} \cdot \nabla_t) \phi_i &= B_{i\alpha\beta j}^0 \partial_\alpha \partial_\beta \phi_j \\
&+ F_i[\mathbf{r}, \phi, t] + \eta_i(\mathbf{r}, t), \quad (3.1)
\end{aligned}$$

where B^0 is the usual elastic matrix, η_i represents ‘‘thermal’’ noise (which as we will see in Sec.V can appear even at zero physical temperature), and the random force F_i is given by Eqs.1.12 and 1.13 and contains all nonlinearities. Note that we have kept both the equilibrium and nonequilibrium components contained in F_i , since, although these are of differing order in $\tilde{\Gamma}$, they cannot be regarded as corrections to any zeroth order terms. One important ingredient which has been left out of Eq. 3.1 is the set of KPZ non-linearities ($C_{i\alpha j \beta k}$ terms). While these coefficients are probably small, they may very well modify the asymptotic long-distance behavior. Based on previous work on somewhat simpler (but instructive!) models,^{22,25} we expect that these effects will only *increase* the distortions of the moving lattice, and furthermore, that the increase in displacements will be most pronounced in the longitudinal direction.

We therefore proceed with the analysis of Eq. 3.1, expecting that our results *underestimate* the roughness in the moving lattice, and therefore provide a necessary (but not sufficient) condition for its stability. To proceed, we note that, as pointed out by Giamarchi and Le Doussal²⁶, many of the terms in the random force, Eq. 2.59, are oscillatory in time. Such oscillatory terms average out at large sliding velocities, when the ‘‘washboard’’ frequencies $\omega_{\mathbf{Q}} = \mathbf{Q} \cdot \mathbf{v}$ are large. Even when they are not large, they generate only finite renormalizations of the other parameters in the model. We therefore drop this oscillatory part of \mathbf{F} , keeping only the Fourier components of the force orthogonal to the mean velocity,

$$F_i[\mathbf{r}, \phi] \rightarrow \sum_{\mathbf{Q}\cdot\mathbf{v}=0} e^{i\mathbf{Q}\cdot(\mathbf{x}-\phi)} F_i^s(\mathbf{r}), \quad (3.2)$$

where we have dropped the explicit time dependence t inside F_i , since it has disappeared in this approximation. Recall that the ϕ -independent force $F_i^s(\mathbf{r})$ contains both equilibrium and nonequilibrium contributions, with the corresponding correlators given in Eqs. 2.46–2.51.

In this section we will further simplify the problem and linearize the nonequilibrium hydrodynamic equations (3.1). We will then discuss the predictions of the linearized theory for the decay of translational and temporal order in the driven lattice.

We recall that we have used the labels longitudinal (l) and transverse (t) to denote the directions along the oriented manifolds and transverse to them, respectively. The d -dimensional position vector was then written in

terms of a transverse coordinate \mathbf{x} and a longitudinal coordinate vector \mathbf{z} as $\mathbf{r} = (\mathbf{x}, \mathbf{z})$. We now choose the x direction (one of the d_t \mathbf{x} coordinates) along the direction of the driving force ($\mathbf{v} = v\hat{\mathbf{x}}$) and denote by \mathbf{r}_\perp the $d-1$ directions transverse to the external drive ($d = d_l + d_t$). These $d-1$ directions can be further broken up into components transverse and longitudinal to the oriented manifolds, $\mathbf{r}_\perp = (\mathbf{y}, \mathbf{z})$, with \mathbf{y} a d_t-1 -dimensional vectors denoting the components of the transverse displacement that are also perpendicular to the external driving force. The d_t -dimensional transverse coordinate space is then described by a 1-dimensional coordinate x (not to be confused with \mathbf{x}) and \mathbf{y} , respectively parallel and perpendicular to the direction of motion, with $\mathbf{x} = (x, \mathbf{y})$. The d -dimensional position vector is written as $\mathbf{r} = (\mathbf{x}, \mathbf{z}) = (x, \mathbf{y}, \mathbf{z})$. We will also use the labels parallel (\parallel) and perpendicular (\perp) to denote the directions parallel and perpendicular to the external drive. For concreteness we specialize to a lattice where the d_l directions along the manifolds that compose the lattice are isotropic and the longitudinal elastic properties are described by a single elastic constant, denoted by c_{44} . We assume the d_t -dimensional lattice is described by isotropic elasticity, with two elastic constants, a compressional modulus c_{11} and a shear modulus c_{66} . Our model hydrodynamic equations for the driven lattice are then given by,

$$\gamma\left(\partial_t + v\partial_x\right)\phi_i = [c_{66}\nabla_t^2 + c_{44}\nabla_z^2]\phi_i \quad (3.3)$$

$$+ c_{11}\partial_i\nabla_t \cdot \phi + F_i[\mathbf{r}, \phi],$$

where for the purposes of this section we have dropped thermal noise, thereby ignoring the *subdominant* thermal fluctuations. These equations describe the important physical case of the lattice of magnetic flux lines in a three-dimensional superconductors ($d_l = 1$, $d_t = 2$). For $d_l = 0$ and $d_t = 2$ the equations describe the elastic properties of driven vortex lattices in superconducting films, driven magnetic bubble arrays, or driven Wigner crystals.

The displacement field can be split into components parallel and perpendicular to the mean motion, $\phi = (\phi_x, \phi_y)$. The transverse displacement ϕ_y is a $(d_t - 1)$ -dimensional vector. The pinning force is then seen to be independent of ϕ_x :

$$F_i[\mathbf{r}, \phi_y] = \sum_{\mathbf{Q}\cdot\mathbf{v}=0} e^{i\mathbf{Q}\cdot(\mathbf{x}-\phi_y)} \times [F_i^{\text{eq}}(\mathbf{r}) + F_i^{\text{neq}}(\mathbf{r})], \quad (3.4)$$

The independence of the static pinning force on ϕ_x is a consequence of the precise time-translational invariance of the system. This requires that the equation of motion be unchanged upon transforming $t \rightarrow t + \tau$, $\phi_x \rightarrow \phi_x + v\tau$. As argued above, all explicitly time dependent terms are irrelevant at low frequencies, thereby implying independence of ϕ_x in the same limit. Eq. 3.3 is thus *linear* in the longitudinal displacement ϕ_x , which can therefore be treated exactly.

The only remaining nonlinearity in the equation of motion, Eq.3.3 is in ϕ_y , entering through the random force $F_i[\mathbf{r}, \phi_y]$, which, in this section, we treat perturbatively. We stress that the validity of this perturbative calculation requires the displacements ϕ_y transverse to the mean motion to be small, but places no constraints on the size of the displacements along the direction of motion. The perturbation theory in $F_i[\mathbf{r}, \phi_y]$ thus gives a complete description of the behavior of positional correlations in the x direction out to asymptotic length scales for the model of Eq. 3.1. In contrast, the predictions of the perturbation theory for the correlations of the *transverse* displacement ϕ_y presented below are only valid in the Larkin regime; RG methods of Sections V,VI must be used to go beyond the Larkin length scale.

To lowest order in the random force, we simply neglect the displacement field ϕ_y in $F_i[\mathbf{r}, \phi_y]$, Eq. (3.4). The Fourier components of the pinning force are then given by

$$F_i^{(0)}(\mathbf{q}) = \sum_{\mathbf{Q}\cdot\mathbf{v}=0} F_i^s(\mathbf{q}_t + \mathbf{Q}, \mathbf{q}_z), \quad (3.5)$$

with correlations

$$[F_i^{(0)}(\mathbf{q})F_j^{(0)}(\mathbf{q}')]_{\text{ens.}} = (2\pi)^{d_l}\delta^{(d_l)}(\mathbf{q}_z + \mathbf{q}'_z)(2\pi)^{d_t}\delta^{(d_t)}(\mathbf{q}_t + \mathbf{q}'_t)\Delta_{ij}, \quad (3.6)$$

and

$$\Delta_{ij} = g_{ij} + \sum_{\mathbf{Q}\cdot\mathbf{v}=0} Q_i Q_j \tilde{\Gamma}(Q)$$

$$= (\Delta + g_0)(\delta_{ij} - \delta_{ix}\delta_{jx}) + g_1\delta_{ix}\delta_{jx}. \quad (3.7)$$

The disorder strength Δ is the variance of the equilibrium part of the static pinning force,

$$\Delta = \frac{1}{d_t} \sum_{\mathbf{Q}\cdot\mathbf{v}=0} Q^2 \tilde{\Gamma}(Q). \quad (3.8)$$

The coefficients g_0 and g_1 are determined by the correlations g_{ij} of the nonequilibrium part of the static pinning force, according to

$$g_{ij} = g_0(\delta_{ij} - \delta_{ix}\delta_{jx}) + g_1\delta_{ix}\delta_{jx}. \quad (3.9)$$

They are evaluated in Appendix C, where it is shown that for large sliding velocities and short-ranged pinning potential ($\xi \ll a$, with ξ the range of the pinning potential),

$$g_{0,1} \sim \frac{\Delta^2}{v^{(2d_t-d_l)/2}}. \quad (3.10)$$

The components of the mean square displacement tensor are given by

$$B_{ij}(\mathbf{r}) = 2 \int_{\mathbf{q}} \int_{\omega} [1 - \cos(\mathbf{q}\cdot\mathbf{r})] \times [\langle \phi_i(\mathbf{q}, \omega) \rangle \langle \phi_j^*(\mathbf{q}, \omega) \rangle]_{\text{ens.}} \quad (3.11)$$

The correlation functions of the displacement field are easily calculated in Fourier space. The linear equation of motion for the disorder induced displacement yields

$$\langle \phi_i(\mathbf{q}, \omega) \rangle = \left[G_L(\mathbf{q}, \omega) P_{ij}^L(\mathbf{q}_t) + G_T(\mathbf{q}, \omega) P_{ij}^T(\mathbf{q}_t) \right] \times 2\pi\delta(\omega) F_i^{(0)}(\mathbf{q}), \quad (3.12)$$

where $G_L(\mathbf{q}, \omega)$ and $G_T(\mathbf{q}, \omega)$ are the longitudinal and transverse elastic propagators, respectively,

$$G_L(\mathbf{q}, \omega) = \frac{1}{i\gamma(\omega - vq_x) + (c_{11} + c_{66})q_t^2 + c_{44}q_z^2}, \quad (3.13)$$

$$G_T(\mathbf{q}, \omega) = \frac{1}{i\gamma(\omega - vq_x) + c_{66}q_t^2 + c_{44}q_z^2}, \quad (3.14)$$

and $P_{ij}^L(\mathbf{q}_t) = \hat{q}_{ti}\hat{q}_{tj}$ and $P_{ij}^T(\mathbf{q}_t) = \delta_{ij} - \hat{q}_{ti}\hat{q}_{tj}$ are the familiar longitudinal and transverse projection operators, with $\hat{\mathbf{q}}_t = \mathbf{q}_t/q_t$. The correlation functions of the displacement field are given by

$$\begin{aligned} [|\langle \phi_x(\mathbf{q}, \omega) \rangle|^2]_{\text{ens.}} &= 2\pi\delta(\omega) \left[\frac{g_1}{(\gamma v q_x)^2 + [c_{66}q_t^2 + c_{44}q_z^2]^2} \right. \\ &\quad \left. + \mathcal{O}\left(\Delta \frac{q_x^2}{q_y^2} |G_L|^2\right) \right] \delta(0), \end{aligned} \quad (3.15)$$

$$\begin{aligned} [|\langle \phi_y(\mathbf{q}, \omega) \rangle|^2]_{\text{ens.}} &= 2\pi\delta(\omega) \left[\frac{\Delta + g_0}{(\gamma v q_x)^2 + [(c_{11} + c_{66})q_t^2 + c_{44}q_z^2]^2} \right. \\ &\quad \left. + \mathcal{O}\left(g_1 \frac{q_x^2}{q_y^2} |G_T|^2\right) \right] \delta(0), \end{aligned} \quad (3.16)$$

where $\delta(0) \equiv (2\pi)^{d+1} \delta(\omega = 0) \delta^d(\mathbf{q} = \mathbf{0})$. Because the wavevector integral in Eq. 3.11 is dominated by $q_x \sim (c q_y^2 / \gamma v)$, terms containing $(q_x^2 / q_y^2) |G_T|^2$ or $(q_x^2 / q_y^2) |G_L|^2$ yield less divergent (generally bounded) contributions to the fluctuations compared to the terms without this angular factor. The behavior in real space is displayed here for the case $d_t = 0$, relevant to vortex lattices in thin superconducting films. The corresponding expressions for $d_t = 1$, describing flux-line arrays in three-dimensional superconductors, are given in Appendix D. For $d_t = 0$ we obtain,

$$B_{xx}(x, \mathbf{y}) \sim g_1 \frac{|y|^{3-d_t}}{\gamma v c_{66}} \mathcal{F}_0^{(d_t)} \left(\frac{|x| c_{66}}{\gamma v y^2} \right), \quad (3.17)$$

$$\begin{aligned} B_{\perp\perp}(x, \mathbf{y}) &\sim (\Delta + g_0) \frac{|y|^{3-d_t}}{\gamma v (c_{11} + c_{66})} \\ &\quad \times \mathcal{F}_0^{(d_t)} \left(\frac{|x| (c_{11} + c_{66})}{\gamma v y^2} \right), \end{aligned} \quad (3.18)$$

where

$$\mathcal{F}_0^{(d_t)}(s) = \int \frac{d^{d_t-1} \mathbf{u}}{(2\pi)^{d_t-1}} \frac{1}{u^2} \left[1 - \cos(\hat{\mathbf{y}} \cdot \mathbf{u}) e^{-su^2} \right]. \quad (3.19)$$

The asymptotic behavior of the scaling function is given by $\mathcal{F}_0^{(d_t)}(0) = \text{constant}$ and $\mathcal{F}_0^{(d_t)}(s) \sim s^{(3-d_t)/2}$ for $s \gg 1$.

Fluctuations in the direction of the driving force are dominated by the *nonequilibrium* part of the random drag and by *shear* modes. As discussed earlier, the corresponding power-law scaling of ϕ_x holds out to arbitrary length scales. Since

$$B_{xx} \sim |y|^{3-d_t}, \quad \text{for } y^2 \gg (c_{66}/\gamma v)|x|, \quad (3.20)$$

$$B_{xx} \sim |x|^{(3-d_t)/2}, \quad \text{for } y^2 \ll (c_{66}/\gamma v)|x|, \quad (3.21)$$

longitudinal density correlations are short-ranged in $d_t < 3$, with a stretched-exponential decay. Since, as argued above, this behavior will persist even once the full nonlinear form for $F_i[\mathbf{r}, \phi_{\mathbf{y}}]$ is taken into account, the validity of the elastic model itself is in doubt. In particular, for the physical case of $d_t = 2$, the spatial correlations are in fact exponentially decaying, and it is natural to expect that this drives the unbinding of dislocations with Burger's vectors parallel to the drive. If this is the case, both translational and temporal order for $\mathbf{Q} \cdot \mathbf{v} \neq 0$ are short range in the driven steady state.

In contrast, both the equilibrium and nonequilibrium parts of the static pinning force contribute to fluctuations in the transverse direction, which are controlled by the *compressional* modes of the system. For large sliding velocity or weak disorder and intermediate length scales, the equilibrium part of the static pinning force will dominate as $g_0 \sim (\Delta/v)^2 \ll \Delta$ in this limit. The perturbation theory employed here breaks down, however, at lengths larger than the Larkin lengths, R_c^y and R_c^x defined by $B_{\perp\perp}(R_c^x, R_c^x) \sim \xi^2$, where ξ is the range of the pinning potential. The Larkin volume is defined for deformations of the lattice in the transverse direction ($\phi_y \sim \xi$) and it is anisotropic, with

$$R_c^y \sim \left(\frac{\xi^2 v c_{11}}{\Delta} \right)^{1/(3-d_t)} \quad (3.22)$$

$$R_c^x \sim v (R_c^y)^2 / c_{11}. \quad (3.23)$$

It is elongated in the longitudinal direction at large sliding velocities. Longitudinal displacements (ϕ_x) grow without bound on *all* length scales in $d_t < 3$ and a Larkin domain cannot be defined in this case. As usual, the nonlinearities in the static pinning force must be incorporated non-perturbatively to describe the asymptotic decay of the correlations beyond the Larkin length scales. We will consider this problem in more detail in the following sections. A natural suspicion is, however, that at asymptotically large distances at a finite temperature in two dimensions, the nonequilibrium random drag, g_0 , will dominate, destroying also the transverse periodicity.

We stress that longitudinal fluctuations - that grow without bound - are induced by shear modes of the lattice. This is consistent with the intuition that shear

modes (rather than compressional ones) play the dominant role in melting a crystal. In contrast, transverse fluctuations are controlled by compressional modes. Compressional modes are present in both solids and liquids and are generally not expected to generate the unbounded strains needed to yield dislocation unbinding.

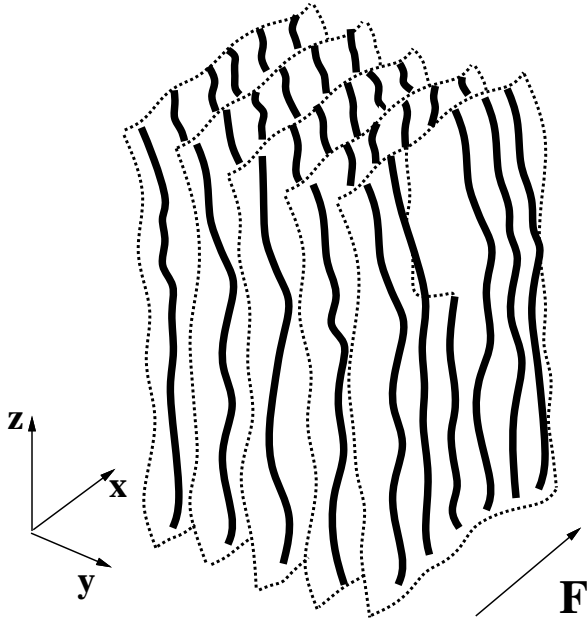


Fig.4:Schematic illustration of a driven line smectic, i.e. smectic in three dimensions, with $d_t = 2$, $d_l = 1$.

IV. DRIVEN SMECTIC DYNAMICS

It was shown in the previous section that disorder-induced fluctuations parallel to the direction of the mean motion grow algebraically in $d_t < 3$. This algebraic growth of fluctuations yields short-range positional correlations along the direction of the external drive, and it is our belief that this implies the breakdown of the elastic description along the direction of motion (x). While we have not considered explicitly the role of dislocations here, analysis of similar equations of motion *including non-linearities*^{22,25} suggests that this should occur (for $d_t \leq 2$) via the unbinding of dislocations with Burgers vectors *parallel* to the driving force²⁷. This mechanism should convert the longitudinal translation and temporal correlations to the exponential (or stretched exponential) form typical of a liquid. This is also in agreement with real space images of driven two-dimensional vortex lattices ($d_t = 2$, $d_l = 0$) obtained via numerical simulations.²⁸ Therefore for $d_t = 2$ and $d_l = 0$ the driven lattice can only retain periodicity at reciprocal lattice vectors *transverse* to the direction of motion. At best, therefore, it consists of a stack of one-dimensional liquid-like channels, sliding parallel to the direction of motion¹⁹ and has the spatial symmetry of a smectic li-

quid crystal. It is, however, important to stress that in real, *equilibrium* smectic liquid crystals the underlying rotational symmetry (which is broken *spontaneously*) enforces soft *Laplacian* in-layer elasticity.²⁹ In contrast, the rotational symmetry of the nonequilibrium “driven smectic” discussed here is *explicitly* broken by the external drive. These systems are therefore characterized by conventional *gradient* elasticity.

For the case $d_t = 2$ and $d_l = 1$, corresponding to magnetic flux-line arrays in three-dimensional superconductors, the driven crystal is potentially stable as translational correlations decay logarithmically also in the direction of the applied force. We recall, however, that the results obtained here by dropping the KPZ terms are expected to strongly underestimate the growth of longitudinal fluctuations of a moving *crystal*. Since in $d = 3$ the transverse line smectic state is equally stable it is possible to have a phase transition between the transverse smectic (expected at intermediate velocities) and a moving glass (stabilized at high velocities). The nonequilibrium smectic state (illustrated in Fig. 4) then consists of liquid-like sheets of flux lines lying in planes parallel to the zx plane. These sheets are periodically spaced in the y direction, normal to the external drive. Within each sheet, however, there is no positional order of the flux lines and the correlations are liquid-like.

In a smectic liquid crystal the density field ρ becomes an independent variable, as it is no longer slaved to the displacement field. The density is a conserved quantity and therefore a density fluctuation relaxes at a rate that vanishes in the long-wavelength limit, i.e., it is a hydrodynamic variable. In addition, the system still has broken translational symmetry in the direction perpendicular to that of the mean motion. *Both* the Goldstone modes of the broken translation symmetry (the displacement $\phi_{\mathbf{y}}$) and the conserved density field (ρ) must be retained in a hydrodynamic description. In the remainder of this section we consider the case $d_t = 2$ and $d_l = 0$ of a two-dimensional lattice driven over a disordered substrate. The hydrodynamic variables of the driven smectic are then a conserved density field ρ and the one-dimensional displacement vector $\phi_{\perp}(\mathbf{x}, z) \rightarrow \phi(\mathbf{x}, z)$, describing displacements of the layers in the directions normal to the external drive and to the layers themselves. As we are only interested in overdamped systems here, the momentum and energy are not conserved and therefore need not be included explicitly in our hydrodynamic description.

The continuum hydrodynamic free energy for the overdamped smectic is given by

$$\mathcal{F}_s = \frac{1}{2} \int_{\mathbf{x}} \left\{ c_L \left(\frac{\delta \rho}{\rho_0} \right)^2 + c_{11}^y (\partial_y \phi)^2 + K_1 (\partial_x \phi)^2 + 2K_2 (\partial_y \phi) \frac{\delta \rho}{\rho_0} \right\}, \quad (4.1)$$

where $\delta \rho = \rho - \rho_0$, with ρ_0 the equilibrium density. Here c_L is the smectic bulk modulus, c_{11}^y the in-layer compressibility and K_1 the layer bending stiffness. The cou-

pling constant K_2 also has dimensions of an elastic constant. The hydrodynamic equations of the driven smectic contain additional nonequilibrium terms, as compared to their equilibrium counterpart. The nonequilibrium terms can be constructed by preserving the invariance under inversions about the direction of the external drive ($y \rightarrow -y$, $\phi \rightarrow -\phi$) and the fact that physical properties are invariant under the “phase shift” $\phi \rightarrow \phi + a$.

Density conservation requires that ρ satisfies a continuity equation,

$$\partial_t \delta \rho + \nabla \cdot \mathbf{j} = 0, \quad (4.2)$$

where \mathbf{j} is the number current density. The equation for the layer displacement is given by

$$(\partial_t + v \partial_x) \phi = \frac{j_y}{\rho} - \frac{\Gamma_0}{\rho_0} \left(\frac{\delta \mathcal{F}_s}{\delta \phi} - F_y[\mathbf{x}, \phi] \right), \quad (4.3)$$

with Γ_0 a kinetic coefficient and F_y the y -component of the non-oscillating part of the pinning force given in Eq. 3.2. We neglect here the oscillatory contributions to the pinning force that only give small corrections to the non-oscillatory part. We also neglect other contributions to the pinning force that couple to the density. These would be important for a full systematic RG treatment, which we do not attempt here. A discussion of more general equations for the driven smectic that incorporate these terms is left for future work.

To close the equations, a constitutive relation for the current flux \mathbf{j} is needed. This is given by

$$j_x = v \delta \rho + v_1 \delta \rho + \rho_0 v_2 \partial_y \phi - \rho_0 \Gamma_1 \partial_x \frac{\delta \mathcal{F}_s}{\delta \rho}, \quad (4.4)$$

$$j_y = \rho_0 v_3 \partial_x \phi - \rho_0 \Gamma_2 \partial_y \frac{\delta \mathcal{F}_s}{\delta \rho}. \quad (4.5)$$

The first term on the right hand side of Eq. (4.4) arises from the transformation to the laboratory frame. The terms proportional to the coefficients v_1 , v_2 and v_3 are nonequilibrium terms that can be generated upon coarse-graining, by the method described in Section II for the driven lattice. Other nonequilibrium terms that yield contributions that are higher order in the gradients, and therefore subdominant, have been neglected here. By inserting the constitutive equation for the current in Eqs. (4.2) and (4.3), one obtains,

$$(\partial_t + \tilde{v}_1 \partial_x) \delta \rho = -\rho_0 \tilde{v}_2 \partial_x \partial_y \phi + [D_1 \partial_x^2 + D_2 \partial_y^2] \delta \rho, \quad (4.6)$$

and

$$(\partial_t + \tilde{v}_3 \partial_x) \phi = D_5 \partial_y \frac{\delta \rho}{\rho_0} + [D_3 \partial_x^2 + D_4 \partial_y^2] \phi + \frac{\Gamma_0}{\rho_0} F_y[\mathbf{x}, \phi]. \quad (4.7)$$

Additional “velocities” \tilde{v}_1 , \tilde{v}_2 , \tilde{v}_3 have been defined as

$$\tilde{v}_1 = v + v_1, \quad (4.8a)$$

$$\tilde{v}_2 = v_2 + v_3, \quad (4.8b)$$

$$\tilde{v}_3 = v - v_3 \quad (4.8c)$$

The coefficients D_i have dimensions of diffusion constants and are given by

$$D_1 = \Gamma_1 c_L / \rho_0, \quad (4.9a)$$

$$D_2 = \Gamma_2 c_L / \rho_0, \quad (4.9b)$$

$$D_3 = \Gamma_0 K_1 / \rho_0, \quad (4.9c)$$

$$D_4 = (\Gamma_0 c_{11}^y - \Gamma_2 K_2) / \rho_0, \quad (4.9d)$$

$$D_5 = (\Gamma_0 K_2 - \Gamma_2 c_L) / \rho_0. \quad (4.9e)$$

By solving the hydrodynamic equations in the long wavelength limit, one finds that the decay of density and displacement fluctuations is governed by two diffusive modes with eigenfrequencies,

$$\omega_\phi = \tilde{v}_3 q_x - i \left[D_3 q_x^2 + \left(D_4 - \frac{\tilde{v}_2 D_5}{\tilde{v}_1 - \tilde{v}_3} \right) q_y^2 \right], \quad (4.10)$$

$$\omega_\rho = \tilde{v}_1 q_x + i \left[D_1 q_x^2 + \left(D_2 + \frac{\tilde{v}_2 D_5}{\tilde{v}_1 - \tilde{v}_3} \right) q_y^2 \right]. \quad (4.11)$$

For stability we must have $D_4 - \frac{\tilde{v}_2 D_5}{\tilde{v}_1 - \tilde{v}_3} > 0$ and $D_2 + \frac{\tilde{v}_2 D_5}{\tilde{v}_1 - \tilde{v}_3} > 0$. The diffusion constants D_1 and D_3 are clearly positive defined. The first mode describes long-wavelength deformations of the layers and governs the decay of displacement fluctuations. The second mode corresponds to the permeation mode of the driven “smectic” and describes the transport of mass across the layers that can occur in these systems without destroying the layer periodicity. It is associated with density fluctuations and it has important physical consequences for the response of the driven smectic to an additional small driving force applied normal to the layers (see Sec.VII).

An important physical quantity that can be measured in both simulations and experiments is the structure factor of the driven periodic medium. As the driven smectic has broken translational symmetry in the y direction, normal to the layers and to the external drive, the density field can be written as

$$\rho(\mathbf{x}) = \rho_L(\mathbf{x}) + \sum_{Q_y} \rho_{Q_y}(\mathbf{x}) e^{i Q_y y}, \quad (4.12)$$

where $Q_y = n 2\pi / a$ are the reciprocal lattice vectors corresponding to a layer spacing a , with n an integer, ρ_{Q_y} are the corresponding Fourier components of the density, and $\rho_L(\mathbf{x})$ is the smooth (liquid-like) part of the density field. The smectic structure factor is then given by

$$S(\mathbf{q}_\perp) = S_L(\mathbf{q}_\perp) + \sum_{Q_y} \int_{\mathbf{x}} e^{-i q_x x} e^{-i (q_y - Q_y) y} \langle \rho_{Q_y}(\mathbf{x}) \rho_{-Q_y}(\mathbf{0}) \rangle, \quad (4.13)$$

with $S_L(\mathbf{q}_\perp) = \langle |\rho_L(\mathbf{q}_\perp)|^2 \rangle$. The smectic structure function should therefore consists of a broad liquid-like background $S_L(\mathbf{q}_\perp)$, with superimposed peaks at the reciprocal lattice vectors Q_y , normal to the direction of mean

motion (see Fig. 2(b)). As discussed in the Introduction, in a Gaussian theory the correlator of the order parameters $\rho_{Q_y}(\mathbf{x})$ can be written in terms of the mean square displacement, according to

$$\langle \rho_{Q_y}(\mathbf{x}) \rho_{Q_y}^*(\mathbf{0}) \rangle \approx \rho_1^2 e^{-Q_y^2 \langle [\phi(\mathbf{x}) - \phi(\mathbf{0})]^2 \rangle}. \quad (4.14)$$

The disorder-induced transverse mean square displacement is easily calculated from Eqs. 4.6 and 4.7 by treating the the random force $F_y[\mathbf{x}, \phi]$ as a perturbation, in an analysis similar to that of Sec.III. Conceptually simple but algebraically tedious calculations show that including the coupling to the density does not change the resulting decay of the correlation function. For simplicity we therefore neglect this coupling in Eq. (4.7) (i.e., let $\delta\rho = 0$) and obtain

$$\langle [\phi(\mathbf{x}) - \phi(\mathbf{0})]^2 \rangle_{\text{ens.}} = \frac{(\Delta + g_0)\Gamma_0^2}{2\pi\rho_0^2 D_4 \tilde{v}_3} y \mathcal{F}_0^{(2)} \left(\frac{|x|D_4}{\tilde{v}_3 y^2} \right). \quad (4.15)$$

The scaling function $\mathcal{F}_0^{(2)}(s)$ is identical to that obtained in Eq. (3.17) and it has the asymptotic behavior $\mathcal{F}_0^{(2)}(0) = \text{constant}$ and $\mathcal{F}_0^{(2)}(s) \sim \sqrt{s}$ for $s \gg 1$. The perturbation theory therefore predicts that the smectic Bragg peaks at $q_y = Q_y$ decay exponentially with the system size. In other words, disorder would destroy the transverse periodicity of the smectic. In fact, we will see in the following sections that this result continues to hold non-perturbatively. The power-law scaling of transverse Bragg peaks obtained in simulations of two-dimensional driven vortex lattices²⁸ is therefore most likely an artifact of small systems and weak disorder, and would crossover to a disordered form at longer distances. We will return to this point later in Sec. VII.

V. RENORMALIZATION GROUP FOR “TOY” SMECTIC

A. Model and MSR formulation

In this section, we will consider a simplified model for the smectic phase, in which the hydrodynamic fluctuations of the conserved density are neglected. This “toy” smectic is then modeled simply by dropping Eq. 4.6 and setting $\delta\rho = \text{const.}$, leaving the single equation of motion

$$\gamma(\partial_t + v\partial_x)\phi = K_{\parallel}\partial_x^2\phi + K_{\perp}\nabla_{\perp}^2\phi + F(\phi, \mathbf{r}) + \eta(\mathbf{r}, t), \quad (5.1)$$

Here we have pulled out a factor of $\gamma = \rho_0/\Gamma_0$, let $K_{\parallel} \equiv D_3\rho_0/\Gamma_0$, $K_{\perp} \equiv D_4\rho_0/\Gamma_0$, and $F_{\perp} \rightarrow F$. For simplicity we assume longitudinal and transverse elasticity are governed by the same elastic constant K_{\perp} . We have also added the random time-dependent “thermal” noise η , satisfying

$$\langle \eta(\mathbf{r}, t) \eta(\mathbf{r}', t') \rangle = 2\gamma T \delta(\mathbf{r} - \mathbf{r}') \delta(t - t'). \quad (5.2)$$

The random force F is characterized by the correlator

$$[F(\phi, \mathbf{r}) F(\phi', \mathbf{r}')]_{\text{ens.}} = \Delta(\phi - \phi') \delta(\mathbf{r} - \mathbf{r}'). \quad (5.3)$$

The function $\Delta(\phi)$ is periodic with the smectic lattice spacing, which we take to be $a = 2\pi$. It includes both the equilibrium and non-equilibrium components. The latter can be viewed as simply an overall constant contribution to $\Delta(\phi)$. In addition to discounting density fluctuations, Eq. 5.1 also neglects an allowed KPZ non-linear term of the form

$$F_{\text{KPZ}} = C \partial_x \phi \partial_y \phi, \quad (5.4)$$

which should be added to the right hand side of the equation of motion. Simple power-counting shows, however, that, in contrast to a driven *lattice* this term is strongly *irrelevant* in a transverse smectic (see below).

To analyze Eq. (5.1), we use the method of MSR to transform the stochastic equation of motion into a field theory, similar to what was already done in the Sec.IIB to perform the single-step coarse-graining. In this case, the MSR “partition function” is

$$Z = \int [d\hat{\phi}] [d\phi] e^{-S}, \quad (5.5)$$

where $S = S_0 + S_1$, with

$$S_0 = \int_{\mathbf{r}t} \left\{ \hat{\phi}_{\mathbf{r}t} [\gamma(\partial_t + v\partial_x) - K_{\parallel}\partial_x^2 - K_{\perp}\nabla_{\perp}^2] \phi_{\mathbf{r}t} - \gamma T \hat{\phi}_{\mathbf{r}t}^2 \right\}, \quad (5.6)$$

and the interaction term

$$S_1 = -\frac{1}{2} \int_{\mathbf{r}, tt'} \hat{\phi}_{\mathbf{r}t} \hat{\phi}_{\mathbf{r}t'} \Delta(\phi_{\mathbf{r}t} - \phi_{\mathbf{r}t'}). \quad (5.7)$$

By construction, $Z = 1$; non-trivial correlation and response functions are obtained, however, by inserting appropriate $\hat{\phi}$ and ϕ operators into the functional integrand.

B. Power counting

Let us first consider under what conditions the random force is a *relevant* perturbation in the sense of the renormalization group (RG) using simple power-counting. To do so, we rescale the coordinates and fields by a scale factor $b > 1$:

$$\mathbf{x}_{\perp} \rightarrow b\mathbf{x}_{\perp}, \quad (5.8)$$

$$x \rightarrow b^{\zeta} x, \quad (5.9)$$

$$t \rightarrow b^z t, \quad (5.10)$$

$$\hat{\phi} \rightarrow b^{\hat{\chi}} \hat{\phi}. \quad (5.11)$$

Note that, anticipating a periodic fixed point, we will not rescale ϕ . To fix the exponents ζ and $\hat{\chi}$, we choose to keep the terms γv and K_\perp fixed in the quadratic action S_0 . This implies $d-3+z+\zeta+\hat{\chi}=0$ and $d-1+z+\hat{\chi}=0$, or

$$\zeta = 2, \quad (5.12)$$

$$\hat{\chi} = -d + 1 - z. \quad (5.13)$$

Note that because ϕ was kept invariant, the temperature T necessarily rescales

$$T \rightarrow b^{1-d}T. \quad (5.14)$$

Clearly this is a somewhat artificial choice for $\Delta = 0$, since the theory retains no memory of the periodicity of ϕ . It is rather natural, however, for $\Delta \neq 0$, and will be returned to below. The exponent z is more subtle. Naively, it should be determined by the condition that γ be invariant under rescaling. Neglecting the random force, we then obtain

$$z_{\text{naive}} = 2. \quad (5.15)$$

We will see that even for small non-zero Δ , this is actually very far from correct.

Fortunately, the rescaling of $\Delta(\phi)$ and C is in fact independent of z . The KPZ non-linearity is strongly irrelevant:

$$C \rightarrow C/b \rightarrow 0, \quad (5.16)$$

while the disorder correlator obeys

$$\Delta(\phi) \rightarrow b^{3-d}\Delta(\phi). \quad (5.17)$$

We therefore see that for $d > 3$, the random force is irrelevant, and at long length scales has a negligible effect on the moving smectic. For $d \leq 3$, however, power-counting is insufficient to determine the fate of the system.

C. Zero temperature RG

To proceed, we will perform a systematic RG, working perturbatively in S_1 , expanding it from the exponential and integrating out “fast” modes with large *transverse* momenta. This is simplest in the scheme with neither a frequency ω nor longitudinal momentum q_x cut-off. The fields are first decomposed into their slow ($<$) components with $q_\perp < \Lambda/b$ and fast ($>$) components with $\Lambda/b < q_\perp < \Lambda$, where Λ is a hard transverse momentum-space cut-off. That is,

$$\phi = \phi_{<} + \phi_{>}, \quad \hat{\phi} = \hat{\phi}_{<} + \hat{\phi}_{>} \quad (5.18)$$

Then the partition function is

$$Z = \int [d\hat{\phi}_{<}][d\phi_{<}] e^{-S_0[\phi_{<}, \hat{\phi}_{<}]} \left\langle e^{-S_1[\phi_{<} + \phi_{>}, \hat{\phi}_{<} + \hat{\phi}_{>}]} \right\rangle_{>}, \quad (5.19)$$

where the brackets denote an average over the fast fields with respect to the quadratic action $S_0[\phi_{>}, \hat{\phi}_{>}]$. Relabeling the surviving slow fields $\phi_{<} \rightarrow \phi$, $\hat{\phi}_{<} \rightarrow \hat{\phi}$, the renormalization of the effective action due to the mode elimination is given by

$$e^{-S_{\text{eff.}}[\phi, \hat{\phi}]} = e^{-S_0[\phi, \hat{\phi}]} \left\langle e^{-S_1[\phi + \phi_{>}, \hat{\phi} + \hat{\phi}_{>}]} \right\rangle_{>}. \quad (5.20)$$

A cumulant expansion gives

$$\langle e^{-S_1} \rangle_{>} = \exp \left\{ -\langle S_1 \rangle_{>} + \frac{1}{2} \langle S_1^2 \rangle_{>,c} + \dots \right\}, \quad (5.21)$$

where the subscript c indicate the cumulant (connected) correlator. From Eq. 5.14, it is natural to suspect that much of the interesting physics is dominated by small (renormalized) temperatures. With this in mind, we first consider the RG in the extreme $T = 0$ case. Then the only non-vanishing expectation values correspond to *response* functions:

$$\begin{aligned} G_{>}(\mathbf{r}, t) &= \langle \phi(\mathbf{r}' + \mathbf{r}, t' + t) \hat{\phi}(\mathbf{r}', t') \rangle_{>} \quad (5.22) \\ &= \int_{\Lambda/b}^{\Lambda} \frac{d^d \mathbf{q}_\perp}{(2\pi)^{d-1}} \int \frac{dq_x}{2\pi} \int \frac{d\omega}{2\pi} \frac{e^{-i\mathbf{q}_\perp \cdot \mathbf{r} + i\omega t}}{i\gamma(\omega - vq_x) + K_\parallel q_x^2 + K_\perp q_\perp^2}. \end{aligned}$$

It is instructive to perform some of the integrations above and bring out the dependence on x and t . We are primarily interested in the limit $K_\parallel \rightarrow 0$, since K_\parallel is obviously less relevant than γv , which has one less x derivative. In that limit these integrals are trivial, and we obtain

$$G_{>}(\mathbf{r}, t) = \int_{\Lambda/b}^{\Lambda} \frac{d^{d-1} \mathbf{q}_\perp}{(2\pi)^{d-1}} \frac{1}{\gamma} e^{-i\mathbf{q}_\perp \cdot \mathbf{r}} e^{-(K_\perp/\gamma)q_\perp^2 t} \theta(t) \delta(x - vt). \quad (5.23)$$

From this we see that the response function is causal and represents unidirectional propagation along the positive x axis. Including a non-zero K_\parallel simply spreads out the δ -function over a distance $\delta x \propto \sqrt{K_\parallel}t$. The irrelevance of K_\parallel is indicated by the smallness of this width relative to the distance vt propagated in the large t limit.

Working first to $O(\Delta)$, consider the term

$$\begin{aligned} &\langle S_1 \rangle_{>} - S_1[\phi, \hat{\phi}] \\ &\approx \int_{\mathbf{r}t} \hat{\phi}_{\mathbf{r}t} [\Delta'(0) + \Delta''(0)(t - t') \partial_t \phi_{\mathbf{r}t}] G_{>}(0, t - t'). \quad (5.24) \end{aligned}$$

By symmetry, $\Delta'(0) = 0$, and we need to evaluate

$$\begin{aligned} \int_\tau \tau G_{>}(\mathbf{0}, \tau) &= \int_{\mathbf{q}_\perp}^> \int_{\omega\tau} \frac{\tau e^{i\omega\tau}}{i\gamma(\omega - vq_x) + K_\parallel q_x^2 + K_\perp q_\perp^2} \\ &= \frac{2\gamma K_\parallel \Lambda^{d-1} C_{d-1}}{(\gamma^2 v^2 + 4K_\parallel K_\perp \Lambda^2)^{3/2}} dl \\ &= \frac{\bar{\kappa}}{1 + 2\bar{\kappa}} \frac{\Lambda^{d-3} C_{d-1}}{vK_\perp} dl, \quad (5.25) \end{aligned}$$

where we defined

$$\bar{\kappa} \equiv \frac{2K_{\parallel}K_{\perp}}{\gamma^2 v^2} \Lambda^2, \quad (5.26)$$

chosen the infinitesimal rescaling factor $b = e^{dl}$, and defined $C_d = S_d/(2\pi)^d$ in terms of the surface area of a d -dimensional sphere $S_d = 2\pi^{d/2}/\Gamma(d/2)$. Inserting this result above gives a renormalization of the friction drag coefficient (the inverse mobility):

$$\partial_l \gamma|_{O(\Delta)} = -\frac{\bar{\kappa}}{1+2\bar{\kappa}} \frac{\Lambda^{d-3} C_{d-1}}{v K_{\perp}} \Delta''(0). \quad (5.27)$$

Note that we have obtained no renormalization of the spatial gradient terms. This is actually a general conse-

$$\delta S_2 = -\frac{1}{2} \int_{\mathbf{r}_1 t_1 t'_1}^{\mathbf{r}_2 t_2 t'_2} \left\langle \hat{\phi}_{\mathbf{r}_1 t_1} \hat{\phi}_{\mathbf{r}_1 t'_1} \Delta(\phi_{\mathbf{r}_1 t_1} - \phi_{\mathbf{r}_1 t'_1}) \hat{\phi}_{\mathbf{r}_2 t_2} \hat{\phi}_{\mathbf{r}_2 t'_2} \Delta(\phi_{\mathbf{r}_2 t_2} - \phi_{\mathbf{r}_2 t'_2}) \right\rangle_c. \quad (5.29)$$

At this point we are aided by a simplifying feature that actually makes this part of the calculation easier than the equilibrium one. Since we have a propagating mode along the x axis, in the limit of zero longitudinal damping, $K_{\parallel} = 0$, the response function vanishes unless $x > 0$. This means that two response fields at different x points cannot be contracted, since this would give the product $G(\mathbf{x} - \mathbf{x}', \cdot) G(\mathbf{x}' - \mathbf{x}, \cdot)$, which vanishes for any x . Instead, a non-vanishing contribution obtains only when both $\hat{\phi}$ fields are taken from the same term. This gives

$$\begin{aligned} \delta S_2 = & -\frac{1}{2} \int_{\substack{\mathbf{r}_1 t_1 t'_1 \\ \mathbf{r}_2 t_2 t'_2}} \hat{\phi}_{\mathbf{r}_1 t_1} \hat{\phi}_{\mathbf{r}_1 t'_1} \Delta(\phi_{\mathbf{r}_2 t_2} - \phi_{\mathbf{r}_2 t'_2}) \Delta''(\phi_{\mathbf{r}_1 t_1} - \phi_{\mathbf{r}_1 t'_1}) \\ & \times [G_{>}(\mathbf{r}_1 - \mathbf{r}_2, t_1 - t_2) G_{>}(\mathbf{r}_1 - \mathbf{r}_2, t_1 - t'_2) - G_{>}(\mathbf{r}_1 - \mathbf{r}_2, t_1 - t_2) G_{>}(\mathbf{r}_1 - \mathbf{r}_2, t'_1 - t'_2)]. \end{aligned} \quad (5.30)$$

Each term contains two response functions, which constrain their arguments to be small. To leading (zeroth) order in gradients of ϕ , we may approximate $\phi_{\mathbf{r}_2 t_2} \approx \phi_{\mathbf{r}_1, t_1}$ and $\phi_{\mathbf{r}_2 t'_2} \approx \phi_{\mathbf{r}_1 t'_1}$ in the first term, while in the second $\phi_{\mathbf{r}_2 t'_2} \approx \phi_{\mathbf{r}_1 t'_1}$. This leads to the simpler formula

$$\delta S_2 = -\frac{I}{2} \int_{\mathbf{r}_1 t_1 t'_1} \hat{\phi}_{\mathbf{r}_1 t_1} \hat{\phi}_{\mathbf{r}_1 t'_1} \Delta''(\phi_{\mathbf{r}_1 t_1} - \phi_{\mathbf{r}_1 t'_1}) [\Delta(0) - \Delta(\phi_{\mathbf{r}_1 t_1} - \phi_{\mathbf{r}_1 t'_1})], \quad (5.31)$$

where the same integral I occurs in both terms. In the limit $K_{\parallel} \rightarrow 0$, it becomes

$$I = \int_{\mathbf{q}_{\perp}}^> \int_{q_x} G_{>}(\mathbf{q}, \omega = 0) G_{>}(-\mathbf{q}, \omega = 0) \approx \frac{\Lambda^{d-3} C_{d-1}}{2\gamma v K_{\perp}} dl. \quad (5.32)$$

This gives the second order contribution to the renormalization of $\Delta(\phi)$:

$$\partial_l \Delta(\phi)|_{O(\Delta^2)} = -\frac{\Lambda^{d-3} C_{d-1}}{2\gamma v K_{\perp}} \Delta''(\phi) [\Delta(\phi) - \Delta(0)]. \quad (5.33)$$

At $T = 0$, these are all the necessary mode-elimination contributions. Combining these results with the scale-changes, we thus arrive at the zero temperature RG equations

$$\begin{aligned} \partial_l \Delta(\phi) = & (3-d)\Delta(\phi) \\ & -\frac{\Lambda^{d-3} C_{d-1}}{2\gamma v K_{\perp}} \Delta''(\phi) [\Delta(\phi) - \Delta(0)], \end{aligned} \quad (5.34)$$

quence of taking an ultra-local (i.e. δ -function correlated) random force. For such a force, it is straightforward to show that the static response function

$$G(\mathbf{q}, \omega = 0) = \frac{1}{-i\gamma v q_x + K_{\parallel} q_x^2 + K_{\perp} q_{\perp}^2} \quad (5.28)$$

is unrenormalized, i.e. exact even when F is included in the equation of motion. Thus γv , K_{\parallel} , and K_{\perp} suffer no diagrammatic corrections at any order.

The next step is to examine the renormalization of Δ . The first corrections (for $T = 0$) arise at $O(\Delta^2)$. To determine these, we must compute the next term in the cumulant expansion. This is

$$\partial_l \gamma = \left[2 - z - \frac{\bar{\kappa}}{1+2\bar{\kappa}} \frac{\Lambda^{d-3} C_{d-1}}{\gamma v K_{\perp}} \Delta''(0) \right] \gamma, \quad (5.35)$$

$$\partial_l K_{\parallel} = -2K_{\parallel}, \quad (5.36)$$

$$\partial_l \bar{\kappa} = -2\bar{\kappa}, \quad (5.37)$$

where the flow for the dimensionless parameter $\bar{\kappa}$ is exact and independent of the choice of the rescaling exponents z , ζ and $\hat{\chi}$.

1. Behavior in $d = 3 - \epsilon$ dimensions

As a first attempt at an analysis of these results, we consider the problem in $d = 3 - \epsilon$ dimensions. Defining the dimensionless random-force correlator

$$\Gamma(\phi) \equiv \frac{\Lambda^{d-3} C_{d-1}}{\gamma v K_{\perp}} \Delta(\phi) \quad (5.38)$$

the RG flow equation for this dimensionless random force variance is given by

$$\partial_l \Gamma(\phi) = (3-d)\Gamma(\phi) - \frac{1}{2} \Gamma''(\phi) [\Gamma(\phi) - \Gamma(0)]. \quad (5.39)$$

For $\epsilon \ll 1$, we thus expect to find a fixed point with $\Gamma = O(\epsilon)$. However, evaluating Eq. 5.39 at $\phi = 0$ demonstrates that (in contrast to equilibrium case, where there was an additional stabilizing $-\Gamma'(\phi)^2/2$ term) this is only possible if $\Gamma(0)^* = 0$. Like other functional RG equations at $T = 0$, Eq. 5.39 leads to a non-analytic force-force correlator. This can be seen directly by differentiating twice above and evaluating at the origin:

$$\partial_l \Gamma''(0) = (3-d)\Gamma''(0) - \frac{1}{2} [\Gamma''(0)]^2. \quad (5.40)$$

Since $\Gamma''(0; l=0) < 0$, this equation leads directly to a divergence. In fact, all “fixed points” (see below for an explanation of the quotation marks here) have a slope discontinuity at the origin. A little analysis demonstrates that the large l behavior of Γ is

$$\Gamma(\phi; l) \sim \epsilon \min_n \left\{ (\phi - \pi - 2\pi n)^2 - \frac{\pi^2}{3} \right\} + \Gamma_0(l), \quad (5.41)$$

where Γ_0 is the zero Fourier component of $\Gamma(\phi)$ and satisfies

$$\partial_l \Gamma_0 = \epsilon \Gamma_0 + \frac{2\pi^2}{3} \epsilon^2 \quad (5.42)$$

Note that although $\Gamma_0 = -2\pi^2\epsilon/3$ provides a formal fixed point solution, it is unphysical: for this value, $\Gamma(0) = 0$, which would imply the (positive semidefinite) variance of $F(\phi, \mathbf{r})$ vanishes, and hence that F is uniformly zero, clearly in contradiction with $\Gamma(\phi) \neq 0$. For any physical situation Γ_0 will be *larger*. For instance, equilibrium initial conditions require that the force arise as a derivative of a random potential, and hence that the integral over $\Delta(\phi)$ vanish. For the solution above, this gives $\Gamma_0 = 0 > -2\pi^2\epsilon/3$. Indeed, Γ_0 can be identified as the variance of the *static* force calculated using the single-step coarse graining in Sec.II B.

For physical situations, it is clear from Eq. (5.42) that Γ_0 is a strongly *relevant* variable which will flow off under

$$C_{>}(\mathbf{r}, t) = \langle \phi_{\mathbf{r}+\mathbf{r}', t+t'} \phi_{\mathbf{r}t'} \rangle_{>} = \int_{\mathbf{q}\omega}^> \frac{2\gamma T e^{-i\mathbf{q}\cdot\mathbf{r}+i\omega t}}{\gamma^2(\omega - vq_x)^2 + (K_{\parallel}q_x^2 + K_{\perp}q_{\perp}^2)^2} \quad (5.43)$$

is now non-zero. This now makes it possible to contract two ϕ fields when renormalizing the MSR functional. It is sufficient to work only to linear order in Δ (or Γ). Following the same method as earlier, we find

$$\delta S_1^{(T)} = \langle S_1 \rangle_{>}^{(T)} = -\frac{1}{2} \int_{\mathbf{r}t t'} \hat{\phi}_{\mathbf{r}t} \hat{\phi}_{\mathbf{r}t'} \Delta''(\phi_{\mathbf{r}t} - \phi_{\mathbf{r}t'}) [C_{>}(\mathbf{0}, 0) - C_{>}(\mathbf{0}, t-t')]. \quad (5.44)$$

This gives two terms. The first contributes a renormalization of Δ . That correlation function gives

the RG. Luckily, as pointed out by Narayan and Fisher in their study of CDW depinning³⁰, this does not really present a problem. It can be easily shown that the static random force does not effect the dynamics, by the same argument used above to demonstrate the exact static response function (i.e. shifting it away and showing that the distribution of the shifted force is unmodified). This is also essentially the same argument used in the Cardy-Ostlund problem, in which there is also a runaway random force (which is, in that case however, the gradient of a potential).

The non-analyticity of Γ has important consequences for the dynamics. Indeed inspection of Eq. 5.35 shows that it is problematic: the quantity $\Delta''(0)$ is (minus) infinity at the fixed point (and indeed becomes infinite at a finite length scale). Physically, the non-analyticity of Γ is related to the existence of multiple metastable minima in the effective potential on the scale l and a concurrent “sharpness” of this potential. At zero temperature, this sharpness leads to trapping of the phase ϕ and hence to a breakdown of the simple assumption of analyticity in the coarse-grained dynamics. A detailed analysis²⁵ shows that the divergence of $\Delta''(0)$ can be interpreted as the signature of a multi-valued force reminiscent of static friction, and corresponds to the existence of a non-zero transverse critical force to “depin” the smectic³¹.

D. Finite temperature RG

A simpler means of controlling these singularities is to include non-zero thermal fluctuations, which act to locally average the effective potential and effect thermally activated motion between different metastable states on long time scales. In hopes of obtaining a workable dynamics, we are thus led to consider the effects of a non-zero temperature. At the same time we must also ask if temperature is a relevant or irrelevant perturbation around the $T = 0$ fixed point considered here. Naively, from Eq. 5.14, we would expect T be strongly irrelevant for d near three. In equilibrium, the corresponding (power-counting there gives $2-d$) result is exact; again due to Galilean invariance and the FDT, there are no diagrammatic renormalizations to T ³².

Because of the lack of FDT, we will, surprisingly, be led to a completely different conclusion! Consider the mode elimination at a non-zero temperature. The correlation function,

$$C_{>}(\mathbf{0}, 0) = \int_{\mathbf{q}_\perp}^> \int_{\omega q_x} \frac{2T\gamma}{\gamma^2(\omega - vq_x)^2 + (K_\parallel q_x^2 + K_\perp q_\perp^2)^2} = \frac{T}{2\sqrt{K_\parallel K_\perp}} \Lambda^{d-2} C_{d-1} dl. \quad (5.45)$$

Note that the integral is singular in the $K_\parallel \rightarrow 0$ limit. Physically, this is because some damping is needed to control the thermal fluctuations excited in the propagating longitudinal mode. Incorporating this piece in the RG equation for Γ gives

$$\partial_l \Gamma(\phi) = \left[(3-d) + \bar{T} \frac{\partial^2}{\partial \phi^2} \right] \Gamma(\phi) - \frac{1}{2} \Gamma''(\phi) [\Gamma(\phi) - \Gamma(0)], \quad (5.46)$$

where

$$\bar{T} \equiv \Lambda^{d-2} C_{d-1} \frac{T}{2\sqrt{K_\perp K_\parallel}}. \quad (5.47)$$

The second term in Eq. 5.44 gives a correction to the temperature. This is simple to see, since in this term $|t - t'|$ is kept small, so that $\phi_{\mathbf{r}t'} \approx \phi_{\mathbf{r}t}$ (and likewise for $\hat{\phi}$). This gives

$$\delta S = \frac{1}{2} \int_{\mathbf{r}t} \left(\hat{\phi}_{\mathbf{r}t} \right)^2 \Delta''(0) \int_{t'} C_{>}(\mathbf{0}, t - t'). \quad (5.48)$$

This integral is finite in the limit $K_\parallel \rightarrow 0$, giving

$$\begin{aligned} \int_{t'} C_{>}(\mathbf{0}, t - t') &= \int_{\mathbf{q}_\perp}^> \int_{q_x} \frac{2T\gamma}{\gamma^2 v^2 q_x^2 + K_\perp^2 q_\perp^4} \\ &= \frac{T}{K_\perp v} \Lambda^{d-3} C_{d-1} dl. \end{aligned} \quad (5.49)$$

This is a renormalization of γT . Taking into account the renormalization of γ obtained earlier (Eq. 5.35), one finds

$$\partial_l T = \left[1 - d - \left(\frac{1}{2} - \frac{\bar{\kappa}}{1 + 2\bar{\kappa}} \right) \Gamma''(0) \right] T. \quad (5.50)$$

Using the definition of the dimensionless temperature, this becomes

$$\partial_l \bar{T} = \left[2 - d - \left(\frac{1}{2} - \frac{\bar{\kappa}}{1 + 2\bar{\kappa}} \right) \Gamma''(0) \right] \bar{T}. \quad (5.51)$$

1. $d = 3 - \epsilon$ redux

Eqs. 5.46 and 5.51 complete the modified set of RG flows at non-zero temperature. Let us focus again on the behavior for $d = 3 - \epsilon$, discussed above for $T = 0$. As suspected, the presence of the diffusion-like term in Eq. 5.46 indeed acts to smooth out the cusp in $\Gamma(\phi)$ (a simple heuristic argument for this rounding is given in Ref. 34). To see this, consider the ‘‘adiabatic’’ approximation in which Eq. 5.46 is solved for fixed non-zero \bar{T} , ignoring

corrections to $\partial_l \Gamma$ arising from the scale dependence of \bar{T} . To carry this out, we search for a solution

$$\Gamma(\phi, l) = \Gamma(0, l) - (3-d) \tilde{\Gamma}(\phi, \bar{T}(l)), \quad (5.52)$$

where $\tilde{\Gamma}(0, l) = 0$. Evaluating Eq. 5.46 at $\phi = 0$ gives the flow equation for $\Gamma(0, l)$, which in turn implies an equation for $\tilde{\Gamma}(\phi)$ in the ‘‘adiabatic’’ approximation.

$$\partial_l \Gamma(0, l) = (3-d) \Gamma(0) + \bar{T} \Gamma''(0), \quad (5.53)$$

$$\mu \tilde{\Gamma}''(0) = \tilde{\Gamma}(\phi) + \mu \tilde{\Gamma}'''(\phi) + \frac{1}{2} \tilde{\Gamma}''(\phi) \tilde{\Gamma}(\phi), \quad (5.54)$$

where $\mu = \bar{T}/\epsilon \ll 1$. Multiplying Eq. 5.54 through by $\tilde{\Gamma}'(\phi)$, allows one to perform one integral, and thereby to solve for $\tilde{\Gamma}(\phi)$ exactly in an implicit form. One finds

$$\int_0^{\tilde{\Gamma}} d\hat{\Gamma} \left[\frac{\pi^2}{|\ln \mu|} \ln(1 + \hat{\Gamma}/2\mu) - \hat{\Gamma} \right]^{-1/2} = 2\phi, \quad (5.55)$$

for $0 \leq \phi \leq 2\pi$. For $|\phi - 2\pi n| \gg \mu \sqrt{|\ln \mu|}$ (with integer n), this reduces to the zero temperature solution in Eq. 5.41. It contains, however, a boundary layer near $\phi = 2\pi n$. Inside this boundary layer $\Gamma(\phi)$ remains smooth, and a simple computation finds

$$\Gamma''(0) = -\frac{\pi^2 \epsilon^2}{\bar{T} \ln(\epsilon/\bar{T})}. \quad (5.56)$$

Putting this result back into Eq. 5.51 gives, to leading order in ϵ ,

$$\partial_l \bar{T} = -\bar{T} + \frac{\pi^2 \epsilon^2}{2 \ln(\epsilon/\bar{T})}. \quad (5.57)$$

The new term leads to a fixed point at a non-zero temperature given by

$$\bar{T}^* \sim \frac{\pi^2 \epsilon^2}{2 |\ln \epsilon|}. \quad (5.58)$$

Note that in equilibrium, i.e., in $v \rightarrow 0$ limit, $\bar{\kappa} \rightarrow \infty$, $\bar{\kappa}/(1 + 2\bar{\kappa}) \rightarrow 1/2$, and two terms appearing inside the parentheses in Eq. 5.51— exactly cancel due to the FDT, preserving the power-counting result and leaving \bar{T} irrelevant. Here, for any finite v , they do not, and the noise renormalization (first term) overwhelms the dynamic renormalization (second term) due to strong irrelevance of $\bar{\kappa}$ (or equivalently K_\parallel), thereby destabilizing the zero-temperature fixed point! The asymptotic flow of \bar{T} is then given by

$$\partial_l \bar{T} = \left[2 - d - \frac{1}{2} \Gamma''(0) \right] \bar{T}. \quad (5.59)$$

E. Behavior in three dimensions

In three dimensions, we expect that \bar{T} flows to zero, and the above analysis is invalid. To analyze this case, consider first the behavior of $\Gamma(\phi)$ at $T = 0$. From Eq. 5.40, we see that even for $d = 3$, $\Gamma''(0)$ diverges at a finite scale, and the non-analyticity remains. Indeed, for $T = 0$, a solution (presumably the asymptotic attractor for an arbitrary initial condition) of Eq. 5.39 is

$$\Gamma(\phi; l; T = \epsilon = 0) = a(l) \min_n \left\{ (\phi - \pi - 2\pi n)^2 - \frac{\pi^2}{3} \right\} + \Gamma_0(l), \quad (5.60)$$

where

$$\partial_l a(l) = -a^2, \quad (5.61)$$

$$\partial_l \Gamma_0 = \frac{2\pi^2}{3} a^2. \quad (5.62)$$

Thus the amplitude of the ‘‘cuspy’’ part of the disorder correlator decays slowly to zero,

$$a(l) = \frac{a(0)}{1 + la(0)}. \quad (5.63)$$

Employing again the adiabatic approximation for small $\bar{T} \neq 0$, one finds

$$\Gamma''(0, l; d = 3) = \frac{-\pi^2 [a(l)]^2}{\bar{T}(l) \ln(a(l)/\bar{T}(l))}. \quad (5.64)$$

Putting this back into Eq. 5.51, the ‘‘fixed point’’ for $\epsilon \neq 0$ now drifts slowly down towards zero. The correct asymptotic behavior is obtained simply by substituting $\epsilon \rightarrow a(l)$ in Eq. 5.58, giving

$$\bar{T}(l) \sim \frac{\pi^2 a^2}{2 |\ln a|} \sim \frac{\pi^2}{2l^2 |\ln l|}, \quad (5.65)$$

for large l . Note that this is faster than the usual case of a marginally irrelevant operator ($\sim 1/l$), but much slower than the naive power-counting result ($\sim e^{-l}$).

VI. DYNAMICS OF 2+ ϵ -DIMENSIONAL SMECTIC

In this section, we study the toy model for the driven smectic near *two* dimensions. Based on an extrapolation of the results of the previous section (Eq. 5.58), we expect that in this case the governing stable fixed point should occur at a renormalized temperature of order one. In this regard $d = 2$ plays a special role, since (see Eq. 5.59) dimensionless temperature \bar{T} becomes marginal.

For temperatures of $O(1)$, the character of the functional RG (Eq. 5.46) is substantially changed. This is because the linear operator

$$\hat{\mathcal{L}} = 3 - d + \bar{T} \frac{\partial^2}{\partial \phi^2} \quad (6.1)$$

has a *discrete* spectrum (defined in the space of 2π -periodic functions),

$$\hat{\mathcal{L}} \cos n\phi = (3 - d - \bar{T}n^2) \cos n\phi. \quad (6.2)$$

For $\bar{T} > 3 - d$, therefore, all the harmonics but the constant ($n = 0$) are irrelevant, and $\Delta(\phi) \rightarrow \Delta_0$. For $(3 - d)/4 < \bar{T} < 3 - d$, we can study the onset of non-trivial random-force correlations by truncating the Fourier expansion of Δ at $n = 1$:

$$\Delta(\phi) = \Delta_0 + \Delta_1 \cos \phi. \quad (6.3)$$

Eq. 6.3 displays one distinct advantage over the full functional RG treatment in the previous section: $\Delta(\phi)$ in this limit is manifestly *analytic*, so perturbation theory is uniformly valid. By contrast, the treatment for $d \approx 3$, while physically reasonable, is considerably less controlled. Indeed, from Eq. 5.59 or Eq. 5.56, $\Gamma''(0)^* = -2(d - 2)$ is $O(1)$ in this limit, and although $\Gamma(\phi)$ is $O(\epsilon)$, it is unclear how the singular derivatives might enter into higher order corrections.

To implement the complimentary, strictly controlled approach for $d = 2 + \epsilon$, we simply insert Eq. 6.3 into Eq. 5.46, dropping harmonics with $n \geq 2$. This gives

$$\frac{d\bar{\Delta}_0(l)}{dl} = (3 - d)\bar{\Delta}_0(l) + \frac{1}{4}\bar{\Delta}_1^2, \quad (6.4)$$

$$\frac{d\bar{\Delta}_1(l)}{dl} = (3 - d - \bar{T})\bar{\Delta}_1 - \frac{1}{2}\bar{\Delta}_1^2, \quad (6.5)$$

$$\frac{d\bar{T}(l)}{dl} = (2 - d + \frac{1}{2}\bar{\Delta}_1)\bar{T}(l), \quad (6.6)$$

where $\bar{\Delta}_{0,1} \equiv \Delta_{0,1} C_{d\perp} \Lambda^{d-3} / (K_\perp \gamma |v|)$. We pause to point out that Eq. 6.3 is equivalent to the physical approximation of the equation of motion,

$$\begin{aligned} \gamma(\partial_t + v\partial_x)\phi(\mathbf{r}, t) &= (K_\parallel \partial_x^2 + K_\perp \nabla_\perp^2)\phi(\mathbf{r}, t) + F_0(\mathbf{r}) \\ &\quad + F_1(\mathbf{r}) \cos[y - \phi(\mathbf{r}, t)] + \eta(\mathbf{r}, t), \end{aligned} \quad (6.7)$$

with

$$[F_0(\mathbf{r})F_0(\mathbf{r}')]_{\text{ens.}} = 2\Delta_0 \delta^{(d)}(\mathbf{r} - \mathbf{r}'), \quad (6.8)$$

$$[F_1(\mathbf{r})F_1(\mathbf{r}')]_{\text{ens.}} = 2\Delta_1 \delta^{(d)}(\mathbf{r} - \mathbf{r}'). \quad (6.9)$$

For completeness, we rederive Eqs. 6.4–6.6 directly from Eqs. 6.7–6.9 in Appendix E. Note that Eq. 6.4 implies that the random ϕ -independent drag correlator $\bar{\Delta}_0$ is always generated by the disorder and is relevant, even if it is not present in the ‘‘bare’’ equation of motion. Although $\bar{\Delta}_0$ runs off to infinity, as discussed in the previous subsection, its effects can luckily be taken into account exactly, by a simple transformation on the field ϕ . The

remaining flow equations for $\bar{\Delta}_1(l)$ and $\bar{T}(l)$ contain three fixed points

$$\text{Gaussian: } \bar{T}^* = 0, \bar{\Delta}_1^* = 0, \quad (6.10)$$

$$\text{Zero Temperature: } \bar{T}^* = 0, \bar{\Delta}_1^* = 2(3-d), \quad (6.11)$$

$$\text{Driven Smectic: } \bar{T}^* = 5-2d, \bar{\Delta}_1^* = 2(d-2). \quad (6.12)$$

Of these, only the Driven Smectic is globally stable. Fortunately, it is also perturbative, and hence controlled, for d near 2, and indeed becomes exact in the $d \rightarrow 2^+$ limit. Furthermore, the Driven Smectic fixed point that is perturbative near $d = 2$ appears to smoothly match onto the finite disorder, finite temperature fixed point that was obtained at strong coupling by a functional renormalization group calculation near $d = 3$ in Sec. VD.

Equations 6.5–6.6 are also the nonequilibrium analog of the Cardy-Ostlund fixed line³⁵ that describes the 1+1 dimensional vortex glass state¹⁸ and the super-rough phase of a crystal surface grown on a random substrate^{36,37}. Because of the lack of fluctuation-dissipation theorem for the driven system considered here, the Cardy-Ostlund fixed line is destabilized by the nontrivial renormalization of temperature. This disorder generated thermal renormalization ($\bar{\Delta}_1$ -dependent term in Eq.6.6) is reminiscent of the “shaking” temperature, discussed by Koshelev and Vinokur³⁸. Note, however, that the “heating” found here is a multiplicative rather than an additive effect, as was suggested in Ref. 38.

In $d = 2 + \epsilon$ dimensions the flow equations have an interesting spiral structure around the Driven Smectic fixed point, as is illustrated in Fig.5

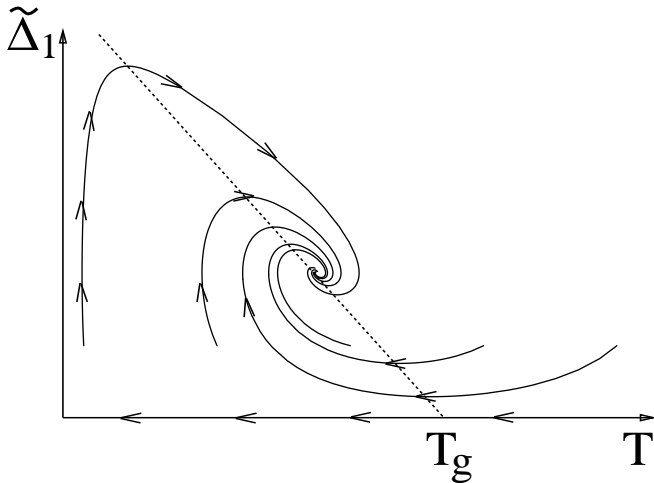


Fig.5.:Renormalization group flow diagram (for $2 < d = 2 + 0.3 < 3$) in the disorder Δ_1 temperature T plane, for a set of initial conditions with $\bar{\Delta}_1(0) = 0.2$ and $\bar{T}(0)$ ranging from 0.05 to 0.85, in increments of 0.2

The structure of the renormalization group flow in the physically interesting case of $d = 2$ is displayed in Fig.6.

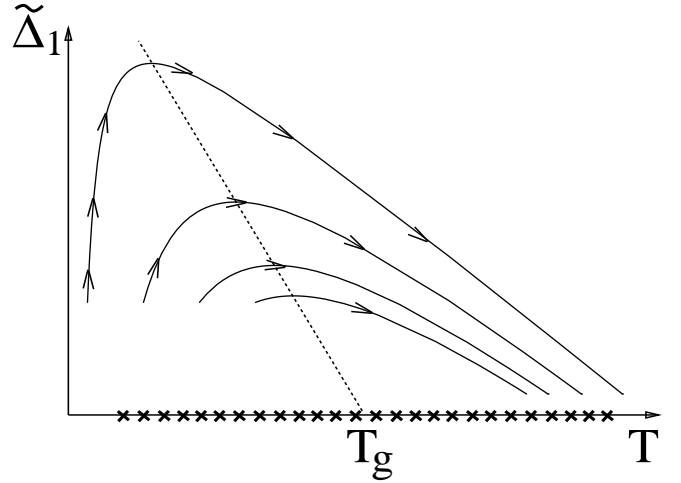


Fig.6: Renormalization group flow diagram (for $d = 2$) in the disorder Δ_1 temperature T plane, for a set of initial conditions with $\bar{\Delta}_1(0) = 0.2$ and $\bar{T}(0)$ ranging from 0.05 to 0.65, in increments of 0.2

In $d = 2$ the Driven Smectic fixed point moves down to zero disorder and merges into the zero-disorder fixed line. Despite the absence of a globally stable finite disorder fixed point in $d = 2$, we expect nontrivial observable effects associated with the interesting RG flows displayed in Fig.6. Qualitatively, a moving lattice at temperature T with disorder Δ_1 behaves at long times and length scales as a thermal moving smectic with an effective disorder-enhanced temperature $T_{\text{eff}}(T, \Delta_1)$.

To determine T_{eff} , we take advantage of the solvability of Eqs. 6.5–6.6 in two dimensions. Dividing Eq. 6.5 by Eq. 6.6 gives

$$\frac{d\bar{\Delta}_1(\bar{T})}{d\bar{T}} = 2\frac{1-\bar{T}}{\bar{T}} - \frac{\bar{\Delta}_1}{\bar{T}}. \quad (6.13)$$

This has the exact solution

$$\bar{\Delta}_1^{\text{eff}} = 2 - \bar{T}_{\text{eff}} + f/\bar{T}_{\text{eff}}, \quad (6.14)$$

where f is given by the initial conditions $\bar{\Delta}_1(l=0) = \bar{\Delta}_1$, $\bar{T}(l=0) = \bar{T}$ as

$$f = \bar{T} [\bar{\Delta}_1 - 2 + \bar{T}]. \quad (6.15)$$

The asymptotic effective temperature is determined from Eq. 6.14 by setting $\bar{\Delta}_1^{\text{eff}} = 0$, which gives

$$\bar{T}_{\text{eff}} = 1 + \sqrt{1 + \bar{T}(\bar{\Delta}_1 + \bar{T} - 2)}. \quad (6.16)$$

This effective temperature has the following meaning: asymptotically, the *connected* correlation and response functions of a moving smectic at temperature \bar{T} in the presence of disorder $\bar{\Delta}_1$ are given by the noninteracting, disorder-free functions with T replaced by $T_{\text{eff}}(\bar{T}, \bar{\Delta}_1)$. Of course the details of the approach to the zero disorder fixed line and to this effective temperature will determine subdominant q -dependent corrections to the correlation and the response functions.

VII. NONEQUILIBRIUM RESPONSE AND CORRELATION FUNCTIONS

We now turn our attention to the dynamic response and correlation functions of a moving smectic. We will consider only mean (disorder-averaged) properties here. The mean response function is defined by

$$R(\mathbf{r}, t) = \left[\frac{\delta \langle \phi(\mathbf{r} + \mathbf{r}', t + t') \rangle}{\delta \eta(\mathbf{r}', t')} \right]_{\text{ens.}} = \left[\langle \phi(\mathbf{r} + \mathbf{r}', t + t') \hat{\phi}(\mathbf{r}', t') \rangle \right]_{\text{ens.}}. \quad (7.1)$$

We similarly define a mean correlation function,

$$C(\mathbf{r}, t) = \left[\langle (\phi(\mathbf{r} + \mathbf{r}', t + t') - \phi(\mathbf{r}', t'))^2 \rangle \right]_{\text{ens.}}. \quad (7.2)$$

Given the results of the renormalization group analysis of the previous two sections, the long length and time asymptotics of these functions can be computed using standard matching techniques. For the momentum-shell regularization used here, this matching is most directly done in momentum and frequency space. Consider first the correlation function, which for transverse momentum \mathbf{k}_\perp and rescaling factor $1 < b \leq |\Lambda/\mathbf{k}_\perp|$ satisfies the relation

$$C(\mathbf{k}, \omega; \{\lambda_i\}) = b^{d_\perp + \zeta + z} C(\mathbf{k}_\perp b, k_x b^\zeta, \omega b^z; \{\lambda_i(b)\}). \quad (7.3)$$

Here $\{\lambda_i(b)\}$ denotes the set of running coupling constants at scale b . The prefactor on the right hand side arises from the (conventional) definition of the Fourier transform,

$$C(\mathbf{r}, t) = \int_{\mathbf{k}\omega} 2 [1 - e^{-i\mathbf{k}\cdot\mathbf{r} + i\omega t}] C(\mathbf{k}, \omega), \quad (7.4)$$

and the dimensionlessness of $\phi(\mathbf{r}, t)$.

To calculate the correlators at long length and time scales, we will choose $b = \Lambda/|\mathbf{k}_\perp| \gg 1$ and evaluate the right-hand-side of Eq. 7.3. This is simple because the rescaled correlator is evaluated at a large rescaled transverse wavevector $|\mathbf{k}_\perp|b = \Lambda$ equal to the uv cut-off, at which fluctuations are small, and therefore can be taken into account perturbatively, without encountering any infa-red divergences. However, the computation of the rescaled propagator requires a knowledge of the running couplings $\{\lambda_i(b)\}$.

These flows have been studied in Sections IV-V. Throughout, unless explicitly indicated otherwise, all running couplings *without* arguments refer to the bare couplings, i.e., $\lambda_i \equiv \lambda_i(b=1)$. It is convenient to choose $z = \zeta = 2$ and $\hat{\chi} = -d - 1$. With this choice, K_\perp and γv are invariant, i.e.

$$K_\perp(b) = K_\perp, \quad (7.5)$$

$$\gamma v(b) = \gamma v. \quad (7.6)$$

The remaining parameters behave nontrivially. The rescaled temperature and longitudinal elastic modulus follow from Eq.5.47 and Eq. 5.37, respectively:

$$T(b) \underset{b \gg 1}{\sim} \frac{2(K_\perp K_\parallel)^{1/2}}{\Lambda^{d-2} C_{d-1}} \bar{T}(b) b^{-1}, \quad (7.7)$$

$$\bar{\kappa}(b) = \bar{\kappa} b^{-2}. \quad (7.8)$$

In $d = 2$, the dimensionless temperature flows to the fixed half-line (and is hence non-universal), while in $d = 3$, it flows logarithmically to zero, i.e.

$$\bar{T}(b = e^l) \underset{b \gg 1}{\sim} \begin{cases} \bar{T}_{\text{eff}} > 1, & d = 2 \\ \pi^2/2l^2 |\ln l| & d = 3 \end{cases}. \quad (7.9)$$

For $2 < d < 3$ it flows to a universal value (see Eqs. 5.58 and 6.12), which is sadly of only formal interest since the 2.5-dimensional smectic is currently experimentally inaccessible.

The mobility is more complicated, but using Eq. 5.35 and Eq. 7.8, we obtain

$$\gamma(b) = \gamma e^{\Phi(b)}, \quad (7.10)$$

with

$$\Phi(b) = - \int_0^{\log b} dl \frac{\bar{\kappa} e^{-2l}}{1 + 2\bar{\kappa} e^{-2l}} \Gamma''(0, l). \quad (7.11)$$

The integrand in Eq. 7.11 is exponentially suppressed at large l , so that $\Phi(b)$ has a finite limit as $b \rightarrow \infty$. This implies the finite renormalization

$$\gamma(b) \underset{b \rightarrow \infty}{\sim} \gamma_R = \gamma e^{\sigma K_\parallel K_\perp \Lambda^2 / (\gamma v)^2}. \quad (7.12)$$

Because, for large v (small $\bar{\kappa}$) the integral in Eq. 7.11 is dominated by small l (due to the exponential behavior of $\kappa(l)$), the constant σ is highly nonuniversal. Above two dimensions at sufficiently high velocities and temperatures ($\bar{\kappa} \ll 1$ and $\bar{T} \gg a_0^2$ in 3d), \bar{T} flows rapidly to a unique fixed-point, and it becomes parameter-independent, with $\sigma = 2(d-2)$. For $d = 2$, σ depends upon the bare disorder strength even for $\bar{\kappa} \ll 1$, due to the semi-infinite fixed line with $\bar{T}_{\text{eff}} > 1$. More interesting is the extreme low-temperature limit, in which (see Eqs. 5.56, 5.64) $\Gamma''(0)$ becomes singular. In 3d, this limit gives

$$\sigma \approx \frac{\pi^2 a_0^2}{\bar{T} \ln(a_0/\bar{T})}, \quad \bar{T} \ll a_0^2. \quad (7.13)$$

The corresponding low-temperature regime in two dimensions is outside the limits of the controlled RG, but we expect a result similar to Eq. 7.13 to hold with, however, a_0 of order one. Note that in all cases γ_R is strongly enhanced as the velocity of the moving smectic is lowered.

The remaining flow parameter is the force-force correlator $\Delta(\phi)$. Again, we quote here the results only directly in $d = 2, 3$.

In two dimensions, the correlator is well-described asymptotically in the single-harmonic approximation (Eq. 6.3). From Eq. 6.4, $\overline{\Delta}_0$ grows linearly with b ,

$$\overline{\Delta}_0(b) \xrightarrow{b \rightarrow \infty} \tilde{\Delta} b, \quad (7.14)$$

where $\tilde{\Delta} > \Delta_0$, and for $\overline{\Delta}_1 \ll 1$ and $\overline{T} > 1/2$ can be estimated by

$$\tilde{\Delta} \approx \Delta_0 + \frac{1}{4\pi\Lambda K_\perp \gamma v} \frac{\Delta_1^2}{2\overline{T} - 1}. \quad (7.15)$$

As can be easily seen from Eq.6.5, in $d = 2$, the first harmonic flows asymptotically to zero according to

$$\Delta_1(b) \xrightarrow{b \rightarrow \infty} \tilde{\Delta}_1 b^{-(\overline{T}_{\text{eff}}-1)}. \quad (7.16)$$

In three dimensions, we have instead logarithmic flows, and simple manipulations of Eqs. 5.60–5.63 give

$$\Delta(\phi, l) \xrightarrow{b \rightarrow \infty} 2\pi\gamma v K_\perp \frac{a_0}{1 + la_0} \frac{1}{n} \min\{(\phi - \pi - 2\pi n)^2 - \pi^2\} + \tilde{\Delta}, \quad (7.17)$$

where

$$\tilde{\Delta} = 2\pi\gamma v K_\perp \left[\Gamma_0 + \frac{2\pi^2}{3} a_0 \right]. \quad (7.18)$$

We are now in a position to evaluate the right-hand-side of Eq. 7.3. Setting $b = e^l = \Lambda/|\mathbf{k}_\perp|$ and using the above results, we obtain

$$C(\mathbf{k}, \omega) = \begin{cases} \mathcal{D}^{-1}(\mathbf{k}, \omega) \left[4\pi K \gamma_R \overline{T}_{\text{eff}} + \tilde{\Delta} \delta(\omega) \right], & d = 2 \\ \mathcal{D}^{-1}(\mathbf{k}, \omega) \left[\frac{1}{k_\perp} \frac{4\pi^3 a^2 K \gamma_R}{|\ln a|} + \tilde{\Delta} \delta(\omega) \right], & d = 3 \end{cases}, \quad (7.19)$$

where

$$\mathcal{D}(\mathbf{k}, \omega) = (\gamma_R \omega - \gamma v k_x)^2 + (K_\parallel k_x^2 + K_\perp k_\perp^2)^2, \quad (7.20)$$

we have defined $K = \sqrt{K_\perp K_\parallel}$ and from Eq. 5.63, the three-dimensional logarithmic coupling constant is

$$a = \frac{a_0}{1 + a_0 \ln(\Lambda/k_\perp)}. \quad (7.21)$$

Eqs. 7.19–7.21 have simple physical significance. The first term in each of the square brackets in Eq. 7.19 represents time-dependent “thermal” fluctuations. The second, δ -function term represents a static, time-independent distortion of the smectic, and is in fact identical in form to the perturbative expressions of Section IV. This is roughly because at the uv momentum cut-off (where the rescaled correlator is evaluated), the displacement fluctuations are strongly suppressed, and dominated by the value of the random force at origin $\phi = 0$ (as in the naive Larkin approximation).

To further explore the implications of Eqs. 7.19–7.21, we now discuss the corresponding expressions in real space and time. First consider the long-time limit $C_{\text{EA}}(\mathbf{r}) = \lim_{t \rightarrow \infty} C(\mathbf{r}, t)$,

$$C_{\text{EA}}(\mathbf{r}) = \int_{\mathbf{k}} \frac{2\tilde{\Delta} [1 - e^{-i\mathbf{k} \cdot \mathbf{r}}]}{(\gamma v k_x)^2 + (K_\parallel k_x^2 + K_\perp k_\perp^2)^2}. \quad (7.22)$$

This correlator is analogous to the Edwards-Anderson correlator in a spin-glass, and represents a static but random conformation of the ϕ field that persists at long times. Performing the above integration, we find two limits. For $d < 4$ and $x < K_\parallel/\gamma v$, the static roughness *scales* isotropically (similarly to the equilibrium case), with *finite* anisotropy arising due to the difference between K_\perp and K_\parallel

$$C_{\text{EA}}(\mathbf{r}) = \frac{\tilde{\Delta}}{K} \left(\frac{K_\parallel}{K_\perp} \right)^{(d-2)/4} r_\perp^{4-d} f_\Delta^{(1)} \left(\frac{|x| K_\perp^{1/2}}{r_\perp K_\parallel^{1/2}} \right), \quad (7.23)$$

where the scaling function obeys $f_\Delta^{(1)}(x \rightarrow 0) \rightarrow \text{constant}$ and $f_\Delta^{(1)}(x \rightarrow \infty) \rightarrow x^{4-d}$. For $d \leq 3$, in the asymptotic limit $x > K_\parallel/\gamma v$, $C_\Delta(\mathbf{r})$ becomes infinitely anisotropic owing to the difference between the convective behavior along the direction of motion (x) and diffusive transport transverse to it (along r_\perp). We find

$$C_{\text{EA}}(\mathbf{r}) = \tilde{\Delta} \frac{r_\perp^{3-d}}{\gamma v K_\perp} f_\Delta^{(2)} \left(\frac{|x| K_\perp}{r_\perp^2 \gamma v} \right), \quad (7.24)$$

where the asymptotics of the scaling function are

$$f_\Delta^{(1)}(x) \propto \begin{cases} \text{constant}, & \text{for } x \rightarrow 0 \\ x^{(3-d)/2}, & \text{for } x \rightarrow \infty \end{cases}. \quad (7.25)$$

In three dimensions, the power-law in Eq. 7.24 should be replaced by the logarithm $(r_\perp)^0 \rightarrow \ln |\Lambda r_\perp|$.

The other important physical correlator measures the thermal fluctuations around the static distortion measured by C_{EA} . The thermal correlator is naturally defined as

$$C_{\text{T}}(\mathbf{r}, t) \equiv C(\mathbf{r}, t) - C_{\text{EA}}(\mathbf{r}). \quad (7.26)$$

For simplicity, we consider only the equal-time thermal fluctuations; corresponding results for non-equal times are easily obtained from Eqs. 7.19–7.21. In two dimensions, the thermal correlator is logarithmic,

$$C_{\text{T}}(\mathbf{r}, 0) \sim 2\overline{T}_{\text{eff}} \ln \sqrt{\aleph x^2 + \aleph^{-1} y^2}, \quad (7.27)$$

where $\aleph = \sqrt{K_\perp/K_\parallel}$. Note that the (in 2d nonuniversal) coefficient of the logarithm above is proportional to the effective temperature, and therefore *bounded* below! This is a consequence of the roughly semicircular RG flows in Fig. 6. It is interesting to further note that by extending above calculations to $2 + \epsilon$ dimensions, using

results of Sec.VI, we find that the logarithmic growth of thermal correlation function is in fact super-universal (i.e., independent of d) for $2 < d < 3$, with the prefactor $\overline{T}_{\text{eff}}$ above replaced by a *universal* fixed point value of $\overline{T}^* = 1 - 2\epsilon$ (Eq.6.12).

In three dimensions, the logarithmic decay of a in Eq. 7.21 renders the Fourier transform of the thermal term in Eq. 7.19 non-divergent. The thermal correlator thus *saturates* at long distances in $d = 3$,

$$C_T(\mathbf{r}, 0) \xrightarrow{|r| \rightarrow \infty} C_{T,0} \propto \frac{a_0}{|\ln a_0|}. \quad (7.28)$$

Comparing the static (EA) and thermal correlators above, we see that at any fixed time, the static contribution to $C(\mathbf{r}, t)$ dominates at long distances, i.e.

$$C(\mathbf{r}, t) \xrightarrow{|r| \rightarrow \infty} C_{\text{EA}}(\mathbf{r}). \quad (7.29)$$

Thus the naive perturbative results of section IV are essentially correct for the long-distance properties of the correlation functions. In particular, *the structure function in the smectic phase displays power-law smectic Bragg peaks (translational QLRO) in three dimensions, with fully rounded smectic peaks (translation SRO) in two dimensions.*

Similar analysis of the response function $R(\mathbf{k}, \omega)$ shows that to the leading order in disorder it is given by

$$R(\mathbf{k}, \omega) = \frac{1}{i(\gamma_R(k_\perp)\omega - \gamma v k_x) + K_\parallel k_x^2 + K_\perp k_\perp^2}, \quad (7.30)$$

and is identical to the response function in the linearized theory of Sec.III, but with a drag coefficient γ multiplying ω (but *not* k_x) replaced by the disorder enhanced renormalized $\gamma_R(k_\perp)$,

$$\gamma_R(k_\perp) = \gamma e^{\Phi(\Lambda/k_\perp)}, \quad (7.31)$$

$$\widetilde{k_\perp \ll \Lambda} \gamma_R. \quad (7.32)$$

Since γ_R is finite, the renormalized response function $R(\mathbf{k}, \omega)$ implies an *analytic* response to a uniform transverse external force, and a *finite linear* mobility γ_R^{-1} in the limit of vanishing transverse force.

We now turn our attention to the *nonlinear* dynamic response to a transverse force f_\perp . A true calculation of the non-linear response to f_\perp is beyond the current capabilities of these methods. A relatively simple scaling argument suffices, however, to obtain a rough picture of the dynamics. Consider introducing an explicit force into the MSR functional. Since it couples directly to ϕ , simple rescaling and use of the relations between the scaling exponents $\hat{\chi}$, z and ζ leads to a strong growth of the rescaled force $f_\perp(b)$ under the RG,

$$f_\perp(b) = f_\perp b^2. \quad (7.33)$$

When this rescaled force becomes large, of the order of the typical depinning force $f_c \sim \Lambda^{d/2} \sqrt{\Delta''(0)}$, it becomes a strong perturbation and the damping coefficient

γ should cease to renormalize. Choosing $f_\perp b^2 = f_c$ defines a (f_\perp -dependent) rescaling factor b at which to evaluate γ via Eqs. 7.10–7.11. This gives an effective drag coefficient

$$\gamma_{\text{eff}}(f_\perp) = \gamma_R e^{-\nu(f_\perp/f_c)}, \quad \text{for } f_\perp < f_c, \quad (7.34)$$

$$= \gamma, \quad \text{for } f_\perp > f_c, \quad (7.35)$$

where $\nu \equiv \sigma K_\parallel K_\perp \Lambda^2 / (\gamma v)^2$. Combining this result with the definition of γ

$$v_\perp(f_\perp) = \frac{f_\perp}{\gamma_{\text{eff}}(f_\perp)}, \quad (7.36)$$

we obtain a nonlinear response which interpolates between two different linear responses at small and large f_\perp , schematically displayed in Fig.7. We remark in passing that this simple argument neglects possible renormalizations of f_\perp by the random force. This occurs at zero temperature, and allows for the possibility of a true critical transverse force in that case. A careful treatment of the finite-temperature crossover to the above (generic) behavior is still an open problem.

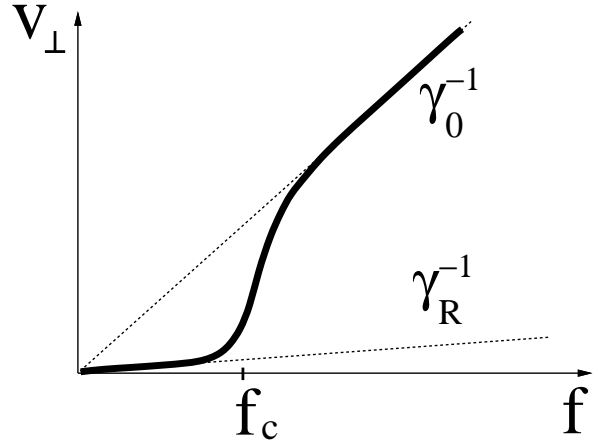


Fig.7: Schematic of the nonlinear transverse response for the moving smectic (neglecting the permeation mode). Including the permeation mode simply adds a linear function of slope μ_{perm} to the above plot.

The finite-temperature “IV” (velocity-force) curve gives an interpolation between two linear regimes, above and below f_c . For small γv , the renormalized mobility γ_R^{-1} is quite small. In this case the IV has a non-linear feature similar to that of a threshold, but nevertheless completely analytic. In addition, the permeation mode provides a second channel for transport, which further enhances the linear mobility. A possible (though highly speculative) scenario at zero temperature is a small linear mobility via the permeation of a small concentration of fluctuating defects “activated” through local chaotic dynamics, superimposed upon a sharp threshold for motion of the smectic density wave. However, we again caution

(as in the Introduction), that zero temperature dynamics may be highly nonuniversal, with qualitatively different behavior occurring in different systems.

VIII. DISCUSSION

A. Relation to previous work

Much of the recent interest in driven solids stems from the work of Koshelev and Vinokur (KV),³⁸ who applied perturbation theory to compute the mean-square displacement of the driven solid and argued that the driven system might exhibit a nonequilibrium phase transition from a moving liquid to an ordered moving solid.³⁹ The argument was based on the notion that at large velocities the effect of pinning could be described by an effective “shaking” temperature $T_{sh} \sim 1/v^2$. With this assumption, KV recast the problem into equilibrium form. This suggested only thermal roughness for the driven lattice, so that the mean square displacement would always be bounded in $d > 2$ (with translational QLRO in $d = 2$), arguing indeed for the stability of the driven lattice for $d \geq 2$.

Experiments on flux lattices in type-II superconductors have indeed shown evidence for current-induced ordering of the vortex array. This evidence has been obtained both indirectly through transport experiments^{40,41} and by directly probing the structure of a driven vortex lattice by neutron scattering⁴² and decoration experiments^{43,44}. Numerical simulations of driven vortex arrays in two dimensions also provide clear indication of ordering of the sliding lattice at large drives^{45,46,38,47}. We discuss these experiments in more detail below.

The notion that non-equilibrium effects might play an important role was addressed by Balents and Fisher¹⁶ in the simpler context of CDWs. They classified the possible phases of driven CDWs and showed that the KV predictions were violated in this case. In fact, certain static components of the quenched disorder persist in a coarse-grained model even at very large velocity. This static random force arises physically from spatial inhomogeneities in the impurity distribution and represents a sort of random drag. Therefore noise in the nonequilibrium steady state of the sliding CDW never mimics thermal noise, which is uncorrelated in time. As a result these authors concluded that the analogous moving solid phase of a CDW is stable in $3d$ at large velocities, but does not exhibit the true long-ranged translational order of an equilibrium $3d$ crystal. Rather it exhibits the algebraic decay of correlations characteristic of a $2d$ equilibrium crystal (QLRO). In $d = 2$ in contrast the moving CDW appears unstable to the proliferation of phase slips.

A similar reinvestigation of the driven lattice was recently undertaken by Giamarchi and Le Doussal (GL)²⁶. These authors focused on the behavior of fluctuations in the direction transverse to that of the driving force. They

pointed out that periodic static component of the pinning force persist in the transverse direction at large drives and suggested that motion in the driven solid occurs along elastically coupled channels parallel to the direction of motion. These authors assumed that disorder-induced displacements in the direction parallel to the driving force always remain bounded and neglected all fluctuations in this direction. They also suggested that the signature of this anisotropic sliding state, the anisotropic moving Bragg Glass (BG), would be the existence of a finite transverse critical force at zero temperature.

Considerable elements of GL’s work are retained in our calculations. The static periodic transverse force is also non-vanishing in our model, and leads to glassy channel-like motion at very low temperatures. There are, however, several key differences from GLs work. First, we give a *model independent* characterization of the possible phases. Second, we *derive* our equations of motion from a microscopic dynamics. These have a truly *non-equilibrium* form, which cannot be obtained simply by a Galilean boost of the equilibrium equations of motion. Third, we argue that the most stable driven phase is the *transverse* smectic, with *short-range* rather than long-range *longitudinal* order. Fourth, we point out the importance of the *permeation mode* in the transverse smectic, which implies a *non-zero transverse linear response at any finite temperature*. Lastly, we show that the transverse displacements themselves are much less glassy than in equilibrium, owing to the strong enhancement of thermal noise caused by the breakdown of the fluctuation dissipation theorem.

Recent simulations in $d = 2$ have confirmed the anisotropic channel structure of the sliding state.^{28,48} These simulations also indicate that dislocations with Burger’s vectors parallel to the flow are unbound, so that the intra-channel order is liquid-like. The driven array thus indeed appears more consistent with a transverse smectic phase than the moving Bragg glass.

All the aforementioned analytical treatments neglect KPZ-type nonlinearities (C coefficients in Eq. 1.11). These are perturbatively irrelevant in the smectic state, as argued above. They probably play a role in the behavior of longitudinal correlations, and may well determine the length scale at which longitudinal dislocations appear in the moving lattice, i.e., the scale at which a driven lattice is unstable to the transverse smectic. Such effects have recently been studied in a simpler model relevant for CDW motion, which contains *only* longitudinal degrees of freedom.²²

B. Experiments

As discussed in the Introduction, there are many physical realizations of dirty driven periodic media. Among these, the magnetic flux lattice in type-II superconductors is perhaps the system that has been most studied

experimentally in recent years and where our predictions can most easily be tested.

The large majority of experimental work has focused on the nonlinear transport properties of these systems for driving forces near the zero-temperature depinning threshold. Our work, in contrast, focuses on the properties of the sliding state well above threshold, where the velocity-force characteristic approaches a linear form. In this regime one is rather interested in the positional and temporal order of the sliding medium.

The positional correlations in a current-driven magnetic flux-lattice can be studied directly both by numerical simulations and experiments. Numerical work is very useful as it can provide both direct real space images of the sliding lattice as well as quantitative structural information like the structure factor. Recent simulations of two-dimensional flux lattices ($d_t = 2$, $d_l = 0$) by Moon et al.²⁸ are in agreement with our finding that the periodicity of the driven flux lattice *along* the direction of motion is absent, i.e., the sliding lattice is a smectic. Real space images of the driven lattice show that motion occurs along channels that are aligned with the direction of the driving force and periodically spaced in the transverse direction. Phase slips, however, occur at the channel boundaries, indicating that the channels are uncorrelated and the longitudinal structure is liquid-like. The structure factors obtained from these simulations show sharp algebraically-divergent peaks at the reciprocal lattice vectors \mathbf{Q} normal to the external drive. The peaks at the other reciprocal lattice vectors have a very small intensity that decays exponentially with system size. Similar results have also been obtained by other authors.^{48,49} One detailed aspect of the results of Ref. 28 which *does not* agree with our theoretical expectations is the algebraic decay of the smectic Bragg peaks. Our theory predicts in fact (possibly stretched) exponential decay, due to the linear displacement growth in Eq. 7.24. We believe the observed power-law structure factor scaling is likely a crossover phenomenon, perhaps enhanced by the dispersive elastic moduli due to the short-scale logarithmic character of the inter-vortex interaction.

One of the first direct experimental evidence of the ordering of the sliding flux lattice at large velocities was obtained some time ago by neutron diffraction⁴² These experiments have not, however, been able to quantitatively determine the structural properties of the driven state. More recently, the channel structure of the driven flux lattice was observed directly by decorating the current-driven flux array in $NbSe_2$.⁴⁴ By digitizing the decoration images Pardo et al. have also very recently obtained the structure factor of the driven array that indeed has the transverse peaks characteristic of a smectic⁵⁰.

Temporal order in the driven medium should manifest itself in narrow band noise (NBN) and mode-locking phenomena. Both of these have been studied extensively in the context of charge density waves, but have not been observed in flux lattices, indicating that the driven flux lattice lacks long-range temporal order. The spectrum

of voltage fluctuations can be probed by applying a dc current I that yields a driving force $f \sim I$ on the flux lattice. The local field induced by flux motion is given by

$$E_i(\mathbf{r}, t) = -\frac{\phi_0}{c} \epsilon_{ij} \partial_t \tilde{\phi}_j \left[\rho_0 + \sum_{\mathbf{Q}} \rho_{\mathbf{Q},0} e^{i\mathbf{Q} \cdot (\mathbf{x} - \tilde{\phi})} \right], \quad (8.1)$$

with ϕ_0 the flux quantum. In a moving solid we expect $\tilde{\phi} = \mathbf{v}t + \phi$. In a perfect lattice the local voltage contains therefore oscillatory components at the frequencies $\omega_{\mathbf{Q}} = \mathbf{Q} \cdot \mathbf{v}$. The Fourier spectrum of voltage fluctuations, defined as,

$$S(\omega) = \int_{\mathbf{r}, \mathbf{r}'} \int_t e^{i\omega t} \langle E_x(\mathbf{r}, t) E_x(\mathbf{r}', 0) \rangle, \quad (8.2)$$

will then contain, in addition to a dc component, a sharp fundamental peak at $\omega_1 = \mathbf{Q}_1 \cdot \mathbf{v}$, with $Q_1 \sim 2\pi/a$, and smaller peaks at all the higher harmonics. This type of spectrum, usually referred to as NBN, has indeed been observed in sliding CDWs and is generally regarded as the signature of the absence of appreciable phase slips in the system.⁵¹ In contrast, in a liquid phase we expect the Fourier spectrum to have a Lorentzian form, centered at the frequency ω_1 . A broad power spectrum of voltage fluctuations, with an $\omega^{-\alpha}$ decay at large frequencies, known as broad band noise (BBN), is observed in CDWs when macroscopic velocity inhomogeneities arising from phase slips are present in the driven system.⁵² NBN has not been observed in current-driven flux lattices. This is consistent with our finding that correlations along the direction of motion are always liquid-like, indicating longitudinal phase slips are present in the system.

Systems with temporal LRO should also exhibit *complete* mode-locking. Mode locking is an interference effect that can occur in a periodic medium driven by both a dc and an ac force. Keeping fixed the amplitude and the frequency of the ac force and varying the amplitude of the dc component, one observes steps in the dc response, known as Shapiro steps. These steps arise from mode locking of the frequency of the applied ac force with the internal oscillation frequencies $\omega_{\mathbf{Q}}$ of the periodic medium. *Complete* mode locking (steps in the dc response that remain constant over some finite range of dc bias) to an arbitrarily weak external ac drive has again been observed in CDWs.⁵³ Assuming, as our calculations suggest, that the driven flux lattice has only short-range longitudinal order (i.e. SRO for wavevectors with non-zero $\omega_{\mathbf{Q}}$), we would expect at best *incomplete* mode locking above a non-zero (perhaps large) threshold ac drive. For (2+1)-dimensional flux lattices again no complete mode locking is expected in the smectic state, as the driven lattice only has quasi-Bragg peaks along the direction in wavevector space perpendicular to the velocity. If a longitudinally ordered phase (“Bragg glass”) were stable in 3d, it ought to exhibit mode locking and NBN; the available experimental evidence seems not to support this possibility.

Finally, it has been suggested that a sliding flux lattice will exhibit a finite threshold force for response to an additional driving force f_{\perp} transverse to the mean velocity^{26,28} and no transverse linear response at zero temperature. The behavior in a purely dissipative (over-damped) model at zero temperature is somewhat non-universal, and indeed, such a transverse critical force is certainly likely *in many possible phases, including both the smectic and Bragg glass (BG)*. At *finite* temperature, a sharper distinction can be drawn. A naive extrapolation of the Bragg glass theory to finite temperature would predict an *exponentially small, non-linear* transverse response at finite temperatures,

$$v_{\perp}^{\text{BG}} \sim \exp \left[- \left(\frac{f_0}{f_{\perp}} \right)^{\Upsilon} \right], \quad (8.3)$$

with $f_0^{\Upsilon} \propto 1/T$ at low temperatures and small f_{\perp} . Eq. 8.3 relies, however, upon two assumptions: (1) density fluctuations (the permeation mode) can be neglected and (2) the $T = 0$ fixed point is stable. Our works shows that both these assumptions are incorrect and invalidates Eq. 8.3. As discussed, in Section VI, we then expect a velocity-force curve with the crossover behavior shown in Fig. 7. For low transverse driving forces there are two small (but nonzero) *linear* components to the mobility, i.e.

$$v_{\perp}^{\text{sm.}} \sim (\mu_{\text{dw.}} + \mu_{\text{perm.}}(T)) f_{\perp}. \quad (8.4)$$

The mobility of the density wave, $\mu_{\text{dw.}}$, has been estimated in Sec.VII. It is activated at low temperatures, and also suppressed for small sliding (longitudinal) velocities, with the form

$$\mu_{\text{dw.}} = \gamma_R^{-1} \approx \gamma^{-1} e^{-\sigma K_{\parallel} K_{\perp} \Lambda^2 / (\gamma v)^2}, \quad (8.5)$$

where $\sigma \propto 1/T$ at very low temperatures (more details are given in the discussion following Eq. 7.12). The second term is a mobility associated with the permeation mode:

$$\mu_{\text{perm.}}(T) \sim \mu_0 e^{-U_d/T}, \quad (8.6)$$

for $T \ll U_d$. Although we have not analytically derived the above exponential form of the mobility, it seems extremely likely on physical grounds. Such behavior arises from an activated concentration of mobile defects (vacancies or interstitials in 2d, kinks and/or vacancy/interstitial lines in 3d) with finite “energy” cost U_d . These flow linearly in response to a driving force with mobility μ_0 . Additional non-linear behavior will be superimposed upon this linear term, but it is subdominant at small f_{\perp} . At low temperatures these non-linearities sharpen to a threshold-like feature around a finite $f_{\perp c}$, so that the identification of an experimental system as either a BG or a smectic by the transverse “threshold” or critical current may be misleading.

C. Open questions

We conclude with a summary of some of the many remaining open questions. Eqs. 1.11 provide for the first time a complete set of hydrodynamic equations to describe nonequilibrium states of driven periodic media. A systematic RG (or other) treatment of them is, however, daunting. Aside from the obvious algebraic complexity, the structure of the equations also raises some interesting conceptual issues. Naively, since first derivative terms are present in all the variables, all spatial coordinates seem to scale isotropically, with dynamical exponent $z = 1$. This power counting, however, is inconsistent with direct perturbative (and more sophisticated) calculations of physical quantities. Preliminary investigations of this problem suggests novel scaling without unique anisotropy or dynamical exponents.²⁵ A more modest goal, requiring only straightforward (if rather tedious) calculations is to extend the RG treatment of the smectic to include the permeation mode, i.e., the coupling to density fluctuations, as described by Eqs. 4.6–4.7.

A systematic treatment of topological defects in disordered lattices is also lacking. Some recent progress along these lines was made recently for equilibrium elastic glasses in Ref. 12 – it remains to be seen whether this work can be extended to driven systems. When dislocations are present, many interesting questions remain at zero temperature⁵⁴. A possible plastic depinning transition and its properties – the associated scaling, noise, and hysteresis – are not presently understood.

Finally, an extremely interesting line of inquiry is to explore how some of the techniques used here might be extended to inertial models appropriate for friction and lubrication. Such systems presumably are controlled not only by the physics described here, but also by nontrivial mechanisms of dissipation and possibly chaotic dynamics.

ACKNOWLEDGMENTS

It is a pleasure to acknowledge discussions with Matthew Fisher. L. Radzihovsky acknowledges discussions with John Toner. L. Balents was supported by the NSF PHY94–07194. M.C. Marchetti was supported by the NSF through Grant DMR–9419257. L. Radzihovsky acknowledges support by the NSF CAREER award, through Grant DMR–9625111, and partial support by the A.P. Sloan Foundation.

APPENDIX A

In this appendix we carry out the mode-elimination needed to coarse-grain the driven lattice in a *periodic*

potential. Expanding the $e^{-\tilde{S}_1}$ within the brackets in Eq. 2.22 to first order gives

$$\delta S_{\text{eff.}}^{(1)} = - \sum_{\mathbf{x}} \int_{\mathbf{z}t} \left\langle [\hat{u}_{<i}(\mathbf{r}, t) + \hat{u}_{>i}(\mathbf{r}, t)] \times \tilde{F}_i[\mathbf{x} + \mathbf{u}_{<}(\mathbf{r}, t) + \mathbf{u}_{>}(\mathbf{r}, t) + \mathbf{v}t, \mathbf{z}] \right\rangle_{0>} . \quad (8.7)$$

This average can be evaluated by expanding the force $\tilde{\mathbf{F}}$ in $\mathbf{u}_{>}$ and averaging over the fast modes term by term. However, in the absence of thermal noise, the only non-zero fast correlator is the response function, which vanishes by causality at equal times. Since all the fields in the first order term are at equal time, all the terms involving *any* $\mathbf{u}_{>}$ or $\hat{\mathbf{u}}_{>}$ fields are zero, and this average simply gives

$$\delta S_{\text{eff.}}^{(1)} = - \sum_{\mathbf{x}} \int_{\mathbf{z}t} \hat{u}_{<i}(\mathbf{r}, t) \tilde{F}_i[\mathbf{x} + \mathbf{u}_{<}(\mathbf{r}, t) + \mathbf{v}t, \mathbf{z}]. \quad (8.8)$$

To leading order, then, the force is unrenormalized.

The first non-trivial correction arises at second order. This effect is actually physically transparent. At first order the fast modes simply respond linearly to the adiabatic motion of the slow modes. However, because of the mode coupling, this response is fed back and felt *at second order* by the slow modes again. It is this feedback that corrects the motion of the slow degrees of freedom, and is perturbatively estimated in the next correction. This is given by

$$\delta S_{\text{eff.}}^{(2)} = - \frac{1}{2} \sum_{\mathbf{x}\mathbf{x}'} \int_{\mathbf{z}\mathbf{z}'t't'} \left\langle \hat{u}_i \hat{u}'_j \times \tilde{F}_i[\mathbf{x} + \mathbf{u} + \mathbf{v}t, \mathbf{z}] \tilde{F}_j[\mathbf{x}' + \mathbf{u}' + \mathbf{v}t', \mathbf{z}'] \right\rangle_{0>}^c, \quad (8.9)$$

where we have indicated the arguments of \mathbf{u} and $\hat{\mathbf{u}}$ by the presence or absence of a prime, and furthermore suppressed the mode decomposition. The superscript *c* indicates a cumulant, or disconnected average, meaning that

$$\delta f_i[\mathbf{u}_{<}, \mathbf{r}, t] = \sum_{\mathbf{x}'} \int_{\mathbf{z}'t'} \sum_{\mathbf{Q}} iQ_i Q_j Q_k e^{i\mathbf{Q} \cdot (\mathbf{x} - \mathbf{x}' + \mathbf{u} - \mathbf{u}' + \mathbf{v}(t-t'))} |U_{\mathbf{Q}}|^2 G_{jk}(\mathbf{r} - \mathbf{r}', t - t'). \quad (8.13)$$

This is greatly simplified by gradient expanding the difference in displacement fields

$$\mathbf{u} - \mathbf{u}' \approx (\mathbf{r} - \mathbf{r}')^\alpha \partial_\alpha \mathbf{u} + (t - t') \partial_t \mathbf{u} - \frac{1}{2} (\mathbf{r} - \mathbf{r}')^\alpha (\mathbf{r} - \mathbf{r}')^\beta \partial_\alpha \partial_\beta \mathbf{u}. \quad (8.14)$$

We then obtain an expansion for the force corrections,

$$\delta f_i = \sum_{\mathbf{x}'} \int_{\mathbf{z}'t'} \sum_{\mathbf{Q}} iQ_i Q_j Q_k |U_{\mathbf{Q}}|^2 e^{i\mathbf{Q} \cdot (\mathbf{x}' + \mathbf{v}t')} G_{jk}(\mathbf{r}', t') \mathcal{F}[\mathbf{u}_{<}], \quad (8.15)$$

where

$$\mathcal{F}[\mathbf{u}] = 1 + iQ_l \left[x'^m \partial_m + t' \partial_t - \frac{1}{2} (x'^m x'^n \partial_m \partial_n + z'^a z'^b \partial_a \partial_b) \right] u^l, \\ - \frac{1}{2} Q_l Q_m r'^\alpha r'^\beta \partial_\alpha u^l \partial_\beta u^m + \dots \quad (8.16)$$

Including these corrections into the effective action gives Eq. 2.24 in the main text.

half of the square of $\delta S_{\text{eff.}}^{(2)}$ is subtracted off, as demanded by the logarithm in Eq. (2.22). As we saw earlier, only non-equal-time response functions can survive the average. This can occur *only* via the first order expansion of the displacement field out of one of the force terms, to be contracted against the response field at the non-equal time. Taking into account the two ways in which this can be achieved gives the result

$$\delta S_{\text{eff.}}^{(2)} = - \sum_{\mathbf{x}\mathbf{x}'} \int_{\mathbf{z}\mathbf{z}'t't'} \hat{u}_{<i} \partial_k \tilde{F}_i[\mathbf{x} + \mathbf{u}_{<} + \mathbf{v}t, \mathbf{z}] \times \tilde{F}_j[\mathbf{x}' + \mathbf{u}'_{<} + \mathbf{v}t', \mathbf{z}'] G_{jk}(\mathbf{r} - \mathbf{r}', t - t'). \quad (8.10)$$

Here the response function is (in matrix form)

$$G(\mathbf{q}, \omega) = \left[i\omega I + K(\mathbf{q}) \right]^{-1} \theta(|q| - \Lambda). \quad (8.11)$$

The θ -function indicates that only a partial mode elimination has been performed, so that the slow modes remain as dynamical variables in the coarse-grained theory. Generally, however, the expressions obtained in this section have smooth limits as $\Lambda \rightarrow 0$, and are well approximated therefore by using the response function in the full Brillouin zone.

Using the Fourier decomposition, Eq. 2.23, the second order contribution to the effective action can then be cast into the form

$$\delta S_{\text{eff.}}^{(2)} = - \sum_{\mathbf{x}} \int_{\mathbf{z}t} \hat{u}_{<i} \delta f_i[\mathbf{u}_{<}, \mathbf{r}, t], \quad (8.12)$$

where δf_i may be interpreted as an additional effective force in the coarse-grained equation of motion for the slow modes $\mathbf{u}_{<}$. The dominant terms in δf_i are those which do not oscillate as \mathbf{x} is varied. Keeping only these, it takes the form

APPENDIX B

Here we present the details of mode elimination for a lattice driven over a *disordered* potential. Expanding S_1 from the exponential ($e^{-\tilde{S}}$) and averaging it perturbatively over the modes outside of the cut-off gives, to linear order in S_1 ,

$$\langle S_1 \rangle > = \delta S_{\text{eff.}}^{(1a)} + \delta S_{\text{eff.}}^{(1b)}, \quad (8.17)$$

where the first term is, as before

$$\delta S_{\text{eff.}}^{(1a)} = S_1[\mathbf{u} \rightarrow \mathbf{u}_<], \quad (8.18)$$

and simply returns the uncorrected bare random force. The next correction is

$$\delta S_{\text{eff.}}^{(1b)} = \sum_{\mathbf{x}, \mathbf{x}'} \int_{\mathbf{z}\mathbf{z}'t't'} \hat{u}^i(\mathbf{r}, t) G_{jk}(\mathbf{r} - \mathbf{r}', t - t') \times \partial_i \partial_j \partial_k \tilde{\Gamma}[\mathbf{r} - \mathbf{r}' + \mathbf{u}(\mathbf{r}, t) - \mathbf{u}(\mathbf{r}', t') + \mathbf{v}(t - t')]. \quad (8.19)$$

Using Eq. (8.14), this becomes

$$\delta S_{\text{eff.}}^{(1b)} = \sum_{\mathbf{x}, \mathbf{x}'} \int_{\mathbf{z}\mathbf{z}'t't'} \hat{u}^i \left\{ \tilde{\Gamma}_{ijkl}[\mathbf{x}' - \mathbf{v}_0 t', \mathbf{z}'] \right. \quad (8.20)$$

This is explicitly

$$\delta S_{\text{eff.}}^{(2)} = -\frac{1}{8} \sum_{\Gamma=4}^6 \left\langle \hat{u}_1^i \hat{u}_2^j \tilde{\Gamma}_{ij}[\mathbf{x}_1 - \mathbf{x}_2 + \mathbf{u}_1 - \mathbf{u}_2 + \mathbf{v}(t_1 - t_2), \mathbf{z}_1 - \mathbf{z}_2] \times \hat{u}_3^k \hat{u}_4^l \tilde{\Gamma}_{kl}[\mathbf{x}_3 - \mathbf{x}_4 + \mathbf{u}_3 - \mathbf{u}_4 + \mathbf{v}(t_3 - t_4), \mathbf{z}_3 - \mathbf{z}_4] \right\rangle_{0>}^C, \quad (8.22)$$

where we introduced the obvious abbreviation for the four lattice sums and longitudinal space and time integrals. This expectation value contains several terms, depending upon the number of $\hat{\mathbf{u}}$ fields which are contracted to give response functions. Terms with one contraction leave 3 response fields, which represents the generation of a skewness to the distribution of the random force, and can be neglected in what follows. Forming three contractions leaves a single response field, which will give higher-order corrections to the coefficients determined above, and can thus also be neglected (for weak disorder). Forming two contractions leaves two response fields, which is of the proper form to renormalize the random force.

To obtain these terms, the $\tilde{\Gamma}$'s must be expanded to second order in the fast fields $\mathbf{u}_>$. This gives

$$\delta S_{\text{eff.}}^{(2)} = -\frac{1}{8} \sum_{\Gamma=4}^6 \left[\tilde{\Gamma}_{ijm}(12) \tilde{\Gamma}_{klm}(34) \left\langle \hat{u}_1^i \hat{u}_2^j (u_{1>}^m - u_{2>}^m) \hat{u}_3^k \hat{u}_4^l (u_{3>}^n - u_{4>}^n) \right\rangle_{>0}^C + \tilde{\Gamma}_{ijmn}(12) \tilde{\Gamma}_{kl}(34) \left\langle \hat{u}_1^i \hat{u}_2^j (u_{1>}^m - u_{2>}^m) (u_{1>}^n - u_{2>}^n) \hat{u}_3^k \hat{u}_4^l \right\rangle_{>0}^C \right], \quad (8.23)$$

where we have now also abbreviated the arguments of the force correlators. The contractions inside the angular brackets can still be performed in several ways. Each such choice gives rise to a separate term containing two response functions and a combination of slow fields at different space-time points. To determine the desired correction to the random force correlator, we keep only the leading term in a gradient expansion of the slow fields (i.e. zeroth order in the gradients). Lengthy but simple calculation gives

$$\delta S_{\text{eff.}}^{(2)} = \frac{1}{2} \sum_{\mathbf{x}, \mathbf{x}'} \int_{\mathbf{z}\mathbf{z}'t't'} \hat{u}^i(\mathbf{r}, t) \hat{u}^j(\mathbf{r}', t') \delta \Gamma_{ij}[\mathbf{x} - \mathbf{x}' + \mathbf{u}_< - \mathbf{u}'_< + \mathbf{v}(t - t'), \mathbf{z} - \mathbf{z}'], \quad (8.24)$$

where the renormalization of the force-force correlator is

$$\times \left[r'^\alpha \partial_\alpha u_l + t' \partial_{t'} u_l - \frac{1}{2} r'^\alpha r'^\beta \partial_\alpha \partial_\beta u_l \right] + \frac{1}{2} \tilde{\Gamma}_{ijklm}[\mathbf{x}' + \mathbf{v}t', \mathbf{z}'] r'^\alpha r'^\beta \partial_\alpha u_l \partial_\beta u_m \left. \right\} G_{jk}(\mathbf{r}', t'),$$

where we have abbreviated $\Gamma_{ij\dots} = \partial_i \partial_j \dots \Gamma$. This correction to the effective action again represents gradient terms in the coarse-grained equation of motion, of the form of Eq. (2.24). Extracting these coefficients, we obtain the formulae quoted in Section II.B.2 for the derivative coefficients γ, A, B and C .

It remains to consider the renormalization of the force term itself. This vanished in the case of the periodic force, due to the (assumed) incommensurability of the lattice and the substrate. The random potential, however, has Fourier components commensurate with the moving lattice, which thereby generates such a renormalization. To evaluate it, however, we must go to higher order in the disorder variance $\tilde{\Gamma}$. In particular, we consider the second correction term

$$\delta S_{\text{eff.}}^{(2)} = -\frac{1}{2} \langle S_1^2 \rangle_{0>}^C. \quad (8.21)$$

$$\begin{aligned}
\delta\tilde{\Gamma}_{ij}[\mathbf{x}, \mathbf{z}] = & \\
& - \sum_{12} \tilde{\Gamma}_{ikm}[\mathbf{x}-\mathbf{x}_1-\mathbf{v}t_1, \mathbf{z}-\mathbf{z}_1] \tilde{\Gamma}_{jln}[\mathbf{x}+\mathbf{x}_2+\mathbf{v}t_2, \mathbf{z}+\mathbf{z}_2] G_{kn}(1) G_{lm}(2) \\
& + 2 \sum_{12} \tilde{\Gamma}_{ikm}[\mathbf{x}-\mathbf{x}_1-\mathbf{v}t_1, \mathbf{z}-\mathbf{z}_1] \tilde{\Gamma}_{jln}[\mathbf{x}_2+\mathbf{v}t_2, \mathbf{z}_2] G_{kn}(1) G_{lm}(2-1) \\
& + \tilde{\Gamma}_{ijmn}[\mathbf{x}, \mathbf{z}] \sum_{12} \tilde{\Gamma}_{kl}[\mathbf{x}_1-\mathbf{x}_2+\mathbf{v}(t_1-t_2), \mathbf{z}_1-\mathbf{z}_2] G_{km}(1) G_{ln}(2) \\
& - \tilde{\Gamma}_{ijmn}[\mathbf{x}, \mathbf{z}] \sum_{12} \tilde{\Gamma}_{kl}[\mathbf{x}+\mathbf{x}_1-\mathbf{x}_2+\mathbf{v}(t_1-t_2), \mathbf{z}+\mathbf{z}_1-\mathbf{z}_2] G_{km}(1) G_{ln}(2) \\
& + \sum_{12} \tilde{\Gamma}_{ilmn}[\mathbf{x}_1+\mathbf{v}t_1, \mathbf{z}_1] \tilde{\Gamma}_{kj}[\mathbf{x}+\mathbf{x}_2+\mathbf{v}t_2, \mathbf{z}+\mathbf{z}_2] G_{lm}(1) G_{kn}(2) \\
& - \sum_{12} \tilde{\Gamma}_{ilmn}[\mathbf{x}_1+\mathbf{v}t_1, \mathbf{z}_1] \tilde{\Gamma}_{kj}[\mathbf{x}+\mathbf{x}_2+\mathbf{v}t_2, \mathbf{z}+\mathbf{z}_2] G_{lm}(1) G_{kn}(2-1). \tag{8.25}
\end{aligned}$$

Integrating this horrendous equation over \mathbf{r} , one obtains the formula for g_{ij} quoted in the text.

APPENDIX C

Here we estimate the correlator of the nonequilibrium part of the static random force, g_{ij} , given in Eq. 2.51 in the limit of large sliding velocity v . First we note that as g_{ij} is a symmetric tensor, it can be written as

$$g_{ij} = g_0(\delta_{ij} - \hat{v}_i \hat{v}_j) + g_1 \hat{v}_i \hat{v}_j, \tag{8.26}$$

where $\hat{\mathbf{v}} = \mathbf{v}/v$ and

$$\begin{aligned}
g_0 + g_1 = & \int_{\mathbf{q}} q^2 q_k q_l q_m q_n |\Gamma(\mathbf{q})|^2 G_{km}(\mathbf{q}, \mathbf{q}_t \cdot \mathbf{v}) \\
& \times [G_{ln}(\mathbf{q}, -\mathbf{q}_t \cdot \mathbf{v}) - G_{ln}(\mathbf{q}, \mathbf{q}_t \cdot \mathbf{v})], \tag{8.27}
\end{aligned}$$

and

$$\begin{aligned}
g_1 = & \sum_{\mathbf{Q} \neq 0} \int_{\mathbf{k}} \int_{q_z} [(\mathbf{k} + \mathbf{Q}) \cdot \hat{\mathbf{v}}]^2 (k+Q)_k (k+Q)_l (k+Q)_m (k+Q)_n |\Gamma(\mathbf{k} + \mathbf{Q})|^2 \\
& \times G_{km}(\mathbf{k}, q_z, (\mathbf{k} + \mathbf{Q}) \cdot \mathbf{v}) [G_{ln}(\mathbf{k}, q_z, -(\mathbf{k} + \mathbf{Q}) \cdot \mathbf{v}) - G_{ln}(\mathbf{k}, q_z, (\mathbf{k} + \mathbf{Q}) \cdot \mathbf{v})]. \tag{8.29}
\end{aligned}$$

We now split the reciprocal lattice vector sum in Eq. (8.29) in two parts by separating out the terms with $\mathbf{Q} \cdot \mathbf{v} = 0$ and write

$$g_1 = g_1^{(1)} + g_1^{(2)}. \tag{8.30}$$

The term $g_1^{(1)}$ denotes the contribution to g_1 from the sum over reciprocal lattice vectors satisfying $\mathbf{Q} \cdot \mathbf{v} \neq 0$. In this term we neglect everywhere k compared to Q and obtain

$$\begin{aligned}
g_1^{(1)} \approx & \sum_{\mathbf{Q} \cdot \mathbf{v} \neq 0} (\mathbf{Q} \cdot \hat{\mathbf{v}})^2 Q_k Q_l Q_m Q_n |\Gamma(\mathbf{Q})|^2 \int_{\mathbf{k}, q_z} G_{km}(\mathbf{k}, q_z, \mathbf{Q} \cdot \mathbf{v}) \\
& [G_{ln}(\mathbf{k}, q_z, -\mathbf{Q} \cdot \mathbf{v}) - G_{ln}(\mathbf{k}, q_z, \mathbf{Q} \cdot \mathbf{v})]. \tag{8.31}
\end{aligned}$$

In the limit $v \gg 2\pi\gamma/(ac)$, with c a typical elastic constant, we can now approximate the elastic propagators in Eq. (8.31) by neglecting the in-plane elastic matrix compared to the frequency $\gamma\mathbf{Q} \cdot \mathbf{v}$, i.e.,

$$G_{km}(\mathbf{k}, q_z, \mathbf{Q} \cdot \mathbf{v}) \approx \frac{\delta_{km}}{c_{44}q_z^2 + i\gamma\mathbf{Q} \cdot \mathbf{v}} \quad (8.32)$$

By inserting Eq. (8.32) into Eq. (8.31), we obtain

$$g_1^{(1)} \approx 2\rho_0 \sum_{\mathbf{Q} \cdot \mathbf{v} \neq 0} (\mathbf{Q} \cdot \hat{\mathbf{v}}_0)^2 Q^4 |\Gamma(Q)|^2 \times \int_{q_z} \frac{(\gamma\mathbf{Q} \cdot \mathbf{v})^2}{[(c_{44}q_z^2)^2 + (\gamma\mathbf{Q} \cdot \mathbf{v})^2]^2}. \quad (8.33)$$

For $d_l = 0$ this gives

$$g_1^{(1)} \approx \frac{2\rho_0}{\gamma^2 v^2} \sum_{\mathbf{Q} \cdot \mathbf{v}_0 \neq 0} Q^4 |\Gamma(Q)|^2 \approx \left(\frac{\Gamma(Q=0)}{\gamma v} \right)^2 \frac{1}{\xi^6} \approx \left(\frac{\Delta}{\gamma v a} \right)^2, \quad (8.34)$$

where $\Delta \approx \Gamma(Q=0)a/\xi$ is the variance of the equilibrium part of the static pinning force defined in Eq. 3.8. For $d_l = 1$ the q_z -integral is easily performed, with the result,

$$g_1^{(1)} \approx \frac{3\rho_0}{8\sqrt{2c_{44}}} \frac{1}{(\gamma v)^{3/2}} \sum_{\mathbf{Q} \cdot \mathbf{v} \neq 0} |Q_x| Q^4 |\Gamma(Q)|^2 \approx \frac{\Delta^2}{(a\gamma v)^{3/2} \sqrt{c_{44} a \xi^2}}. \quad (8.35)$$

In the contribution $g_1^{(2)}$ from the $\mathbf{Q} \cdot \mathbf{v} = 0$ of the reciprocal lattice vector sum the integral over \mathbf{k} is dominated by k near the center of the Brillouin zone. In this term we can therefore approximate the elastic propagators by their long wavelength form, given in Eqs. 3.13 and 3.14. After some lengthy algebra, one can show that in the limit of large sliding velocities, $v \gg 2\pi\gamma/(ac_{66})$, $g_1^{(2)} \sim (\xi/a)g_1^{(1)}$ and is therefore negligible for short-ranged pinning potentials.

The evaluation of g_0 can be performed by the same method, with the result

$$g_0 \sim g_1 \frac{a}{\xi}, \quad d_l = 0, \\ g_0 \sim g_1 \ln(a/\xi), \quad d_l = 1. \quad (8.36)$$

In summary, we find that at large sliding velocities both components g_0 and g_1 of the correlator of the nonequilibrium part of the static random force have the same asymptotic dependence on v and the disorder strength Δ , with

$$g_{0,1} \approx \frac{\Delta^2}{v^{(2d_t - d_l)/2}}. \quad (8.37)$$

Here we examine the predictions of the perturbation theory described in Section III for the real-space decay of positional correlations in a d_t -dimensional lattice of magnetic flux lines ($d_l = 1$), driven in the x direction. To obtain the mean-square displacement in real space, we need to evaluate integrals of the form,

$$B(\mathbf{r}) = 2 \int'_{\mathbf{q}_t, q_z} \frac{1 - \cos(\mathbf{q} \cdot \mathbf{r})}{(\gamma v q_x)^2 + [c q_t^2 + c_{44} q_z^2]^2}, \quad (8.38)$$

where c stands for either c_{66} or $c_{11} + c_{66}$ and the prime denotes a cutoff at $|q_\perp| = \Lambda$. The integrals over q_x and q_z are easily performed. Letting $u = q_\perp x_\perp$, one obtains,

$$B(\mathbf{r}) = \frac{|y|^{2-d_t}}{\sqrt{c c_{44} \gamma v}} \mathcal{F}_1^{(d_t)}(s, \zeta, \Lambda|y|), \quad (8.39)$$

where $s = |x|c/(v\gamma y^2)$ and $\zeta = \sqrt{c/c_{44}}|z|/|y|$. The scaling function $\mathcal{F}_1^{(d_t)}(s, \zeta, \Lambda|y|)$ is given by

$$\mathcal{F}_1^{(d_t)}(s, \zeta, \Lambda|x_\perp|) = \int \frac{d\hat{\mathbf{u}}}{(2\pi)^{d_t-1}} \int_0^{\Lambda y} u^{d_t-3} \left\{ 1 - \cos(\hat{\mathbf{y}} \cdot \mathbf{u}) \times \left[\cosh(\zeta u) - \frac{1}{2} e^{-\zeta u} \Phi\left(\sqrt{s}u - \frac{\zeta}{2\sqrt{s}}\right) - \frac{1}{2} e^{\zeta u} \Phi\left(\sqrt{s}u + \frac{\zeta}{2\sqrt{s}}\right) \right] \right\}. \quad (8.40)$$

Here \mathbf{u} is a $(d_t - 1)$ -dimensional vector, with $\hat{\mathbf{u}} = \mathbf{u}/u$, and $\Phi(x)$ is the error function. We are interested in the asymptotic behavior of the scaling function for $d_t = 2$. For $\zeta = 0$ we find

$$\mathcal{F}_1^{(2)}(s \rightarrow 0, 0, \Lambda|y|) \sim \ln(\Lambda|y|), \\ \mathcal{F}_1^{(2)}(s \gg 1, 0, \Lambda|y|) \sim \ln\left(\frac{c\Lambda^2|x|}{\gamma v}\right). \quad (8.41)$$

For $\zeta \gg 1$, or $|z| \gg |y|\sqrt{c_{44}/c}$,

$$\mathcal{F}_1^{(2)}(s \rightarrow 0, 0, \Lambda|y|) \sim \ln\left(\frac{|z|}{\Lambda} \sqrt{\frac{c}{c_{44}}}\right), \\ \mathcal{F}_1^{(2)}(s \gg 1, 0, \Lambda|y|) \sim \ln\left(\frac{|x|c}{v\gamma y^2}\right). \quad (8.42)$$

The scaling of the mean square displacement is therefore anisotropic, but logarithmic in all directions.

APPENDIX E

In this appendix we outline the details of the $2 + \epsilon$ RG calculation for the single Fourier mode driven smectic model defined by Eq.6.7 in Sec.VI of the main text. It is convenient to employ the Martin-Siggia-Rose (MSR) formalism²⁴. In this formalism one studies the dynamic generating functional Z which is a trace over the displacements $\phi(\mathbf{r}, t)$, with the constraint that $\phi(\mathbf{r}, t)$ satisfies the equation of motion Eq.6.7, imposed via a functional δ -function as an integral over a response field $\hat{\phi}(\mathbf{r}, t)$. Averaging over the noise $\eta(\mathbf{r}, t)$ and the quenched random force $F_p[\phi(\mathbf{r}, t), \mathbf{r}]$, the problem can be recast in the form of a dynamical field theory,

$$Z = \int [d\hat{\phi} d\phi] e^{-S_0[\hat{\phi}, \phi] - S_1[\hat{\phi}, \phi]}, \quad (8.43)$$

where in addition to the standard quadratic part of the action S_0

$$S_0 = \int_{\mathbf{r}, t} \left[\hat{\phi}(\mathbf{r}, t) \{ \gamma(\partial_t + v\partial_x) - (K_{\parallel}\partial_x^2 + K_{\perp}\nabla_{\perp}^2) \} \phi(\mathbf{r}, t) - \gamma T \hat{\phi}(\mathbf{r}, t)^2 \right], \quad (8.44)$$

there is a contribution S_1 due to disorder

$$S_1 = -\frac{1}{2} \int_{\mathbf{r}, t, t'} \hat{\phi}(\mathbf{r}, t) \hat{\phi}(\mathbf{r}, t') \Delta_1 \cos[q_0(\phi(\mathbf{r}, t) - \phi(\mathbf{r}, t'))]. \quad (8.45)$$

In the above, after averaging over disorder we have kept only the most relevant lowest Fourier component of the random force correlation function. We have also deformed the functional integral contour over the response field $\hat{\phi}$ to the imaginary axis.

We employ the standard momentum shell renormalization group transformation⁵⁵, by writing the displacement field as $\phi(\mathbf{r}, t) = \phi^{<}(\mathbf{r}, t) + \phi^{>}(\mathbf{r}, t)$, integrating perturbatively in Δ_1 the high wavevector field $\phi^{>}(\mathbf{r}, t)$ nonvanishing for $\Lambda e^{-l} < q_{\perp} < \Lambda$ (with no cutoff on the momentum along the direction of motion q_x and on ω), and rescaling the lengths, the time, and long wavelength part of the fields with

$$\mathbf{x}_{\perp} = \mathbf{x}'_{\perp} e^l, \quad (8.46a)$$

$$x = x' e^{\zeta l}, \quad (8.46b)$$

$$t = t' e^{z l}, \quad (8.46c)$$

$$\phi^{<}(\mathbf{r}, t) = e^{\chi l} \phi(\mathbf{r}', t'), \quad (8.46d)$$

$$\hat{\phi}^{<}(\mathbf{r}, t) = e^{\tilde{\chi} l} \hat{\phi}(\mathbf{r}', t'), \quad (8.46e)$$

so as to restore the ultraviolet cutoff back to Λ . Because the random-force correlator Δ_1 term is a periodic function of ϕ , it is convenient (but not necessary) to take the arbitrary field dimension $\chi = 0$, thereby preserving the

period $2\pi/q_0$ under the renormalization group transformation. Under this transformation the resulting effective free energy functional can be restored into its original form Eqs.8.44–8.45 with the effective l -dependent couplings. To zeroth order we obtain:

$$\frac{d\gamma(l)}{dl} = (d_{\perp} + \zeta + \hat{\chi})\gamma(l) \quad (8.47a)$$

$$\frac{d\gamma v(l)}{dl} = (d_{\perp} + z + \hat{\chi})\gamma v(l) \quad (8.47b)$$

$$\frac{dK_{\perp}(l)}{dl} = (d_{\perp} + \zeta + z - 2 + \hat{\chi})K_{\perp}(l) \quad (8.47c)$$

$$\frac{dK_{\parallel}(l)}{dl} = (d_{\perp} - \zeta + z + \hat{\chi})K_{\parallel}(l) \quad (8.47d)$$

$$\frac{d\Delta_1(l)}{dl} = (d_{\perp} + \zeta + 2z + 2\hat{\chi})\Delta_1(l) \quad (8.47e)$$

$$\frac{dT\gamma(l)}{dl} = (d_{\perp} + \zeta + z + 2\hat{\chi})T\gamma(l) \quad (8.47f)$$

As in the calculation of Sec.V statistical symmetry under an arbitrary time-independent shift of the displacement field $\phi(\mathbf{r}, t) \rightarrow \phi(\mathbf{r}, t) + f(\mathbf{r})$ (time-translational invariance) guarantees that γv , K_{\perp} and K_{\parallel} do not acquire any graphical corrections, i.e. their flow equations above are *exact*. Imposing this requirement at the tree level on the first two coefficients, and using Eq.8.47a we obtain $\zeta = 2$ and $\hat{\chi} = -d_{\perp} - z$.

More generally but equivalently we look at the dimensionless coupling constants

$$\bar{T} \equiv \frac{T}{2(K_{\perp}K_{\parallel})^{1/2}} C_{d-1} \Lambda^{d-2} \quad (8.48)$$

$$\bar{\Delta}_1 \equiv \frac{\Delta_1}{K_{\perp}\gamma|v|} C_{d-1} \Lambda^{d-3}, \quad (8.49)$$

which have tree-level flow equations

$$\frac{d\bar{T}}{dl} = (2 - d)\bar{T}(l) \quad (8.50)$$

$$\frac{d\bar{\Delta}_1}{dl} = (3 - d)\bar{\Delta}_1(l), \quad (8.51)$$

whose flow is independent of the arbitrary choice of rescaling exponents appearing in Eqs.8.46a-8.46e.

We now proceed to higher order in Δ_1 , perturbatively integrating the short length modes $\hat{\phi}^{>}(\mathbf{r}, t)$ and $\phi^{>}(\mathbf{r}, t)$

$$Z = \int [d\hat{\phi}^{<} d\phi^{<}] e^{-S_0[\hat{\phi}^{<}, \phi^{<}]} \int [d\hat{\phi}^{>} d\phi^{>}] e^{-S_0[\hat{\phi}^{>}, \phi^{>}]} \times \left[1 - S_1[\hat{\phi}, \phi] + \frac{1}{2} S_1[\hat{\phi}, \phi]^2 + \dots \right], \quad (8.52)$$

$$\equiv \int [d\hat{\phi}^{<} d\phi^{<}] e^{-S_0[\hat{\phi}^{<}, \phi^{<}] - \delta S[\hat{\phi}^{<}, \phi^{<}]}, \quad (8.53)$$

where the graphical correction δS to the action (dropping an unimportant constant) is

$$\delta S[\hat{\phi}^{<}, \phi^{<}] = \langle S_1[\hat{\phi}, \phi] \rangle - \frac{1}{2} \langle S_1[\hat{\phi}, \phi]^2 \rangle^c + \dots, \quad (8.54)$$

where the subscript “c” means cumulant average, and the averages are performed with the quadratic action with correlation and response functions, $C(\mathbf{q}, \omega)V \equiv \langle \phi(\mathbf{q}, \omega)\phi(-\mathbf{q}, -\omega) \rangle$, $G(\mathbf{q}, \omega)V \equiv \langle \phi(\mathbf{q}, \omega)\hat{\phi}(-\mathbf{q}, -\omega) \rangle$, respectively given by

$$C(\mathbf{q}, \omega) = \frac{2T\gamma}{\gamma^2(\omega - vq_x)^2 + (K_\perp q_\perp^2 + K_\parallel q_x^2)^2}, \quad (8.55)$$

$$G(\mathbf{q}, \omega) = \frac{1}{i\gamma(\omega - vq_x) + (K_\perp q_\perp^2 + K_\parallel q_x^2)}, \quad (8.56)$$

which can be read off from Eq.8.44. Although naively one would expect from Eq.6.6 that as in the equilibrium problem for $d > 2$ temperature is an irrelevant variable, as we demonstrate below (consistent with the functional RG treatment of the Sec.V D this zero temperature fixed point is destabilized by the finite velocity motion. We will therefore work at a finite temperature.

The first order correction $\langle S_1[\hat{\phi}, \phi] \rangle$ contributes to the renormalization of γ , $T\gamma$ and Δ_1 , which we designate as $\delta\gamma^{(1)}$, $\delta(T\gamma)^{(1)}$, and $\delta\Delta_1^{(1)}$ and illustrate graphically in Fig. 8.



Fig. 8: Two diagrams that contribute to the renormalization of Δ_1 , $T\gamma$, and γ . The full line corresponds to the correlator $C^>$, the full-wiggle line is the response function $G^>$, wiggly line is the $\hat{\phi}$ field and the vertex is the S_1 nonlinearity. The first diagram, is proportional to T , and is the graphical correction to Δ_1 and $T\gamma$, while the second one, survives even at zero temperature and renormalizes γ .

Expanding to quadratic order in the short-scale fields $\hat{\phi}^>$ and $\phi^>$ and averaging we obtain

$$\begin{aligned} \langle S_1 \rangle &= S_1[\hat{\phi}^<, \phi^<] \\ &+ \frac{\Delta_1}{2} \int_{\mathbf{r}, t, t'} \left[\frac{q_0^2}{2} \hat{\phi}_{\mathbf{r}, t}^< \hat{\phi}_{\mathbf{r}, t'}^< \cos[q_0(\phi_{\mathbf{r}, t}^< - \phi_{\mathbf{r}, t'}^<)] \langle (\phi_{\mathbf{r}, t}^> - \phi_{\mathbf{r}, t'}^>)^2 \rangle \right. \\ &\left. + 2q_0 \hat{\phi}_{\mathbf{r}, t}^< \sin[q_0(\phi_{\mathbf{r}, t}^< - \phi_{\mathbf{r}, t'}^<)] \langle \phi_{\mathbf{r}, t}^> \hat{\phi}_{\mathbf{r}, t'}^> \rangle \right], \quad (8.57) \\ &\approx (1 - q_0^2 C^>(\mathbf{r} = \mathbf{0}, t = 0)) S_1[\hat{\phi}^<, \phi^<] \\ &- \frac{1}{2} q_0^2 \Delta_1 \int_{\mathbf{r}, t} \hat{\phi}_{\mathbf{r}, t}^< \hat{\phi}_{\mathbf{r}, t}^< \int_{\delta t} C^>(\mathbf{r} = \mathbf{0}, \delta t) \\ &+ q_0^2 \Delta_1 \int_{\mathbf{r}, t} \hat{\phi}_{\mathbf{r}, t}^< \partial_t \phi_{\mathbf{r}, t}^< \int_{\delta t} \delta t G^>(\mathbf{r} = \mathbf{0}, \delta t), \quad (8.58) \end{aligned}$$

where in above we used causality (selecting the discretization with $\theta(0) \equiv 0$) and took advantage of the fact that the correlations functions are short-range in time to perform small time gradient expansion. Performing above

integrals over δt (best evaluated in Fourier ω space) and noting that the terms in last part of the Eq.8.58 renormalize Δ_1 , $T\gamma$ and γ , respectively, we find

$$\begin{aligned} \delta\Delta_1^{(1)} &= -\Delta_1 q_0^2 C^>(\mathbf{r} = \mathbf{0}, \delta t = 0) \\ &= -\Delta_1 \frac{Tq_0^2}{2(K_\parallel K_\perp)^{1/2}} C_{d-1} \Lambda^{d-2} dl, \quad (8.59) \end{aligned}$$

$$\begin{aligned} \delta(T\gamma)^{(1)} &= \frac{1}{2} \Delta_1 q_0^2 C^>(\mathbf{r} = \mathbf{0}, \omega = 0) \\ &= \Delta_1 \frac{Tq_0^2}{2K_\perp |v|} C_{d-1} \Lambda^{d-3} dl \quad (8.60) \end{aligned}$$

$$\begin{aligned} \delta\gamma^{(1)} &= \Delta_1 q_0^2 i \partial_\omega G^>(\mathbf{r} = \mathbf{0}, \omega = 0) \\ &= \Delta_1 \frac{2K_\parallel q_0^2}{\gamma^2 |v|^3} C_{d-1} \Lambda^{d-1} dl. \quad (8.61) \end{aligned}$$

The calculation to second order in Δ_1 given by $\delta S_2 \equiv -\frac{1}{2} \langle S_1^2 \rangle^c$ can of course be done directly, however, it is convenient to utilize the functional renormalization group calculation of Sec.V C. There we found for an arbitrary force correlation function $\Delta(\phi)$

$$\begin{aligned} \delta S_2 &= \frac{1}{2} \int_{\mathbf{r}, t, t'} \hat{\phi}_{\mathbf{r}, t}^< \hat{\phi}_{\mathbf{r}, t'}^< \Delta''(\phi_{\mathbf{r}, t}^< - \phi_{\mathbf{r}, t'}^<) \\ &\times (\Delta(\phi_{\mathbf{r}, t}^< - \phi_{\mathbf{r}, t'}^<) - \Delta(0)) \frac{C_{d-1} \Lambda^{d-3}}{2K_\perp \gamma |v|} dl, \quad (8.62) \end{aligned}$$

which when applied to the lowest harmonic $\Delta(\phi) = \Delta_1 \cos[q_0 \phi]$ gives

$$\delta S_2 = \Delta_1^2 q_0^2 \int_{\mathbf{r}, t, t'} \hat{\phi}_{\mathbf{r}, t}^< \hat{\phi}_{\mathbf{r}, t'}^< \left[\cos[\phi_{\mathbf{r}, t}^< - \phi_{\mathbf{r}, t'}^<] - \frac{1}{2} \right] \frac{C_{d-1} \Lambda^{d-3}}{4K_\perp \gamma |v|} dl, \quad (8.63)$$

The diagram that leads to the above contribution to δS_2 , renormalizing the 0th and 1st harmonics, i.e. Δ_0 , and Δ_1 , respectively, is illustrated in Fig.9

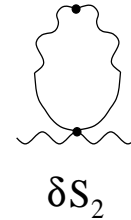


Fig. 9: Diagram that contributes to the renormalization of $\Delta(u)$, to second order in $\Delta(u)$, i.e. renormalizes the 0th and 1st harmonics, Δ_0 and Δ_1 , respectively with the same notation as in Fig.8.

We therefore have to second order in Δ_1

$$\delta\Delta_0^{(2)} = \frac{\Delta_1^2 q_0^2 C_{d-1} \Lambda^{d-3}}{4K_\perp \gamma |v|} dl \quad (8.64)$$

$$\delta\Delta_1^{(2)} = -\frac{\Delta_1^2 q_0^2 C_{d-1} \Lambda^{d-3}}{2K_\perp \gamma |v|} dl, \quad (8.65)$$

where Δ_0 is the zeroth harmonic of the force-force correlator, i.e. the ϕ -independent correlator of the random drag. Combining Eqs.8.65 with the zeroth (trivial dimensional rescaling) and first order results of Eqs.8.47b,8.59–8.61 and rewriting the flow equations for the dimensionless couplings $\overline{\Delta}_0$, $\overline{\Delta}_1$, and \overline{T} defined by Eqs.8.48–8.49, we obtain the RG flow equations quoted in the main text, Sec.VI, Eqs.6.4–6.6.

IX. APPENDIX F

In this appendix we discuss the hydrodynamic equations for the driven smectic of lines (illustrated in Fig. 4) that may be obtained in a three-dimensional superconductor ($d_t = 2$, $d_l = 1$). This smectic of lines has qualitatively new properties as compared to the smectic of point particles described in Section IV. As discussed by Marchetti and Nelson⁵⁷, in an isotropic flux-line liquid the conserved variables associated with hydrodynamic modes are the density field $\rho(\mathbf{r})$ and the two components of a tangent field density $\boldsymbol{\tau}(\mathbf{r}) = (\tau_x, \tau_y)$, describing the instantaneous bending of the lines away from the direction of the external field (z direction). Since flux lines cannot start or stop inside the sample, the density and the two components of the tilt field are not independent dynamical variables, but are related by a continuity equation in the time-like variable z ,

$$\partial_z \delta\rho + \nabla_t \cdot \boldsymbol{\tau} = 0. \quad (9.1)$$

This is simply the condition of no magnetic monopoles. The line smectic retains some degree of periodicity along the transverse direction y . This broken symmetry is described by the layer displacement $\phi_y = \phi$. In addition both the conserved density and one component of the conserved tilt density are associated with independent hydrodynamic modes since they are not slaved to the layer displacement field. Having identified the relevant hydrodynamic variables for the line smectic as a one-dimensional layer displacement ϕ , a density ρ and a tilt density $\boldsymbol{\tau}$, related by Eq. 9.1, we now proceed to construct the phenomenological hydrodynamic equations for the line smectic and to study the spectrum of the hydrodynamic modes of this system.

The continuum hydrodynamic free energy for the overdamped line smectic is given by

$$\mathcal{F}_{ls} = \frac{1}{2} \int_{\mathbf{r}} \left\{ c_L \left(\frac{\delta\rho}{\rho_0} \right)^2 + c_{44} \left(\frac{\boldsymbol{\tau}}{\rho_0} \right)^2 + c_{11}^y (\partial_y \phi)^2 + K_1^x (\partial_x \phi)^2 + K_1^z (\partial_z \phi)^2 + 2K_2 (\partial_y \phi) \frac{\delta\rho}{\rho_0} \right\}, \quad (9.2)$$

where $\delta\rho = \rho - \rho_0$, with ρ_0 the equilibrium density. Here c_L and c_{44} are the smectic bulk and tilt moduli, respectively, c_{11}^y is the in-layer compressibility, K_1^x and K_1^z are layer bending stiffnesses. The coupling constant K_2 has dimensions of an elastic constant. The hydrodynamic equations of the driven smectic contain additional nonequilibrium terms, as compared to their equilibrium counterpart. The nonequilibrium terms can be

constructed by preserving two important symmetries of the driven system, the invariance under inversions about the direction of the external drive ($y \rightarrow -y$, $\phi \rightarrow -\phi$) and the broken translational invariance in the y directions ($y \rightarrow y + a$, $\phi \rightarrow \phi + a$).

Density and tilt density conservation requires the density and the tilt field to satisfy continuity equations⁵⁷,

$$\partial_t \delta\rho + \nabla \cdot \mathbf{j} = 0, \quad (9.3)$$

$$\partial_t \tau_i + \partial_j J_{ij} = \partial_z j_i, \quad (9.4)$$

where \mathbf{j} is the number current density and J_{ij} is the antisymmetric tilt flux tensor. The density and tilt density fields are also related by the ‘‘continuity’’ equation 9.1. The equation for the layer displacement has the same structure as that for the two-dimensional lattice, Eq. 4.3, and is repeated here for completeness

$$(\partial_t + v\partial_x)\phi = \frac{j_y}{\rho} - \frac{\Gamma_0}{\rho_0} \frac{\delta\mathcal{F}_{ls}}{\delta\phi}, \quad (9.5)$$

with Γ_0 a kinetic coefficient. We will not discuss here the role of disorder on the hydrodynamics of the line smectic. Therefore we have not included any pinning force in the equations of motion. The hydrodynamic equations need to be supplemented by constitutive relations for the current flux \mathbf{j} and the tilt flux J_{ij} . For simplicity we only consider here local hydrodynamics, but the non-locality of the elastic constants that is often important in flux-line systems can be trivially incorporated. The constitutive equations for the *driven* line smectic contain, however, new nonequilibrium terms not present in their equilibrium counterpart discussed in Ref. 57. The two components of the current density are given by

$$j_x = (v + v_1)\delta\rho + \rho_0 v_2 \partial_y \phi - a_1 \partial_z \tau_x - \rho_0 \Gamma_1 \left(\partial_x \frac{\delta\mathcal{F}_{ls}}{\delta\rho} - \partial_z \frac{\delta\mathcal{F}_{ls}}{\delta\tau_x} \right), \quad (9.6)$$

$$j_y = \rho_0 v_3 \partial_x \phi - a_2 \partial_z \tau_y - \rho_0 \Gamma_2 \left(\partial_y \frac{\delta\mathcal{F}_{ls}}{\delta\rho} - \partial_z \frac{\delta\mathcal{F}_{ls}}{\delta\tau_y} \right). \quad (9.7)$$

The antisymmetric tilt flux tensor is written as

$$J_{ij} = \epsilon_{ij} \left[v_4 \hat{\mathbf{z}} \cdot (\hat{\mathbf{v}}_0 \times \boldsymbol{\tau}) + \rho_0 \Gamma_\tau \hat{\mathbf{z}} \cdot \left(\nabla_t \times \frac{\delta\mathcal{F}_{ls}}{\delta\boldsymbol{\tau}} \right) \right] \quad (9.8)$$

All the parameters v_i and a_i entering the nonequilibrium terms are proportional to the mean velocity v . Since the longitudinal part of the tilt vector can be eliminated in favor of the density using Eq. 9.1, it is convenient to work in Fourier space. We introduce longitudinal and transverse components of the tilt vector as

$$\boldsymbol{\tau}(\mathbf{q}) = \hat{\mathbf{q}}_t \tau(\mathbf{q}) + (\hat{\mathbf{z}} \times \hat{\mathbf{q}}_t) \tau_T(\mathbf{q}), \quad (9.9)$$

with $\hat{\mathbf{q}}_t = \mathbf{q}_t/q_t$. Then $\tau_L = \hat{\mathbf{q}}_t \cdot \boldsymbol{\tau}$ and $\tau_T = (\hat{\mathbf{z}} \times \hat{\mathbf{q}}_t) \cdot \boldsymbol{\tau}$. By inserting the constitutive equation for the fluxes in Eqs. (9.3), (9.4) and (9.5), we obtain,

$$\left[\partial_t - i\tilde{v}_1 q_x + D_1 q_x^2 + D_2 q_y^2 - (\hat{q}_x^2 D_6 + \hat{q}_y^2 D_7) q_z^2 \right] \delta\rho = \rho_0 \tilde{v}_2 q_x q_y \phi + (D_6 - D_7) \hat{q}_x \hat{q}_y q_z q_t \tau_T, \quad (9.10)$$

$$\left[\partial_t - i\tilde{v}_3 q_x + D_3 q_x^2 + D_4 q_y^2 + D_8 q_z^2 \right] \phi = -i q_y (D_5 - \frac{q_z^2}{q_t^2} D_7) \frac{\delta\rho}{\rho_0} - i q_z \hat{q}_x \frac{D_7}{\rho_0} \tau_T \quad (9.11)$$

$$\begin{aligned} \left[\partial_t + i v_4 q_x + D_9 q_t^2 - (D_6 \hat{q}_x^2 + D_7 \hat{q}_y^2) q_z^2 \right] \tau_T &= \rho_0 q_z q_t (v_2 \hat{q}_y^2 - v_3 \hat{q}_x^2) \phi \\ &+ i(\tilde{v}_1 + v_4) \hat{q}_y q_z \delta\rho + q_z^2 (D_6 - D_7) \hat{q}_x \hat{q}_y \frac{q_z}{q_t} \delta\rho. \end{aligned} \quad (9.12)$$

Finally, the longitudinal part of the tilt density is simply related to the density,

$$\tau_L = -\frac{q_z}{q_t} \delta\rho \quad (9.13)$$

The “velocities” \tilde{v}_1 , \tilde{v}_2 , \tilde{v}_3 have been defined as

$$\tilde{v}_1 = v + v_1, \quad (9.14a)$$

$$\tilde{v}_2 = v_2 + v_3, \quad (9.14b)$$

$$\tilde{v}_3 = v - v_3 \quad (9.14c)$$

The coefficients D_i have dimensions of diffusion constants and are given by

$$D_1 = \Gamma_1 c_L / \rho_0, \quad (9.15a)$$

$$D_2 = \Gamma_2 c_L / \rho_0, \quad (9.15b)$$

$$D_3 = \Gamma_0 K_1 / \rho_0, \quad (9.15c)$$

$$D_4 = (\Gamma_0 c_{11}^y - \Gamma_2 K_2) / \rho_0, \quad (9.15d)$$

$$D_5 = (\Gamma_0 K_2 - \Gamma_2 c_L) / \rho_0, \quad (9.15e)$$

$$D_6 = a_1 - \Gamma_1 c_{44} / \rho_0, \quad (9.15f)$$

$$D_7 = a_2 - \Gamma_2 c_{44} / \rho_0, \quad (9.15g)$$

$$D_8 = \Gamma_0 K_1^z / \rho_0, \quad (9.15h)$$

$$D_9 = \Gamma_\tau c_{44} / \rho_0. \quad (9.15i)$$

By solving the hydrodynamic equations in the long wavelength limit, we can find the hydrodynamic eigenfrequencies that govern the relaxation of density, tilt and displacement fluctuations. All the modes are propagating at finite velocities and are given by

$$\omega_\rho = \tilde{v}_1 q_x + i \left[D_1 q_x^2 + \left(D_2 + \frac{\tilde{v}_2 D_5}{\tilde{v}_1 - \tilde{v}_3} \right) q_y^2 - D_6 q_z^2 \right], \quad (9.16)$$

$$\begin{aligned} \omega_\phi &= \tilde{v}_3 q_x + i \left[D_3 q_x^2 + \left(D_4 - \frac{\tilde{v}_2 D_5}{\tilde{v}_1 - \tilde{v}_3} \right) q_y^2 \right. \\ &\quad \left. + \left(D_8 - \frac{v_3 D_7}{\tilde{v}_3 + v_4} \right) q_z^2 \right], \end{aligned} \quad (9.17)$$

$$\omega_\tau = -v_4 q_x + i \left[D_9 q_t^2 - \left(D_6 + \frac{v_3 D_7}{v_4 + \tilde{v}_3} \right) q_z^2 \right]. \quad (9.18)$$

For stability, in addition to the conditions stated for the two-dimensional smectic, we must have $D_6 < 0$, $D_8 - \frac{v_3 D_7}{v_3 + v_4} > 0$, $D_9 > 0$ and $D_6 + \frac{v_3 D_7}{v_4 + \tilde{v}_3} < 0$. The

first mode corresponds to the permeation mode of smectic liquid crystals and describes the transport of mass across the layers that can occur in these systems without destroying the layer periodicity. The second mode describes long-wavelength deformations of the layers and governs the decay of displacement fluctuations. Finally, the third mode governs the relaxation of tilt fluctuations, that, like density, can occur both in and out of the layers, while preserving the line smectic periodicity.

¹ B. J. Ackerson and N. A. Clark, Phys. Rev. Lett. **46**, 123 (1981); Phys. Rev. A **30**, 906 (1984).

² G. Blatter, M.V. Feigel'man, V.B. Geshkenbein, A.I. Larkin, and V.M. Vinokur, Rev. Mod. Phys. **66**, 1125 (1994).

³ D. Huse and L. Radzihovsky, in Proceedings of 1993 Altenberg Summer School, *Fundamental Problems in Statistical Mechanics VIII*, edited by H. van Beijeren and M. H. Ernst (Elsevier, Netherlands);

⁴ G. Grüner, Rev. Mod. Phys. **60**, 1129 (1988).

⁵ R. Seshadri and R.M. Westervelt, Phys. Rev. B **46**, 5142 & 5150 (1992).

⁶ E.Y. Andrei, G. Deville, D.C. Glattli, F.I.B. Williams, E. Paris, and B. Etienne, Phys. Rev. Lett. **60**, 2765 (1988).

⁷ R.L. Willet, in *Phase Transitions and Relaxation in Systems with Competing Energy Scales*, T. Riste and D. Sherrington, eds., Nato ASI series vol. 415, p. 367 (Kluwer Academic Pub., Dordrecht, 1993); and references therein.

⁸ D. S. Fisher, K. Dahmen, S. Ramanathan, and Y. Ben-Zion, Phys. Rev. Lett. **78**, 4885 (1997); cond-mat/9703029.

⁹ A. Larkin, Sov. Phys. JETP **31**, 784 (1970); A.I. Larkin and Y.N. Ovchinnikov, Sov. Phys. JETP **38**, 854 (1974).

¹⁰ T. Giamarchi and P. Le Doussal, Phys. Rev. Lett. **72**, 1530 (1994); Phys. Rev. B **52**, 1242 (1995).

¹¹ M.J.P. Gingras and D.A. Huse, Phys. Rev. B **53**, 15183 (1996).

¹² D. S. Fisher, Phys. Rev. Lett. **78**, 1964 (1997); cond-mat/9610146.

¹³ H. Fukuyama and P.A. Rice, Phys. Rev. B **17**, 535 (1978).

¹⁴ A.A. Middleton, Phys. Rev. Lett. **68**, 670 (1992).

¹⁵ F. Nori, Science **271**, 1373 (1996).

- ¹⁶ L. Balents and M.P.A. Fisher, Phys. Rev. Lett. **75**, 4270 (1995).
- ¹⁷ The situation is a little simpler for CDWs. In this case in the ordered state the charge density acquires a periodic modulation of wavevector $2k_F$ along a single direction (x direction), that of the most conducting axis of the material. Furthermore the Fourier series can be truncated to the first harmonic as the order parameters defined by higher harmonics in the Fourier expansion of the charge density are not independent. The charge density is then simply written as $\rho(\mathbf{r}) = \rho_0 + \text{Re}\psi e^{i2k_F x}$, where $\psi = \rho_1 e^{i\phi}$ and long wavelength charge fluctuations are described by the CDW phase $\phi(\mathbf{r}, t)$.
- ¹⁸ M. P. A. Fisher, Phys. Rev. Lett. **62**, 1415 (1989); D. S. Fisher, M. P. A. Fisher, and D. A. Huse, Phys. Rev. B **43**, 130 (1991), and references therein.
- ¹⁹ L. Balents, M.C. Marchetti, and L. Radzihovsky, Phys. Rev. Lett. **78**, 751 (1997).
- ²⁰ J.M. Kosterlitz and D.J. Thouless, J. Phys. C **6**, 1181 (1973); B. I. Halperin and D. R. Nelson, Phys. Rev. Lett. **41**, 121 (1978).
- ²¹ Similar equations have apparently been obtained by S. Scheidl, without the nonequilibrium force (S. Scheidl, private communication).
- ²² L.W. Chen, L. Balents, M.P.A. Fisher, and M.C. Marchetti, Phys. Rev. B **54**, 12798 (1996).
- ²³ Strictly speaking, even a crystal at finite temperature always has a non-zero concentration of thermally activated vacancies or interstitials, and their density indeed constitutes an additional hydrodynamic mode. This was first pointed out by P. C. Martin, O. Parodi, and P.S. Pershan, Phys. Rev. A **6**, 2401 (1972). In crystals, however, because this concentration is generally quite small, the defect density mode plays little role.
- ²⁴ P.C. Martin, E.D. Siggia and H.A. Rose, Phys. Rev. A **8**, 423 (1973); H. K. Janssen, Z. Phys. B **23**, 377 (1976); C. De Dominicis and L. Peliti, Phys. Rev. B **18**, 353 (1978); R. V. Jensen, J. Stat. Phys. **25**, 183 (1981).
- ²⁵ L. Balents, unpublished.
- ²⁶ T. Giamarchi and P. Le Doussal, Phys. Rev. Lett. **76**, 3408 (1996).
- ²⁷ The transition from the driven lattice to the smectic resembles the type-I melting proposed some time ago by Ostlund and Halperin (S. Ostlund and B.I. Halperin, Phys. Rev. B **23**, 335 (1981)) for anisotropic two-dimensional crystals. In the equilibrium case considered by these authors the 2d smectic may be stabilized by the coupling to an incommensurate crystalline substrate. In the driven case discussed in our work it is the transverse pinning force that provides the periodic coupling needed to stabilize the smectic.
- ²⁸ K. Moon, R. T. Scalettar, and G. Zimányi, Phys. Rev. Lett. **77**, 2778 (1996).
- ²⁹ G. Grinstein, R. A. Pelcovits, Phys. Rev. Lett. **47**, 856 (1981).
- ³⁰ O. Narayan and D. S. Fisher, Phys. Rev. B **46**, 11520 (1992).
- ³¹ This, however, does *not* imply a vanishing of the transverse linear resistivity in the smectic. The permeation density mode appearing in Eqs.4.6–4.7 allows finite transverse vortex transport even for frozen smectic layers (also see Sec.VII).
- ³² In the *equilibrium* problem, cutting off the nonanalyticity of Δ using finite temperature (which is irrelevant for $d > 2$) leads to divergent (length-scale dependent) correction to the dynamical exponent z , which can be interpreted as activated dynamics over energy barriers that diverge as a power law of length scale (L. Radzihovsky, University of Colorado preprint).
- ³³ It can be easily seen from the functional RG flow equation for $\Gamma(\phi)$, Eq.5.46, that at the Gaussian fixed point, the disorder eigenvalue for the $Q_n = nq_0$ Fourier component of the random potential is $\lambda_n = 3 - d - \overline{T}n^2q_0^2$. This therefore implies that near a finite temperature fixed point one needs to keep only the most relevant lowest Fourier component $Q_1 = q_0$ of the disorder potential.
- ³⁴ L. Balents, Europhys. Lett. **24**, 489 (1993).
- ³⁵ J. L. Cardy and S. Ostlund, Phys. Rev. B **25**, 6899 (1982).
- ³⁶ J. Toner, D. DiVincenzo, Phys. Rev. B **41**, 632 (1990).
- ³⁷ Y. T. Tsai and Y. Shapir, Phys. Rev. Lett. **69**, 1773 (1992)
- ³⁸ A.E. Koshelev and V.M. Vinokur, Phys. Rev. Lett. **73**, 3580 (1994).
- ³⁹ Early theoretical studies of an elastic medium driven through disorder (A. Schmid and W. Hauger, J. Low Temp. Phys. **11**, 667 (1973).) used perturbation theory at large sliding velocities v to obtain nonlinear corrections to the velocity as a function of the external force, but said little about the nature of the sliding state.
- ⁴⁰ S. Bhattacharya and M.J. Higgins, Phys. Rev. Lett. **70**, 2617 (1993); M.J. Higgins and S. Bhattacharya, Physica C **257**, 232 (1996).
- ⁴¹ M.C. Hellerqvist, D. Ephron, W.R. White, M.R. Beasley, and A. Kapitulnik, Phys. Rev. Lett. **76**, 4022 (1996).
- ⁴² U. Yaron *et al.*, Phys. Rev. Lett. **73**, 2748 (1994); Nature **376**, 753 (1995) & **381**, 253 (1996).
- ⁴³ A. Duarte *et al.*, Phys. Rev. B **53**, 11336 (1996).
- ⁴⁴ M. Marchevsky *et al.*, Phys. Rev. Lett. **78**, 531 (1997).
- ⁴⁵ H.J. Jensen, A. Brass, Y. Brechet, and A.J. Berlinsky, Phys. Rev. B **38**, 9235 (1988).
- ⁴⁶ A.-C. Shi and A.J. Berlinsky, Phys. Rev. Lett. **67**, 1926 (1991).
- ⁴⁷ M.C. Faleski, M.C. Marchetti and A.A. Middleton, Phys. Rev. B **54**, 12427 (1996).
- ⁴⁸ S. Ryu, M. Hellerqvist, S. Doniach, A. Kapitulnik, and D. Stroud, Phys. Rev. Lett. **77**, 5114 (1996).
- ⁴⁹ S. Spencer and H.J. Jensen, preprint (cond-mat/96010207).
- ⁵⁰ F. Pardo, private communication.
- ⁵¹ R.M. Fleming and C.C. Grimes, Phys. Rev. Lett. **42**, 1423 (1979).
- ⁵² S. Bhattacharya, J.P. Stokes, M.O. Robbins and R.A. Klemm, Phys. Rev. Lett. **54**, 2453 (1985).
- ⁵³ P. Monceau, J. Richard and M. Renard, Phys. Rev. Lett. **45**, 43 (1980); S. Bhattacharya, J.P. Stokes, M.J. Higgins and R.A. Klemm, Phys. Rev. Lett. **59**, 1849 (1987).
- ⁵⁴ For a first attempt to consider dislocation dynamics in the driven lattice see S. Scheidl and V.M. Vinokur, unpublished (cond-mat/9702014).
- ⁵⁵ K. G. Wilson and J. Kogut, Phys. Rep. C, **12**, 77 (1977).
- ⁵⁶ Since a driving force necessary selects an axis, thereby breaking rotational symmetry explicitly, a hexatic phase has no distinction from the liquid (orientational ordering

can play a role in the dynamics as the applied force tends to zero, changing the nature of the response – this dynamics is an important open problem).

⁵⁷ M.C. Marchetti and D.R. Nelson, *Physica C* **174**, 40 (1991).